NCHRP Web Document 68 (Project 9-27)

Relationships of HMA In-Place Air Voids, Lift Thickness, and Permeability
Volume One

Prepared for:

National Cooperative Highway Research Program

TRANSPORTATION RESEARCH BOARD
OF THE NATIONAL ACADEMIES

Submitted by:

E. Ray Brown
M. Rosli Hainin
Allen Cooley
Graham Hurley
National Center for Asphalt Technology
Auburn University
Auburn, Alabama

September 2004

ACKNOWLEDGMENT

This work was sponsored by the American Association of State Highway and Transportation Officials (AASHTO), in cooperation with the Federal Highway Administration, and was conducted in the National Cooperative Highway Research Program (NCHRP), which is administered by the Transportation Research Board (TRB) of the National Academies.

THE NATIONAL ACADEMIES

Advisers to the Nation on Science, Engineering, and Medicine

The **National Academy of Sciences** is a private, nonprofit, self-perpetuating society of distinguished scholars engaged in scientific and engineering research, dedicated to the furtherance of science and technology and to their use for the general welfare. On the authority of the charter granted to it by the Congress in 1863, the Academy has a mandate that requires it to advise the federal government on scientific and technical matters. Dr. Bruce M. Alberts is president of the National Academy of Sciences.

The **National Academy of Engineering** was established in 1964, under the charter of the National Academy of Sciences, as a parallel organization of outstanding engineers. It is autonomous in its administration and in the selection of its members, sharing with the National Academy of Sciences the responsibility for advising the federal government. The National Academy of Engineering also sponsors engineering programs aimed at meeting national needs, encourages education and research, and recognizes the superior achievements of engineers. Dr. William A. Wulf is president of the National Academy of Engineering.

The **Institute of Medicine** was established in 1970 by the National Academy of Sciences to secure the services of eminent members of appropriate professions in the examination of policy matters pertaining to the health of the public. The Institute acts under the responsibility given to the National Academy of Sciences by its congressional charter to be an adviser to the federal government and, on its own initiative, to identify issues of medical care, research, and education. Dr. Harvey V. Fineberg is president of the Institute of Medicine.

The **National Research Council** was organized by the National Academy of Sciences in 1916 to associate the broad community of science and technology with the Academy's purposes of furthering knowledge and advising the federal government. Functioning in accordance with general policies determined by the Academy, the Council has become the principal operating agency of both the National Academy of Sciences and the National Academy of Engineering in providing services to the government, the public, and the scientific and engineering communities. The Council is administered jointly by both the Academies and the Institute of Medicine. Dr. Bruce M. Alberts and Dr. William A. Wulf are chair and vice chair, respectively, of the National Research Council.

The **Transportation Research Board** is a division of the National Research Council, which serves the National Academy of Sciences and the National Academy of Engineering. The Board's mission is to promote innovation and progress in transportation through research. In an objective and interdisciplinary setting, the Board facilitates the sharing of information on transportation practice and policy by researchers and practitioners; stimulates research and offers research management services that promote technical excellence; provides expert advice on transportation policy and programs; and disseminates research results broadly and encourages their implementation. The Board's varied activities annually engage more than 5,000 engineers, scientists, and other transportation researchers and practitioners from the public and private sectors and academia, all of whom contribute their expertise in the public interest. The program is supported by state transportation departments, federal agencies including the component administrations of the U.S. Department of Transportation, and other organizations and individuals interested in the development of transportation.
www.TRB.org

VOLUME ONE
TABLE OF CONTENTS

Page

LIST OF TABLES

LIST OF FIGURES

RELATIONSHIPS OF HMA IN-PLACE AIR VOIDS, LIFT THICKNESS, AND PERMEABILITY
NCHRP 9-27
Task 3 – Part 1 and 2

1.0 INTRODUCTION AND PROBLEM STATEMENT

Proper compaction of HMA mixtures is vital to ensure that a stable and durable pavement is built. For dense-graded mixes, numerous studies have shown that initial in-place air voids should not be below approximately 3 percent nor above approximately 8 percent (1). Low in-place air voids can result in rutting and shoving, while high air voids allow water and air to penetrate into the pavement leading to an increased potential for water damage, oxidation, raveling, and cracking. Low in-place air voids are generally the result of a mix problem while high in-place voids are generally caused by inadequate compaction.

Many researchers have shown that increases in in-place air void contents have meant increases in pavement permeability. Zube (2) in the 1960's indicated dense-graded pavements become excessively permeable at in-place air voids above 8 percent. Brown et al. (3) later confirmed this value during the 1980s. However, due to problems associated with coarse-graded (gradation passing below the maximum density line) mixes, the size and interconnectivity of air voids have been shown to greatly influence permeability. A study conducted by the Florida Department of Transportation (FDOT) (4) indicated that coarse-graded Superpave mixes can be excessively permeable to water at in-place air voids less than 8 percent. Permeability is also a major concern in stone matrix asphalt (SMA) mixes since they utilize a gap-graded coarse gradation. Data has shown that SMA mixes tend to become permeable when air voids are above approximately 6 percent.

Numerous factors can potentially affect the permeability of HMA pavements. In a study by Ford and McWilliams (5), it was suggested that particle size distribution, particle shape, and density (air voids or percent compaction) affect permeability. Hudson and Davis (6) concluded that permeability is dependent on the size of air voids within a pavement, not just the percentage of voids. Research by Mallick et al. (7) has also shown that the nominal maximum aggregate size (NMAS) and lift thickness for a given NMAS affect permeability.

Work by FDOT indicated that lift thickness can have an influence on density, and hence permeability (8). FDOT constructed numerous pavement test sections on Interstate 75 that included mixes of different NMAS and lift thicknesses. Results of this experiment suggested that increased lift thicknesses could lead to better pavement density and, hence, lower permeability.

The three items discussed (permeability, lift thickness, and air voids) are all interrelated. Permeability has been shown to be related to pavement density (in-place air voids). Increased lift thickness has been shown to allow desirable density levels to be more easily achieved. Westerman (9), Choubane et al. (4), and Musselman et al. (8) have suggested that a thickness to NMAS ratio (t/NMAS) of 4.0 is preferred. Most guidance recommends that a minimum t/NMAS of 3.0 be used (10). However, due to the potential problems of achieving the desired density, it is believed that this ratio should be further evaluated based on NMAS, gradation and mix type (Superpave and SMA).

This report is divided into 5 volumes. The first volume includes the work on Task 3-Part 1 and 2. The second volume includes the work on Task 3-Part 3. The third volume includes the work on Task 5. The fourth volume is the appendix. The fifth

volume is an executive summary of the work.

2.0 OBJECTIVE

The objectives of this study are 1) to determine the minimum t/NMAS needed for desirable pavement density levels to be achievable, and thus impermeable pavements, 2) to evaluate the permeability characteristics of compacted samples at different thicknesses, and 3) to evaluate factors affecting the relationship between in-place air voids, permeability, and lift thickness.

3.0 RESEARCH APPROACH

The laboratory evaluation of the relationship between thickness, density, and permeability was divided into two parts. Part 1 evaluated the relationship of lift thickness, air voids, and permeability in a controlled, statistically designed experiment. Figure 1 illustrates the research approach to evaluate these relationships. The relationship between lift thickness and air voids is essentially one of compactability. Enough mixture is needed on the roadway (lift thickness) so that aggregate particles can orient themselves in such a way that a desirable density can be achieved (assuming sufficient compactive effort). If sufficient mix is not available (lift thickness too thin), then aggregate particles cannot slide past each other and orient in such a way as to allow a desirable density level to be achieved. Another problem with thinner lifts is that the mixture tends to cool more quickly, which also hinders adequate compaction. Therefore, the objective of Part 1 was to identify the minimum thickness(es) of HMA that is needed on the roadway to allow a desirable density to be achieved. Since lift thickness, air voids,

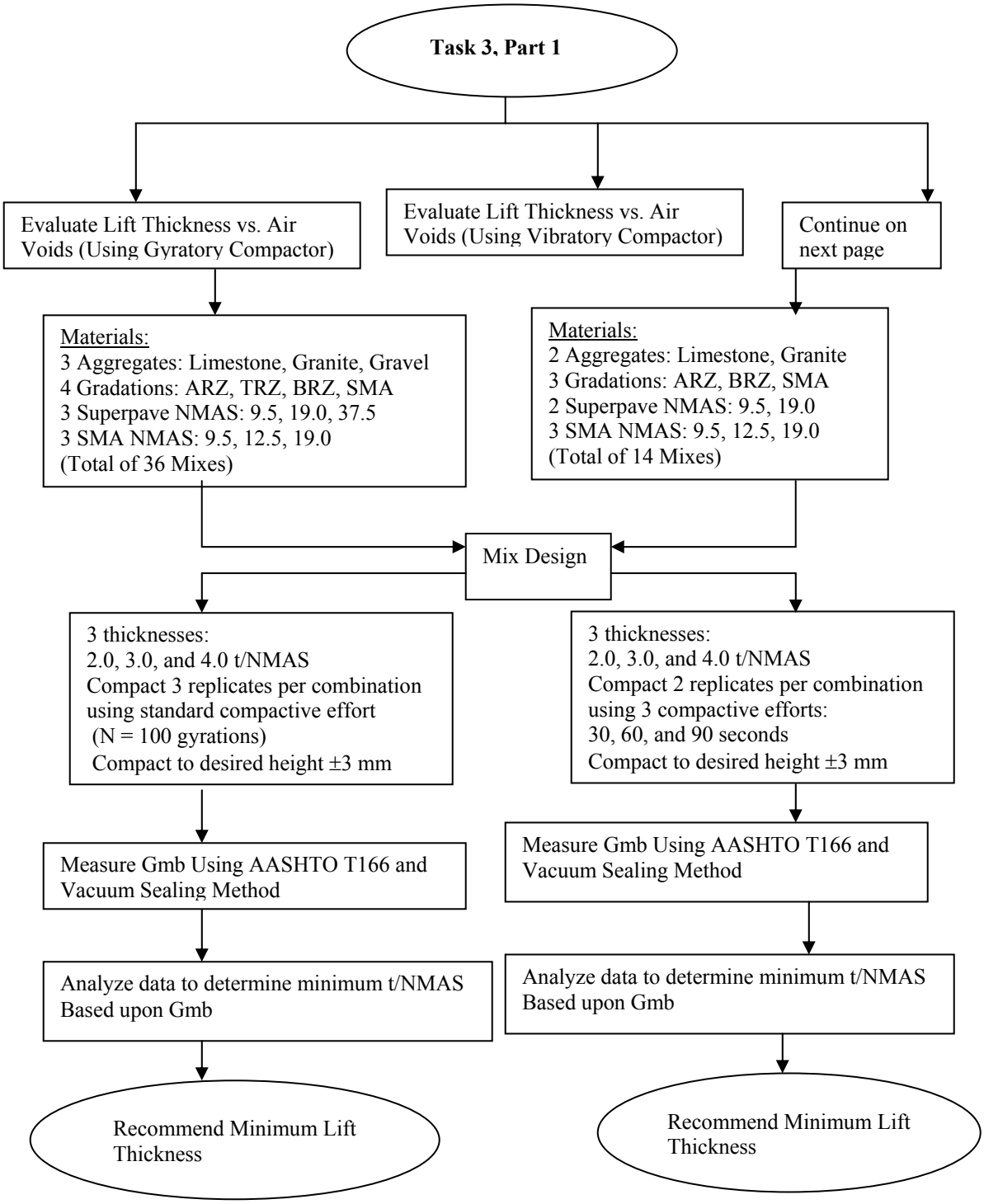

Figure 1: Experimental Plan for Part 1 of Task 3

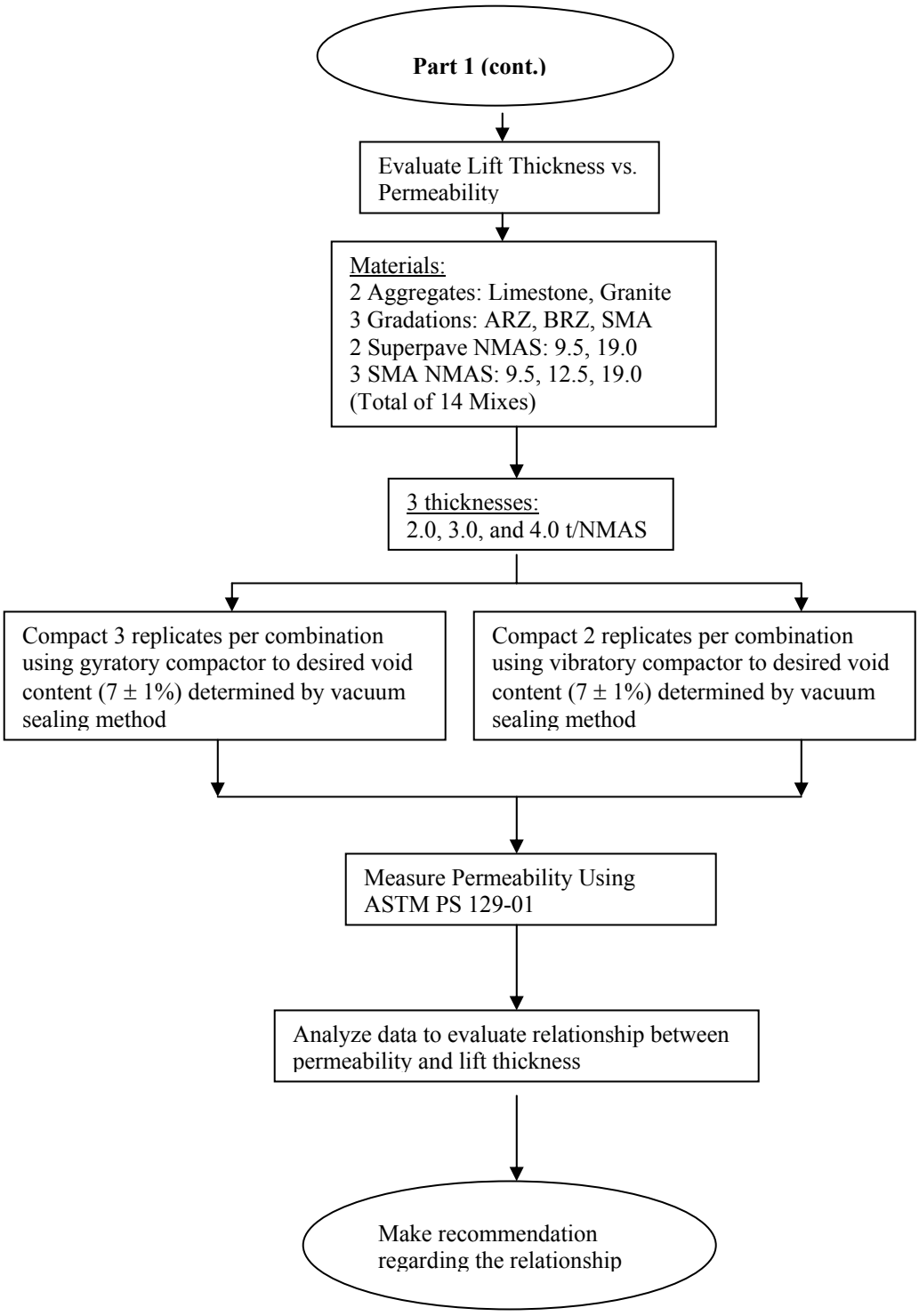

Figure 1 (cont.): Experimental Plan for Part 1

and permeability are interrelated; another objective was to investigate the permeability characteristics of compacted HMA at different thicknesses.

After completion of the laboratory study, NCAT decided to conduct field tests to confirm and improve on the results from the laboratory tests. This was not part of the proposed work but it was considered necessary to better understand the effects of thickness on compaction. The reconstruction of the 2003 NCAT Test Track gave NCAT the opportunity to build sections (off the track) with varying thickness from one end of each section to the other. Through the field experiments, the following issues were also evaluated to strengthen the conclusions of this study: 1) How does lift thickness affect the compactibility of HMA mixes, and 2) What effect does a pneumatic tire roller have on density and permeability as compared to a steel drum roller? Figure 2 illustrates the research approach for this part of the study.

Part 2 of this research project evaluated the relationship between in-place air voids and laboratory permeability of core samples from NCHRP 9-9(1). Figure 3 illustrates the research approach to evaluate this relationship. Other factors influencing the permeability such as gradation, NMAS, lift thickness, and design compactive effort (N_{des}) were also investigated.

3.1 Part 1-Experimental Plan

3.1.1 Evaluation of Effect of t/NMAS on Density Using Gyratory Compactor

In the experimental plan, a total of 36 HMA mixes were designed. Mixes were designed having different aggregates, gradations, and NMASs. The aggregates utilized in this research were a crushed siliceous gravel, a granite, and a limestone. These aggregates

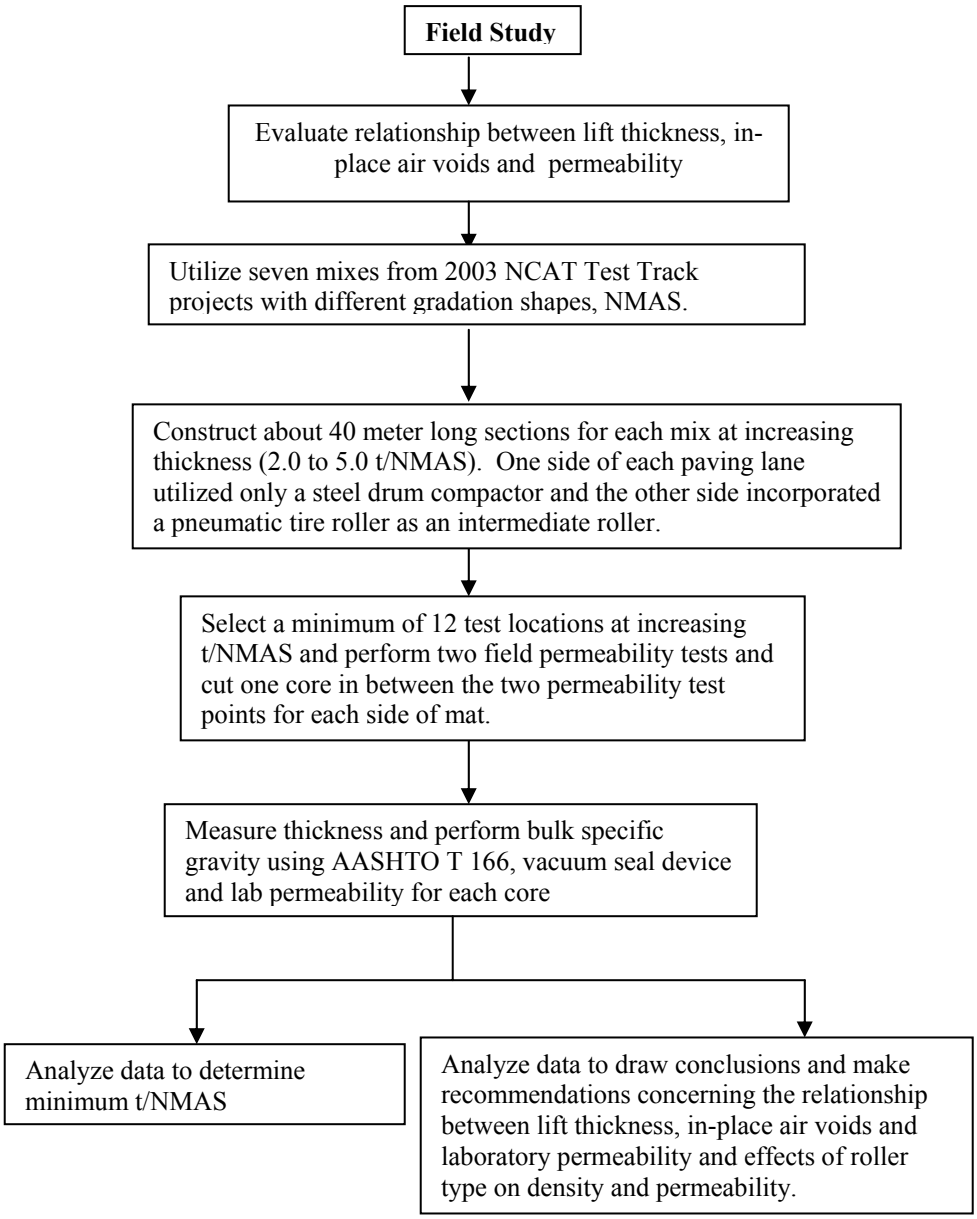

Figure 2: Experimental Plan for Field Study

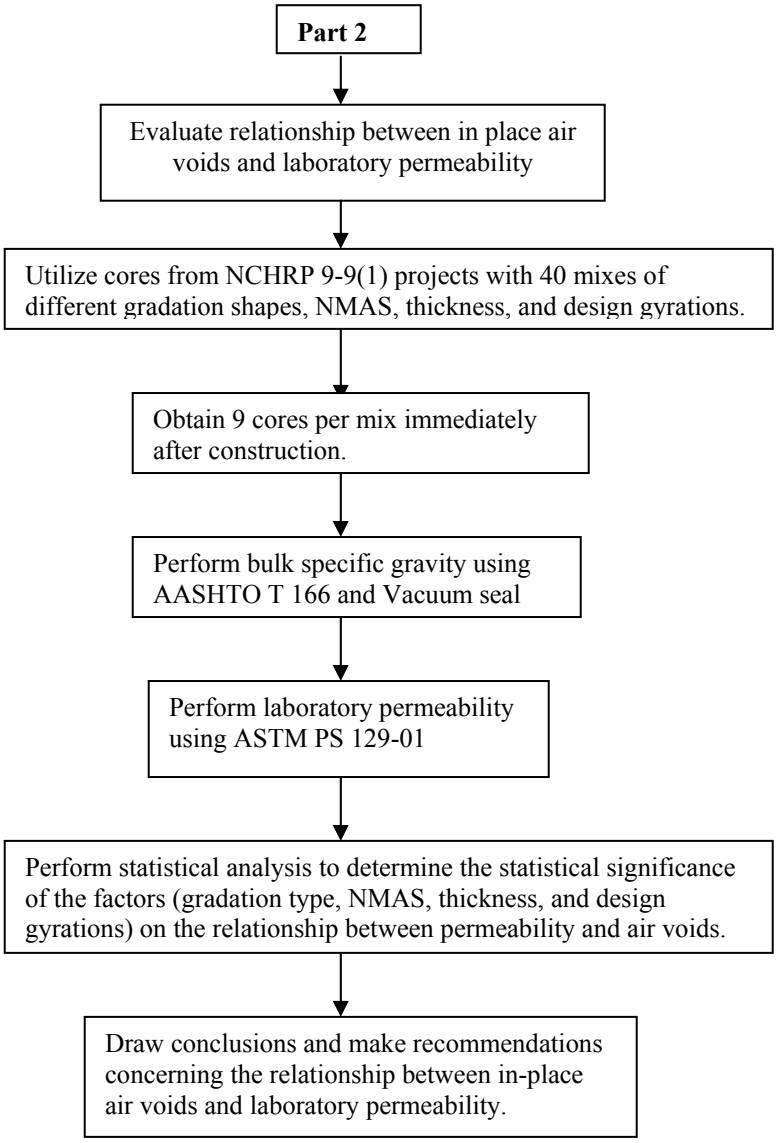

Figure 3: Experimental Plan for Part 2

were selected because they represent a wide range of mineralogical origin, particle shape, and surface texture. The asphalt binder utilized for all mixes was a PG 64-22. All samples were compacted using a Superpave gyratory compactor at the temperature that provides the recommended viscosity for the asphalt binder during the mix design.

The experiment also included four gradation shapes and three nominal maximum aggregate sizes (NMAS). Three gradations fell within Superpave gradation control points and one gradation conformed to stone matrix asphalt specifications. For the gradations meeting the Superpave requirements, NMASs of 9.5, 19.0 and 37.5 mm were investigated. For the SMA gradations, NMASs of 9.5, 12.5, and 19.0 mm were utilized. The three Superpave gradations included one gradation that passed near the upper gradation control limits and above the restricted zone (ARZ), one that resided near the maximum density line and passed through the restricted zone (TRZ), and one that passed near the lower gradation control limits and below the restricted zone (BRZ). This resulted in a total of 36 mix designs.

The property selected to define lift thickness in this experiment was the ratio of thickness to NMAS (t/NMAS). This ratio was selected for two reasons: (1) the ratio normalizes lift thickness for any type of gradation and (2) a general rule-of-thumb for Superpave mixes has been a t/NMAS ratio of 3.0 be used during construction (10). For each NMAS in the experiment, three t/NMAS ratios were investigated. For the 9.5 and 19.0 mm NMAS Superpave mixes and all three SMA NMASs (9.5, 12.5, and 19.0 mm), t/NMAS ratios of 2.0, 3.0, and 4.0 were used. Additional ratios of 8.0 and 6.0 for 9.5 and 12.5 mm NMAS, respectively, were also evaluated to better define the relationship where air voids reach a limiting value (approximately 4.0 percent air voids). For the 37.5 mm NMAS Superpave mixes, ratios of 2.0, 2.5, and 3.0 were investigated. The 4.0 t/NMAS was excluded for the 37.5 mm NMAS mixes since this ratio would produce a 150 mm (6 in.) lift thickness which is unlikely to be used in the field. The desired thicknesses of samples (2.0, 2.5, 3.0, 4.0, 6.0 and 8.0 t/NMAS) were achieved by altering the mass

placed in the mold prior to compaction (as mass changes for a given compactive effort, thickness will change). All samples were short-term aged prior to compaction according to "Standard Practice for Mixture Conditioning of HMA", AASHTO PP2-01. This procedure simulates aging of mixture during production and placement.

Three replicates of each aggregate-gradation-NMAS-thickness combination were compacted using a single Superpave gyratory compactor. For the Superpave mixes, each sample was compacted to 100 gyrations, the upper limit that most state DOTs use. The 100-gyration level was selected because it is probably the compactive effort that presents the most difficulty in obtaining adequate density. For the SMA mixes, each sample was compacted to 75 gyrations in the Superpave gyratory compactor in accordance with the "Standard Practice for Designing SMA", AASHTO PP44-01. The reason for using 75 gyrations was that all the aggregate types had Los Angeles abrasion values of more than 30 percent. Cellulose fiber was used as the fiber within the SMA mixes at 0.3 percent of total mass. Designs were conducted to determine the asphalt binder content necessary to produce 4.0 percent air voids at the design number of gyrations. Testing of each sample after compaction included measuring the bulk specific gravity of each replicate using both AASHTO T166 and the vacuum sealing method. A standard test method has been developed for the vacuum sealing method, ASTM D6752-02a, "Bulk Specific Gravity and Density of Compacted Bituminous Mixtures Using Automatic Vacuum Sealing Method." A statistical analysis of the data was then conducted.

3.1.2 Evaluation of Effect of t/NMAS on Density Using Vibratory Compactor

To further evaluate the relationship between density and lift thickness, a similar

study was conducted but on a smaller scale, using the vibratory compactor as the compaction mode. This was not part of the original proposed work but it was believed that the vibratory compactor might provide compaction that has more typical of in-place compaction. Of the 36 mix designs from Part 1, 14 mixes were selected for this study. Two types of aggregates, granite and limestone were used. For Superpave designed mixes, two gradations were utilized (ARZ and BRZ) along with two NMASs (9.5 mm and 19.0 mm). The 37.5 mm NMAS mix was excluded from the study because the maximum thickness of the vibratory specimen that could be obtained was 75.0 mm, which would only be 2.0 t/NMAS. For the SMA mixes, three NMASs were selected (9.5 mm, 12.5 mm and 19 mm). The t/NMAS ratios utilized were 2.0, 3.0 and 4.0. The compactive effort for each t/NMAS was varied over a range including 30 sec, 60 sec, and 90 sec of compaction. The range of compactive efforts was selected for two reasons: (1) there is no standard compactive effort for the vibratory compactor and (2) the effects of compactive effort on density at different thicknesses could be evaluated. After compaction, the bulk specific gravity was measured and the data was analyzed to provide recommendations concerning the minimum t/NMAS.

3.1.3 Evaluation of Effect of t/NMAS on Density Using Field Experiment

NCAT also conducted a field study to evaluate the acceptable minimum lift thickness. Through the field experiments, the following issues were also evaluated to strengthen the conclusions of this study: 1) How does lift thickness affect the compactibility of HMA mixes, and 2) What effect does a pneumatic tire roller have on density as compared to a steel drum roller?

Seven mixes from the 2003 NCAT Test Track study were selected consisting of the NMASs, gradations, and mix types (Superpave and SMA) shown in Table 1.

Table 1: Mix Information for Field Density Study

Section	NMAS	Gradation	Asphalt Type	Aggregate Type
1	9.5 mm	Fine-Graded Superpave	Unmodified	Granite and Limestone
2	9.5 mm	Coarse-Graded Superpave	Unmodified	Limestone
3	9.5 mm	SMA	Modified	Granite
4	12.5 mm	SMA	Modified	Limestone
5	19.0 mm	Fine-Graded Superpave	Unmodified	Granite and Limestone
6	19.0 mm	Coarse-Graded Superpave	Unmodified	Granite
7	19.0 mm	Coarse-Graded Superpave	Modified	Limestone

The experiment was conducted during the trial mixing stage and included the construction of each section with t/NMAS ratios ranging from approximately 2.0 to 5.0 on the seven sections at the NCAT track facilities. The desired mat thicknesses were achieved by gradually adjusting the screed depth crank of the paver during the laydown operation. To investigate the effect of lift thickness on the rate of cooling in the mat and to ensure the mat was being compacted within the time available for compaction, three locations were selected for temperature measurements for each section; one at the beginning of the section, one at the middle and one at the end of the section. At each location, two thermocouples were placed in the mat immediately after placement and prior to compaction as shown in Figure 4. Surface temperatures were also obtained with an infrared temperature gun. Temperature readings were monitored and recorded every

few minutes and after every roller pass. The air and base temperatures at time of placement, as well as the weather conditions, were also recorded.

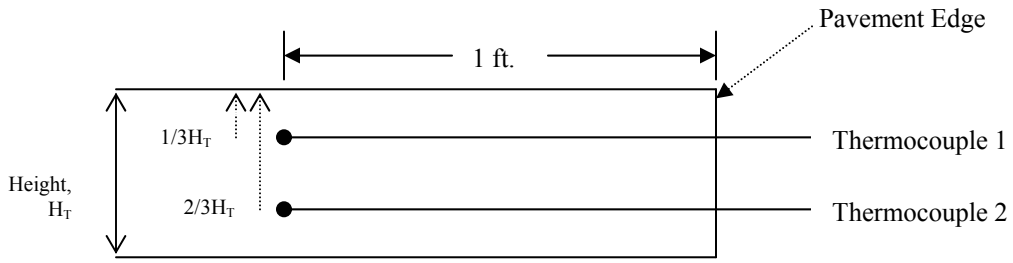

Figure 4: Thermocouple Location in Asphalt Mat

Reasonable and consistent compactive effort was applied throughout the section regardless of the t/NMAS. To study the effect of roller type on density, one side of the mat utilized only a steel drum compactor and the other side incorporated a pneumatic tire roller as an intermediate roller. The steel drum roller operated in both vibratory and static modes. A non-destructive density gauge (Pavement Quality Indicator (PQI)) was used to monitor the density after each pass with the rollers and to determine the rate of densification for the various thicknesses.

A minimum of twelve test locations (at increasing t/NMAS) per compactive effort (steel wheel or pneumatic tire) was selected for testing. At each test location, one field core was obtained approximately 2 ft from the pavement edge. This equated to a total of at least 12 cores for each compactive effort and a total of at least 24 cores for one section (when both roller types were used). The cores obtained were used to determine in-place density, and thickness.

3.1.4 Evaluation of Effect of Temperature on Relationship Between Density and t/NMAS from Field Experiment

Recall from the field experiment that three locations were selected for temperature measurements for each section; one near the beginning of the section, one near the middle, and one near the end of section. This was done because the rate of cooling varied from one end to the other due to change of thickness. The rate of cooling was determined by plotting the average temperature from each location against time. To determine the effect of temperature on the density, the temperature at 20 minutes after placement of mix was selected. This number is somewhat arbitrary but it is realistic because in general, the compaction in the field should be obtained within approximately 20 minutes after paving. Since the mixes in this study used two different types of asphalt binder, (PG 67-22 and PG 76-22), the temperatures at 20 minutes were normalized by subtracting the high temperature grade of the asphalt binder from the measured mat temperatures at 20 minutes. For instance, if the temperature at 20 minutes was 100^{o}C for a mix using PG 67-22, the difference of the temperature was 33^{o}C (100^{o}C – 67^{o}C). This was done because in general the higher PG binder (PG 76-22) would require a higher compaction temperature and hence it is the difference in the mix temperature and the high temperature PG grade that affects compaction.

3.1.5 Evaluation of Effect of t/NMAS on Permeability Using Gyratory Compactor

To investigate the permeability characteristics of HMA at different thicknesses, the same 14 mixes used in the experiment to determine the effect of t/NMAS on density using vibratory compactor were utilized. The gyratory compactor height for t/NMAS

ratios of 2.0, 3.0, and 4.0 was determined and samples were compacted with appropriate mass to produce 7.0 ± 1 percent air voids. The 7.0 percent air voids was selected to simulate the density of a pavement in the field after construction. The bulk specific gravity was measured using the vacuum seal method. Permeability tests were performed on all samples and the relationships between permeability and lift thickness evaluated.

3.1.6 Evaluation of Effect of t/NMAS on Permeability Using Vibratory Compactor

For this study, the same 14 mixes used in the previous vibratory compactor study were utilized. T/NMAS ratios of 2.0, 3.0, and 4.0 were used and two beams of each aggregate-gradation-t/NMAS combination were compacted to 7.0 ± 1 percent air voids. Two 100 mm cores were cut from the beams. Bulk specific gravity for beams and cores was determined using the vacuum seal method. Permeability tests were performed on all core samples and the relationships between permeability and lift thickness evaluated.

3.1.7 Evaluation of the Effect of t/NMAS on Permeability Using Field Experiment

The seven sections constructed to determine the minimum t/NMAS from the field experiment were utilized in this study. The effect of roller type on permeability was also evaluated. A minimum of twelve test locations per compactive effort (steel wheel or pneumatic tire) was selected for testing. Two field permeability tests were performed at the locations where the cores were obtained as shown in Figure 5. Laboratory permeability testing was also performed on the cores obtained from each section. This was done to evaluate the relationships between laboratory and field permeability tests.

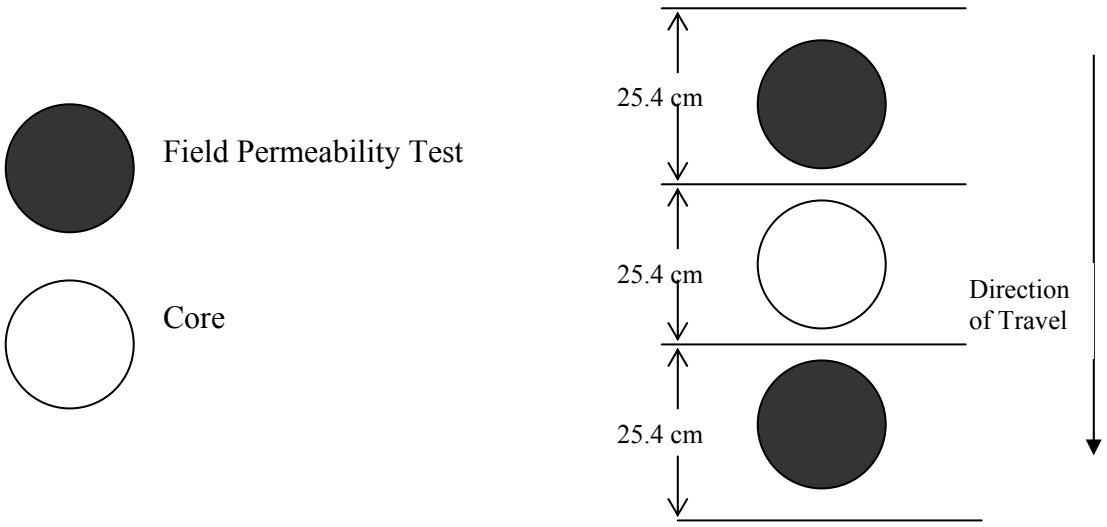

Figure 5: Testing Conducted at Each Test Location.

3.2 Part 2 Experimental Plan – Evaluation of Relationship of Laboratory Permeability, In-place Air Voids, and Lift Thickness of Field Compacted Cores (NCHRP 9-9(1))

Part 2 evaluated the relationship between in-place air voids and laboratory permeability. Figure 2 illustrates the research approach to evaluate this relationship. A total of 40 on-going HMA construction projects were visited by NCAT during NCHRP 9-9(1) "Verification of Gyration Levels in the N_{des} Table". Five different combinations of gradation shape and NMAS were studied: fine-graded 9.5 mm, 12.5 mm, and 19.0 mm NMAS mixes and coarse-graded 9.5 mm and 12.5 mm NMAS mixes. At each of the projects, cores were obtained from the roadway after construction but before traffic so that the actual lift thickness and in-place air voids could be determined. Cores brought back to the laboratory from NCHRP 9-9(1) field projects were sawed and tested for bulk specific gravity (AASHTO T 166 and the vacuum seal methods), thickness, and

laboratory permeability (ASTM PS 129-01). Plant-produced mix was also sampled at each project in order to determine the theoretical maximum density (TMD) and the mixture gradation. The TMD test was performed according to AASHTO T209.

4.0 MATERIALS AND TEST METHODS

4.1 Aggregate and Binder Properties

Properties of the coarse and fine aggregates utilized in the laboratory experiments of Part 1 study are shown in Table 2. The aggregates were selected to represent a range of physical properties, such as bulk specific gravity (2.585 to 2.725), flat and elongated particles (4 to 14 percent at 3:1), Los Angeles abrasion (31 to 37 percent), coarse aggregate angularity (42.9 to 44.0 percent), and fine aggregate angularity (45.7 to 49.4 percent). This variability in aggregate properties, while not very different, should provide some variability of mix properties.

Table 3 presents the test results for the asphalt binder utilized in the study. The binder was classified as PG 64-22 and is commonly used for warm to moderate climates. The binder met high temperature property criteria at a temperature of 67^{o}C and so can be classified as a PG 67-22.

Table 2: Physical Properties of Aggregate

Property		Test Method	Aggregate Type		
			Granite	**Limestone**	**Crushed Gravel**
Coarse Aggregate					
Bulk Specific Gravity		AASHTO T-85	2.654	2.725	2.585
Apparent Specific Gravity		AASHTO T-85	2.704	2.758	2.642
Absorption (%)		AASHTO T-85	0.7	0.4	0.9
Flat and Elongated (%), 3:1, 5:1	19.0 mm	ASTM D4791	14, 0	10, 0	4, 0
	12.5 mm		16, 0	6, 0	16, 2
	9.0 mm		9, 1	16, 3	19, 2
Los Angeles Abrasion (%)		AASHTO T-96	37	35	31
Coarse Aggregate Angularity (%)		AASHTO TP56-99	42.9	43.0	44.0
Percent Crushed (%)		ASTM D5821	100	100	80
Fine Aggregate					
Bulk Specific Gravity		AASHTO T-84	2.678	2.689	2.610
Apparent Specific Gravity		AASHTO T-84	2.700	2.752	2.645
Absorption (%)		AASHTO T-84	0.3	0.9	0.5
Fine Aggregate Angularity (%)		AASHTO T-33 (Method A)	49.4	45.7	48.8
Sand Equivalency (%)		AASHTO T-176	92	93	94

4.2 Aggregate Gradations

The laboratory experiments included four gradation shapes and three nominal maximum aggregate sizes (NMAS). Three gradations fell within the Superpave gradation control points and one gradation conformed to stone matrix asphalt specifications. The mix gradations used are illustrated in Figures 6 through 9.

Table 3: Asphalt Binder Properties

Original Binder		
Properties		**Results**
Specific Gravity		1.028
Flash Point, ^{o}C		313
Viscosity, Pa.s	@ 135^{o}C	0.400
	@ 163^{o}C	0.119
	@ 190^{o}C	0.049
G*/sin δ, kPa @ 67^{o}C		1.078
Rolling Thin Film Oven Aged		
Loss. %		0.08
G*/sin δ, kPa @ 67^{o}C		2.279
Rolling Thin Film Oven Aged + Pressure Aging Vessel Residue		
G*/sin δ, kPa @ 25^{o}C		4752
Stiffness, Mpa		226
m-value		0.325

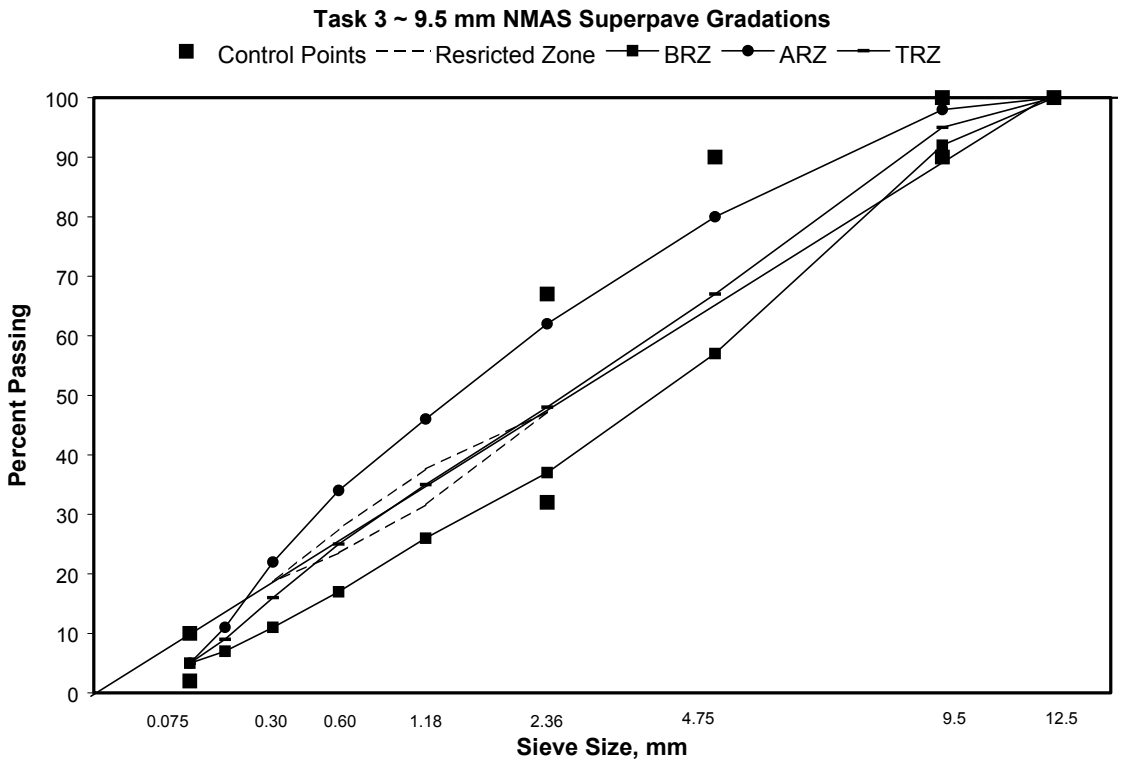

Figure 6: 9.5 mm NMAS Superpave Gradations

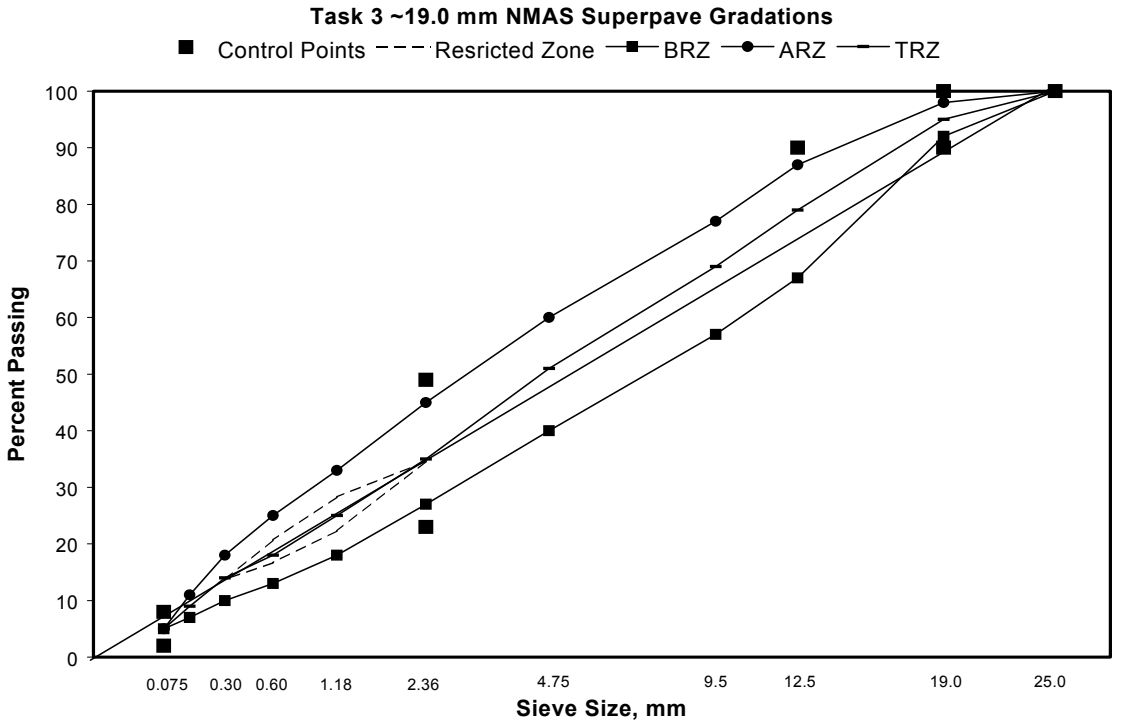

Figure 7: 19.0 mm NMAS Superpave Gradations

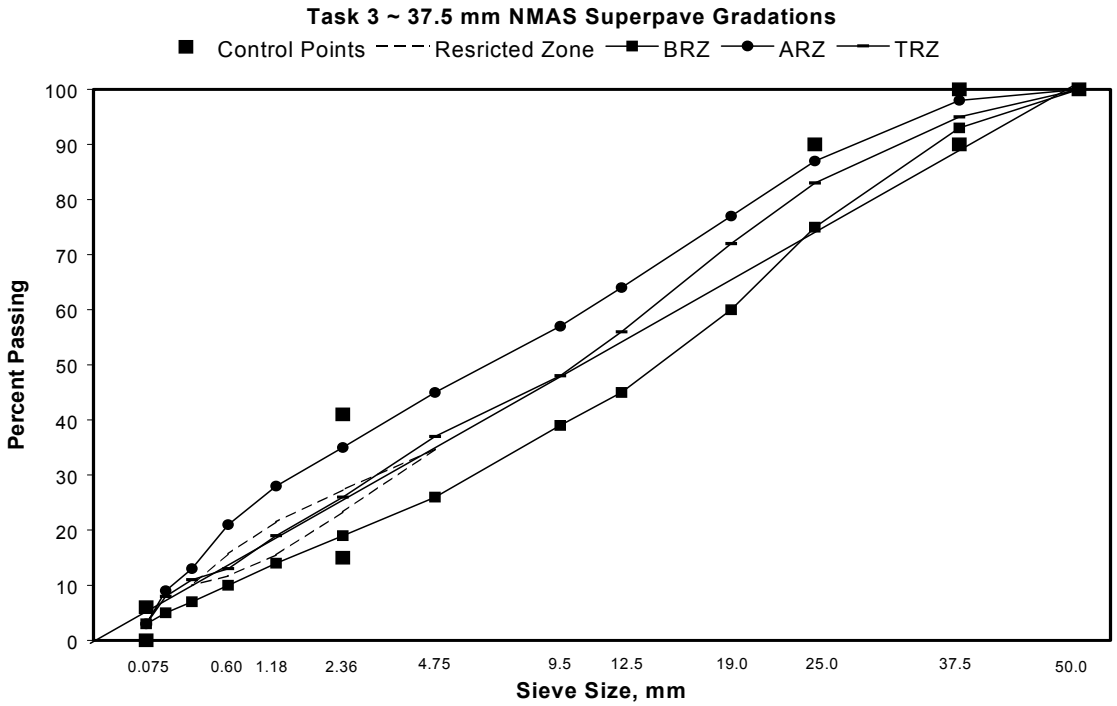

Figure 8: 37.5 mm NMAS Superpave Gradations

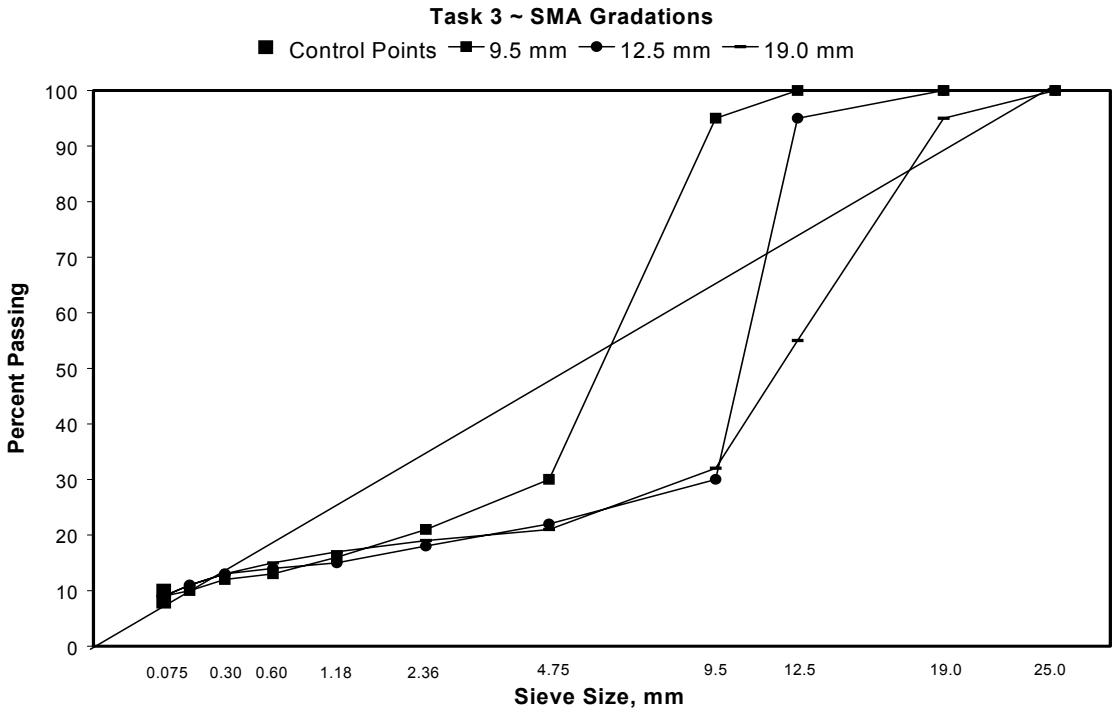

Figure 9: SMA gradations

The field experiment involved seven sections that included three gradation shapes and three NMASs. The section mix information is presented in Table 4. The information includes the gradation for each mix and asphalt content determined from samples from the ignition test, and the volumetric properties i.e. voids in total mix (VTM), voids in mineral aggregate (VMA), voids filled with asphalt (VFA). These were trial mixes and the volumetrics did not always meet the 4 percent air voids requirement. Based on these results mixes were adjusted to be closer to 4 percent air voids prior to placement on the test track. Some of the aggregate gradations also were different than the desired

Table 4: Mix Information for Seven Mixes Used in Field Study

Mix	**9.5 mm FG**	**9.5 mm CG**	**9.5 mm SMA**	**12.5 mm SMA**	**19 mm FG**	**19 mm CG**	**19 mm CG (Mod. AC.)**
Sieve, mm	Percent Passing on Each Sieve						
25	100	100	100	100	100	100	100
19	100	100	100	100	96.7	100	89.6
12.5	100	100	99.6	93.8	90.5	88.4	65
9.5	100	99.9	99.6	74.5	82.7	77.9	53.1
4.75	80.9	78.7	42.1	36.2	68.1	46.2	30.7
2.36	62.1	50.9	21.6	22.3	60.2	29.8	23.1
1.18	49.4	39.4	17.3	16.2	52.2	24	19.6
0.6	36.8	29.3	14.2	13.2	41.5	19.9	16.8
0.3	21	21.1	10.8	11.6	25.1	14.5	9.9
0.15	11.9	14.2	8.1	10.7	15.4	9.1	6.5
0.075	7.2	8.7	5.8	9.6	9.6	5.7	5.0
AC Content, %	6.3	6.2	7.0	6.5	5.2	4.8	4.0
VTM, %	3.6	2.7	6.0	6.1	5.3	2.1	3.7
VMA, %	17.9	13.9	20.4	18.3	16.1	14.2	9.6
VFA, %	79.9	80.4	70.4	66.5	67.3	84.8	60.9

FG- Fine-Graded, CG- Coarse-Graded, AC- Asphalt Cement

gradation, however, it was believed that this wide range of mix types would give a good overall measure of the effect of t/NMAS on density and permeability.

4.3 Determination of Bulk Specific Gravity

The bulk specific gravity of all compacted samples was measured using both AASHTO T166 and vacuum seal device. For AASHTO T166, Method A was utilized. This consists of weighing a dry sample in air, then obtaining a submerged mass after the sample has been placed in a water bath for 4 ± 1 minutes. Upon removal from the water bath, the SSD mass is determined after blotting the sample dry as quickly as possible using a damp towel.

The vacuum seal method was performed in accordance with ASTM D 6752 – 02a, "Standard Test Method for Bulk Specific Gravity and Density of Compacted Bituminous Mixtures Using Automatic Vacuum Sealing Method". It consists of a vacuum-sealing device utilizing an automatic vacuum chamber with a specially designed, puncture resistant plastic bag, which tightly conforms to the sides of the sample and prevents water from infiltrating into the sample. The procedure involved in sealing and analyzing the compacted sample was as follows:

Step 1: Determine the density of the plastic bag (generally manufacturer provided).

Step 2: Place the compacted sample into the bag.

Step 3: Place the bag containing the sample inside the vacuum chamber.

Step 4: Close the vacuum chamber door. The vacuum pump starts automatically and evacuates the chamber.

Step 5: In approximately two minutes, the chamber door automatically opens with

the sample completely sealed within the plastic bag and ready for water displacement testing.

Step 6: Perform water displacement method. Correct the results for the bag density and the displaced bag volume.

4.4 Determination of Permeability

Laboratory permeability tests were conducted in accordance with ASTM PS 129-01, Standard Provisional Test Method for Measurement of Permeability of Bituminous Paving Mixtures Using a Flexible Wall Permeameter. This method utilizes a falling head approach for measuring permeability. Each core was vacuum-saturated for five minutes prior to testing. Water from a graduated standpipe was allowed to flow through the saturated sample and the time to reach a known change in head recorded. Saturation was considered sufficient when the variation between four consecutive time interval measurements was relatively small; in this case all within 10% of the mean. Darcy's Law is then applied to estimate permeability of the sample.

The field permeability testing was performed using the NCAT Field Permeameter. This device has been shown to compare reasonably well with laboratory permeability tests and produce a reasonable relationship with in-place air voids in a pavement.

4.5 Part 2 – Evaluation of Relationship of Laboratory Permeability, Density and Lift Thickness of Field Compacted Cores

Of the 40 different Superpave projects visited during NCHRP 9-9(1), three projects were omitted for the purpose of this study due to damaged samples. A total of

287 usable cores were obtained from the 37 projects. All cores were cut from the roadway prior to traffic. Information about the projects is presented in Table 5. Of the 37 projects, 11 projects utilized a 9.5 mm NMAS gradation, 23 projects utilized a 12.5 mm NMAS gradation, and 3 projects utilized a 19.0 mm NMAS gradation. Gradations for all the mixes are illustrated in Figures 10 through 12, by NMAS from 9.5 to 19.0 mm, respectively. For the purposes of this report, projects were identified as fine-graded or coarse-graded according to the definition given by National Asphalt Pavement Association (NAPA)(11). Percent passing certain sieve sizes for a given NMAS is used to define fine- and coarse-graded mixes as shown in Table 6. Average lift thicknesses for the different projects ranged from 22.3 to 78.8 mm and the N_{des} ranged from 50 to 125 gyrations with a Superpave gyratory compactor.

5.0 TEST RESULTS AND ANALYSIS

5.1 Part 1 - Mix Designs

Of the 36 mix designs, 27 were Superpave designed mixes and 9 were SMA mixes. The optimum asphalt content, the effective asphalt content (P_{be}), voids in mineral aggregate (VMA), voids filled with asphalt (VFA), percent theoretical maximum density at $N_{initial}$ (% G_{mm} at Nini), ratio of dust to effective asphalt content ($P_{0.075}/P_{be}$) for the Superpave mixtures summarized in Table 7; data for SMA mixes is shown in Table 8. The mix design information for both mix types is presented in Appendix A. Optimum asphalt binder content was chosen to provide 4 percent air voids at the design number of gyrations. However, for the 19 mm NMAS limestone SMA mix 4 percent air voids could be achieved with 5.7 percent asphalt content which did not meet the minimum asphalt

Table 5: Project Mix Information

Project No.	NMAS, (mm)	Gradation	Asphalt Performance Grade	N_{des}	Average Thickness, (mm)
1	9.5	Coarse	67 - 22	86	34.3
2	9.5	Coarse	70 - 22	90	40.5
3	9.5	Coarse	70 - 22	90	44.5
4	9.5	Coarse	70 - 22	105	45.7
5	9.5	Coarse	64 - 22	50	31.2
6	9.5	Coarse	76 - 22	100	33.9
7	9.5	Coarse	58 - 22	125	34.9
8	9.5	Coarse	64 - 22	100	44.1
9	9.5	Coarse	70 - 28	100	22.3
10	9.5	Fine	58 - 28	75	40.5
11	9.5	Fine	58 - 28	75	32.4
12	12.5	Coarse	67 - 22	106	39.9
13	12.5	Coarse	67 - 22	100	42.4
14	12.5	Coarse	76 - 22	100	38.0
15	12.5	Coarse	67 - 22	75	33.7
16	12.5	Coarse	76 - 22	125	53.5
17	12.5	Coarse	76 - 22	125	51.0
18	12.5	Coarse	76 - 22	125	52.8
19	12.5	Coarse	76 – 22	125	56.8
20	12.5	Coarse	76 – 28	109	50.6
21	12.5	Coarse	64 – 28	86	47.6
22	12.5	Coarse	76 – 22	100	44.1
23	12.5	Coarse	70 – 22	125	51.1
24	12.5	Coarse	64 – 22	100	78.8
25	12.5	Coarse	70 – 22	125	48.4
26	12.5	Coarse	70 – 28	100	36.3
27	12.5	Fine	64 – 28	86	53.3
28	12.5	Fine	64 – 28	86	44.3
29	12.5	Fine	76 – 22	125	45.8
30	12.5	Fine	64 – 22	68	39.8
31	12.5	Fine	64 – 22	76	51.2
32	12.5	Fine	70 – 28	109	55.2
33	12.5	Fine	70 – 22	100	34.8
34	12.5	Fine	64 – 34	75	38.7
35	19	Fine	67 - 22	95	33.0
36	19	Fine	58 - 28	68	49.6
37	19	Fine	64 - 22	96	48.7

Table 6: Definition of Fine-and Coarse-Graded Mixes (11)

Mixture NMAS	**Coarse-Graded**	**Fine-Graded**
37.5 mm (1 ½")	<35 % Passing 4.75 mm Sieve	>35 % Passing 4.75 mm Sieve
25.0 mm (1")	<40 % Passing 4.75 mm Sieve	>40 % Passing 4.75 mm Sieve
19.0 mm (3/4")	<35 % Passing 2.36 mm Sieve	>35 % Passing 2.36 mm Sieve
12.5 mm (1/2")	<40 % Passing 2.36 mm Sieve	>40 % Passing 2.36 mm Sieve
9.5 mm (3/8")	<45 % Passing 2.36 mm Sieve	>45 % Passing 2.36 mm Sieve
4.75 mm (No. 4 Sieve)	N/A (No standard Superpave gradation)	

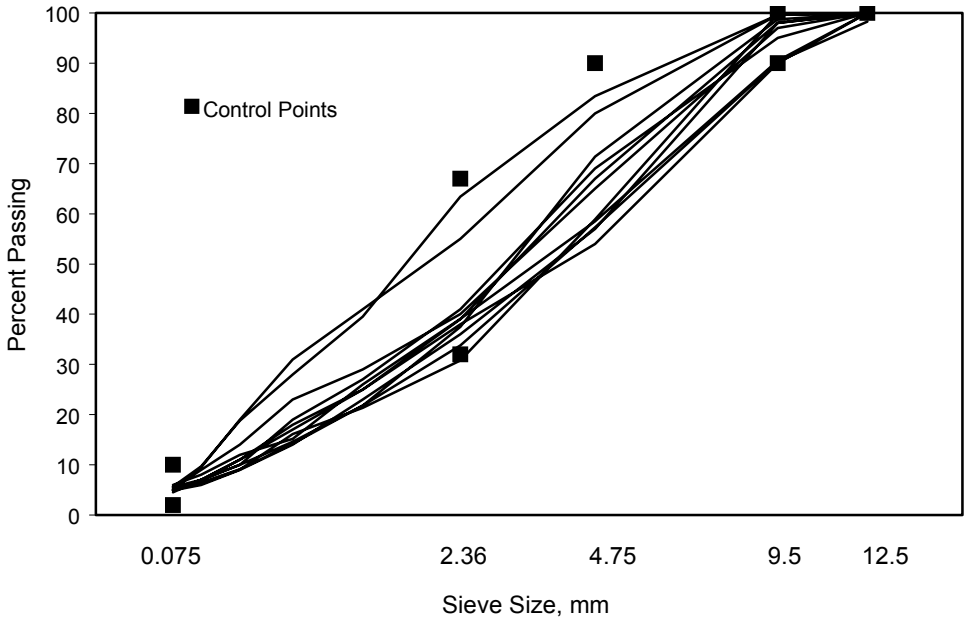

Figure 10: Plot of 9.5 mm NMAS gradations

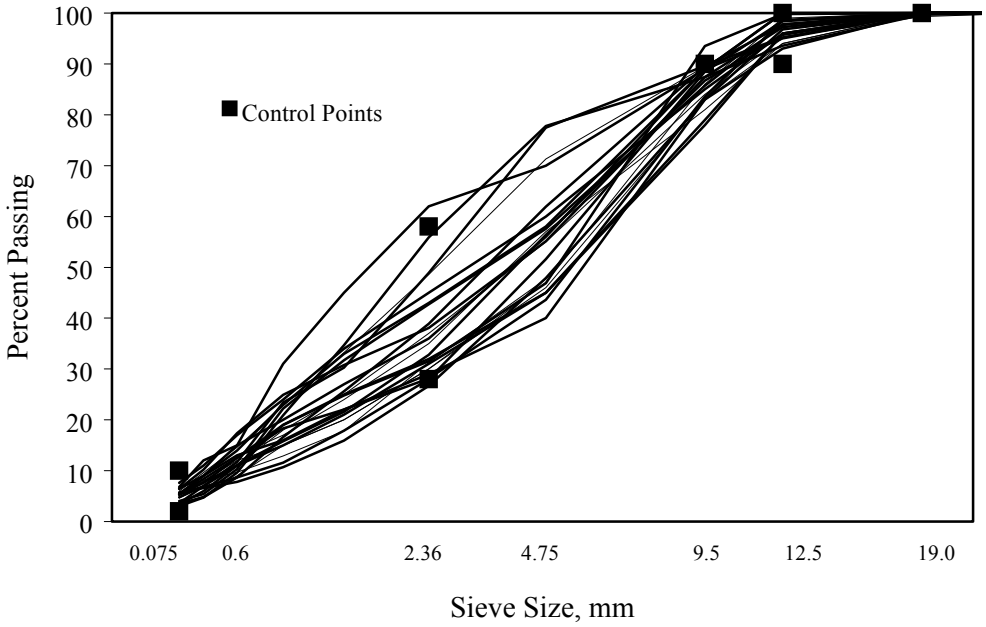

Figure 11: Plot of 12.5 mm NMAS gradations

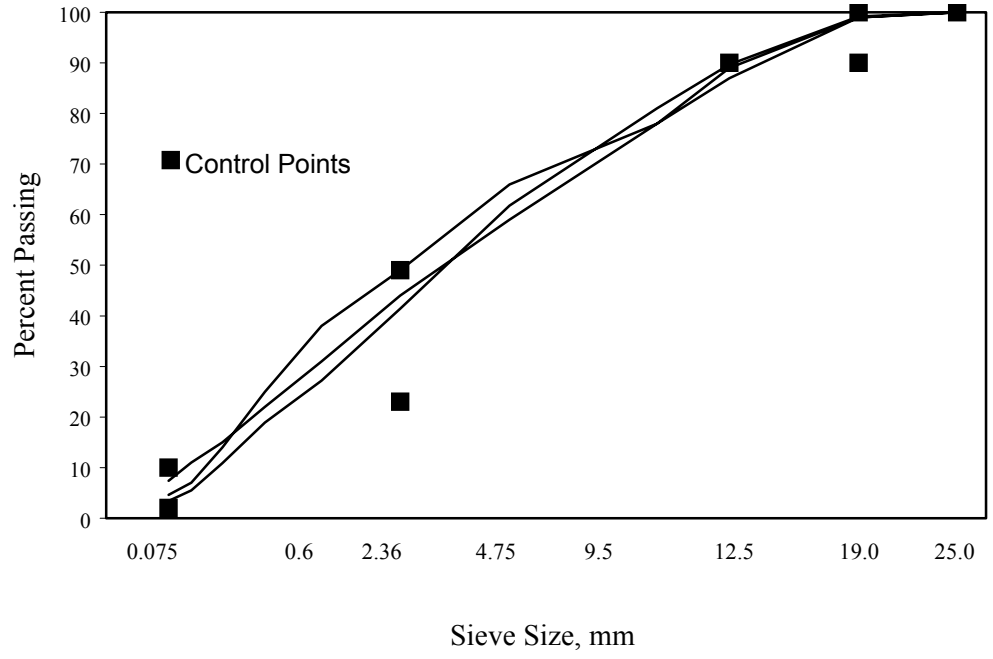

Figure 12: Plot of 19.0 mm NMAS gradations

Table 7: Summary of Mix Design Results for Superpave Mixes

Aggregate	NMAS, mm	Gradation	Optimum Asphalt, %	P_{be}, %	VMA %	VFA %	% G_{mm} at N_{ini}	$P_{0.075}/P_{be}$
Granite	9.5	ARZ	6.7	6.2	18.4	76	89.0	0.8
	9.5	BRZ	5.3	4.9	15.7	73	86.7	1.0
	9.5	TRZ	5.4	5.0	15.6	75	88.9	1.0
	19.0	ARZ	4.7	4.3	14.1	72	89.5*	1.2
	19.0	BRZ	4.4	3.9	13.3	68	86.0	1.0
	19.0	TRZ	4.0	3.6	12.5*	68	88.8	1.4*
	37.5	ARZ	4.2	4.0	13.7	69	89.8*	0.8
	37.5	BRZ	3.3	3.0	11.3	64	86.8	1.0
	37.5	TRZ	3.6	3.3	12.0	65	88.1	0.9
Gravel	9.5	ARZ	6.7	6.5	18.3	78*	88.4	0.8
	9.5	BRZ	6.2	5.6	16.7	75	86.5	0.8
	9.5	TRZ	6.0	5.4	16.3	75	87.7	0.9
	19.0	ARZ	4.9	4.4	14.0	72	88.5	1.1
	19.0	BRZ	4.5	3.9	12.9*	69	86.3	1.3*
	19.0	TRZ	4.4	3.8	12.8*	69	88.0	1.3*
	37.5	ARZ	4.4	3.9	13.0	70	89.7*	0.8
	37.5	BRZ	3.6	3.2	11.7	63	85.5	1.0
	37.5	TRZ	3.9	3.5	12.0	66	85.6	0.9
Limestone	9.5	ARZ	6.0	5.7	17.4	76	87.8	0.7
	9.5	BRZ	5.0	4.6	15.3	72*	85.5	0.9
	9.5	TRZ	4.4	4.2	14.4	70*	86	1.2
	19.0	ARZ	4.1	3.5	12.6*	66	88.3	1.4*
	19.0	BRZ	4.7	4.4	14.3	71	85.5	0.7
	19.0	TRZ	3.3	2.8	11.0*	62*	85.7	1.8*
	37.5	ARZ	3.2	3.1	11.8	64	88.8	1.0
	37.5	BRZ	2.7	2.6	10.6*	60*	86.0	1.2
	37.5	TRZ	2.8	2.6	10.6*	61*	87.7	1.1

*- Did not meet Superpave Design Requirements

content requirement in accordance with the "Standard Practice for Designing SMA", AASHTO PP44-01. Therefore, the minimum asphalt content of 6.0 percent was chosen which resulted in 3.7 percent air voids at the design number of gyrations. Some designs did not meet the requirements for one or more of VMA, VFA, % G_{mm} at N_{ini} and dust/P_{be}. Efforts were made to redesign the respective mixes by changing the gradation until the requirements were met or at least very close to the requirements. This is

important in that the mixes used in this project were intended to duplicate mixes utilized in the field. The adjusted gradations are presented in Tables 9 to 11. However, no modification was made for the TRZ mixes that did not meet the requirements because little could be done to modify gradations and still maintain the gradations passing through the restricted zone.

Table 8: Summary of Mix Design Results for SMA Mixes

Aggregate	NMAS, mm	Optimum Asphalt, %	P_{be}, %	VMA, %	VFA, %	VCA_{mix}, %	VCA_{drc}, %
Granite	9.5	7.2	6.6	18.7	78	30.9	41.9
	12.5	6.6	6.4	18.8	77	30.3	42.7
	19.0	6.4	5.9	17.6	77	29.6	42.0
Gravel	9.5	7.3	6.5	18.6	77	30.4	41.8
	12.5	6.8	6.1	17.7	77	31.1	42.1
	19.0	6.7	6.2	17.8	76	29.3	42.0
Limestone	9.5	6.2	5.8	17.4	76	30.7	38.4
	12.5	7.4	7.0	19.6	80	31.1	38.9
	19.0	6.0	5.6	16.8*	77	29.8	40.3

*- Did not meet SMA Design Requirements

Table 9: Change of Gradation for 9.5 mm NMAS Superpave Mixes

Sieve, mm	Original ARZ Gradation	Adjusted ARZ Limestone	Original Grad. BRZ	Adjusted BRZ Limestone
12.5	100	100	100	100
9.5	98	98	92	92
4.75	80	85	57	67
2.36	62	64	37	35
1.18	46	48	26	23
0.6	34	36	17	15
0.3	22	24	11	9
0.15	11	10	7	6
0.075	5	4	5	4

Table 10: Change of Gradation for 19.0 mm NMAS Superpave Mixes

Sieve, mm	Original ARZ Gradation	Adjusted ARZ Limestone	Original BRZ Gradation	Adjusted BRZ Granite	Adjusted BRZ Limestone
25	100	100	100	100	100
19	98	94	92	92	98
12.5	87	77	67	75	83
9.5	77	67	57	54	68
4.75	60	52	40	37	40
2.36	45	43	27	25	26
1.18	33	35	18	15	15
0.6	25	26	13	11	11
0.3	18	15	10	8	8
0.15	11	9	7	6	6
0.075	5	3	5	4	3

Table 11: Change of Gradation for SMA Mixes

Sieve, mm	Original 12.5 mm SMA	Adjusted 12.5 mm SMA Granite	Adjusted 12.5 mm SMA Limestone	Original 19.0 mm SMA	Adjusted 19.0 SMA
25	100	100	100	100	100
19	100	100	100	95	100
12.5	95	98	98	55	85
9.5	50	50	80	32	26
4.75	22	20	20	21	20
2.36	18	16	16	19	17
1.18	15	14	14	17	16
0.6	14	12	12	15	14
0.3	13	11	11	13	12
0.15	11	10	10	11	10
0.075	9	8	8	9	8

5.2 Evaluation of Effect of t/NMAS on Density Using Gyratory Compactor

Before the evaluation was done to evaluate the effect of t/NMAS on density, the proper method to measure the density was evaluated. Bulk specific gravity for all samples was measured using the AASHTO T166 (SSD) and vacuum sealing (vacuum seal device) methods. The average for the measured thickness, SSD air void contents, vacuum seal device air void contents, and water absorption are summarized by aggregate type in Tables 12 through 14. The results show that as the thickness increases the air void content decreases. For all mix types, there appears to be a difference between the air voids measured by SSD and vacuum seal device. The variations become more significant for samples having higher air void contents that involve coarse–graded and SMA mixes. The average water absorption values increase as the air void content increases. For coarse-graded and SMA mixes, in most cases, the average water absorption values exceeded the 2.0 percent threshold limit.

Figures 13 through 16 illustrate the relationships between the average air voids for the three aggregate types determined from the two methods of measuring bulk specific gravity with respect to gradation of the mixes. The data from this experiment are included in Appendix B. Figure 13 presents the relationships for the ARZ gradation mixes. Based upon this figure, the air voids using the two methods are approximately equal at low air voids and deviate by approximately 0.5 percent at the highest air void level. This figure indicates that for ARZ mixes the two methods provide similar results. Figures 14 through 16 illustrate the relationships between air voids for TRZ, BRZ, and SMA mixes, respectively. The results from the figures suggest that as density decreases the bulk specific gravity measurements for the two methods become farther apart. The

results also indicate that as the gradation becomes coarser the data deviates farther from the line of equality. This finding agrees with the research by Cooley et al. (12) when comparing the two methods. The apparent reason for the difference in the two test methods is loss of water during density measurement and the surface texture. The loss of water when blotting will result in a higher measured density than the actual density. The surface texture can result in the vacuum seal device measuring a lower density than the actual density. Since the vacuum seal device gives a good estimation of density at lower air voids (this indicates that the surface texture does not affect the results), it is also expected to provide good estimation at higher air voids (since the plastic sealer does not penetrate the voids within the mixture. Therefore, for this study, the density determined from the vacuum seal device was used in the analysis (More discussion on density measurement is provided in Volume II of this report).

Table 12: Results for Granite Mixes

NMAS, mm	Gradation	T/NMAS	Average Thickness, mm	Average SSD Air Voids, %	Average Vacuum Seal Air Voids, %	Average Water Abs.,%
9.5	ARZ	2.0	20.5	11.0	11.9	0.7
		3.0	29.3	9.1	9.7	0.4
		4.0	38.0	5.9	6.2	0.1
		8.0	75.1	4.2	4.2	0.0
9.5	BRZ	2.0	20.9	12.6	15.1	4.7
		3.0	30.1	8.4	10.0	1.1
		4.0	40.0	6.8	8.0	0.5
		8.0	76.7	4.5	4.9	0.1
9.5	TRZ	2.0	21.4	14.5	16.0	3.1
		3.0	31.0	11.3	12.4	1.5
		4.0	40.5	9.1	10.0	0.9
		8.0	75.6	4.5	5.1	0.2
9.5	SMA	2.0	21.9	11.2	18.2	6.7
		3.0	30.9	10.2	14.1	5.1
		4.0	39.4	9.3	11.6	3.2
		8.0	77.7	4.8	5.7	0.7
12.5	SMA	2.0	26.7	9.2	17.6	5.2
		3.0	39.1	8.6	15.0	5.1
		4.0	52.3	8.0	12.9	4.1
		6.0	76.3	6.2	8.4	1.8
19	ARZ	2.0	39.6	6.3	6.9	0.4
		3.0	58.3	4.3	4.6	0.2
		4.0	76.9	4.1	4.4	0.2
19	BRZ	2.0	40.7	8.6	11.3	2.7
		3.0	59.0	6.5	8.2	1.2
		4.0	77.5	5.4	6.2	0.8
19	TRZ	2.0	39.7	6.5	7.6	0.9
		3.0	58.6	4.9	5.7	0.6
		4.0	77.3	4.1	4.8	0.5
19	SMA	2.0	39.2	6.8	13.0	3.4
		3.0	58.8	6.1	10.9	2.0
		4.0	77.6	4.8	7.5	0.8
37.5	ARZ	2.0	73.6	4.6	5.6	0.8
		2.5	93.4	4.4	5.2	0.8
		3.0	112.9	4.0	4.8	0.7
37.5	BRZ	2.0	77.4	5.8	9.1	2.4
		2.5	94.9	5.1	6.7	1.9
		3.0	112.3	4.7	5.6	1.4
37.5	TRZ	2.0	75.0	5.9	7.8	1.7
		2.5	93.1	4.3	5.4	1.2
		3.0	112.2	4.0	4.6	1.0

Table 13: Results for Limestone Mixes

NMAS mm	Gradation	T/NMAS	Average Thickness mm	Average SSD Air Voids, %	Average Vacuum Seal Air Voids, %	Average Water Abs.,%
9.5	ARZ	2.0	20.9	12.3	13.0	1.3
		3.0	29.4	8.0	8.4	0.5
		4.0	38.2	6.3	6.7	0.2
		8.0	76.1	3.8	4.2	0.1
9.5	BRZ	2.0	21.6	13.1	15.7	6.4
		3.0	30.6	10.1	11.9	2.6
		4.0	39.2	7.5	9.1	0.8
		8.0	76.8	5.1	6.2	0.3
9.5	TRZ	2.0	21.9	15.4	17.9	5.0
		3.0	30.9	11.0	12.6	1.9
		4.0	39.8	8.7	9.8	0.9
		8.0	77.8	4.3	5.3	0.2
9.5	SMA	2.0	21.2	10.8	17.2	6.4
		3.0	29.8	10.1	13.2	4.4
		4.0	38.5	8.4	10.7	2.5
		8.0	77.2	5.4	6.5	0.7
12.5	SMA	2.0	25.4	10.8	16.9	6.8
		3.0	37.3	8.1	10.8	3.7
		4.0	49.7	7.1	9.1	2.2
		6.0	77.1	6.6	7.7	1.1
19	ARZ	2.0	39.8	8.6	10.3	0.9
		3.0	57.2	6.0	6.5	0.3
		4.0	75.2	4.0	4.4	0.2
19	BRZ	2.0	40.1	8.2	10.2	3.2
		3.0	57.6	5.5	6.3	1.0
		4.0	75.7	4.0	5.1	0.5
19	TRZ	2.0	39.0	10.6	13.4	4.3
		3.0	56.5	6.7	8.0	1.3
		4.0	75.9	4.8	5.7	0.8
19	SMA	2.0	38.5	8.0	16.1	4.6
		3.0	59.0	6.6	9.5	2.6
		4.0	77.9	4.8	6.9	1.4
37.5	ARZ	2.0	72.3	4.5	4.9	0.7
		2.5	91.6	4.5	4.3	0.8
		3.0	112.7	4.4	4.4	0.7
37.5	BRZ	2.0	75.1	4.7	7.8	1.5
		2.5	93.0	4.5	6.3	1.3
		3.0	112.5	4.8	6.3	1.4
37.5	TRZ	2.0	73.5	4.7	5.8	1.2
		2.5	92.1	4.1	4.9	1.2
		3.0	112.9	3.9	5.0	1.0

Table 14: Results for Gravel Mixes

NMAS mm	Gradation	T/NMAS	Average Thickness, mm	Average SSD Air Voids, %	Average Vacuum Seal Air Voids, %	Average Water Abs.,%
9.5	ARZ	2.0	20.5	11.5	12.3	0.7
		3.0	29.1	7.8	8.2	0.4
		4.0	37.6	5.7	6.1	0.2
		8.0	73.9	4.0	4.0	0.1
9.5	BRZ	2.0	21.3	12.8	18.2	4.1
		3.0	29.7	8.5	9.8	1.3
		4.0	38.7	6.6	7.7	0.6
		8.0	74.1	3.3	4.3	0.2
9.5	TRZ	2.0	20.8	12.0	13.4	1.7
		3.0	29.9	8.2	8.7	0.6
		4.0	38.9	6.3	7.0	0.2
		8.0	76.4	4.1	4.4	0.1
9.5	SMA	2.0	21.1	10.7	19.4	6.0
		3.0	30.3	10.4	15.0	5.1
		4.0	38.3	9.3	12.4	3.5
		8.0	77.4	5.8	6.8	0.9
12.5	SMA	2.0	27.2	8.2	17.6	5.0
		3.0	38.5	8.0	13.6	4.0
		4.0	52.7	7.7	11.5	3.7
		6.0	76.9	5.9	7.7	1.7
19	ARZ	2.0	38.9	7.4	8.2	0.4
		3.0	57.1	4.5	4.8	0.2
		4.0	75.5	3.7	4.0	0.1
19	BRZ	2.0	40.6	7.9	9.9	2.5
		3.0	58.1	4.5	5.6	0.6
		4.0	75.7	3.2	4.0	0.3
19	TRZ	2.0	39.7	7.8	9.7	1.5
		3.0	57.2	4.4	5.0	0.5
		4.0	75.9	3.2	3.4	0.2
19	SMA	2.0	39.2	7.0	13.2	3.8
		3.0	57.8	5.7	8.0	2.1
		4.0	77.7	5.5	8.2	1.8
37.5	ARZ	2.0	72.1	4.7	5.2	0.5
		2.5	91.1	4.2	4.4	0.5
		3.0	111.2	4.2	4.7	0.4
37.5	BRZ	2.0	73.8	5.1	7.3	2.0
		2.5	92.5	4.5	6.1	1.8
		3.0	111.6	4.4	5.5	1.4
37.5	TRZ	2.0	73.5	4.2	5.2	1.0
		2.5	92.2	3.6	4.3	0.9
		3.0	111.5	3.4	4.1	0.7

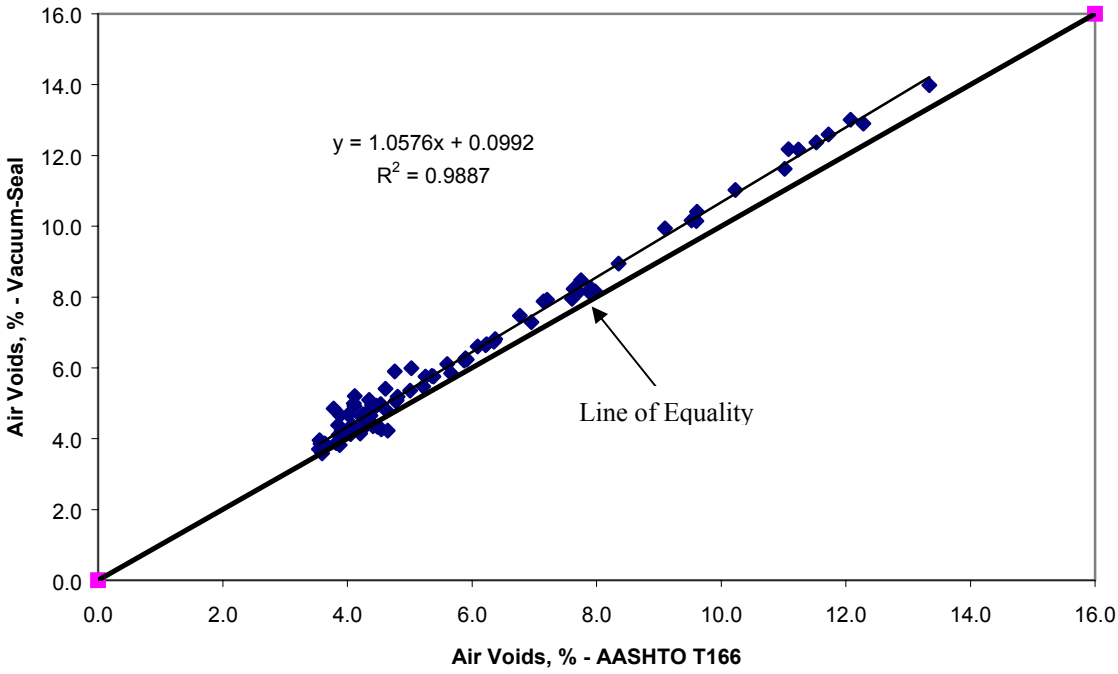

Figure 13: Relationship Between Air voids for ARZ Mixes

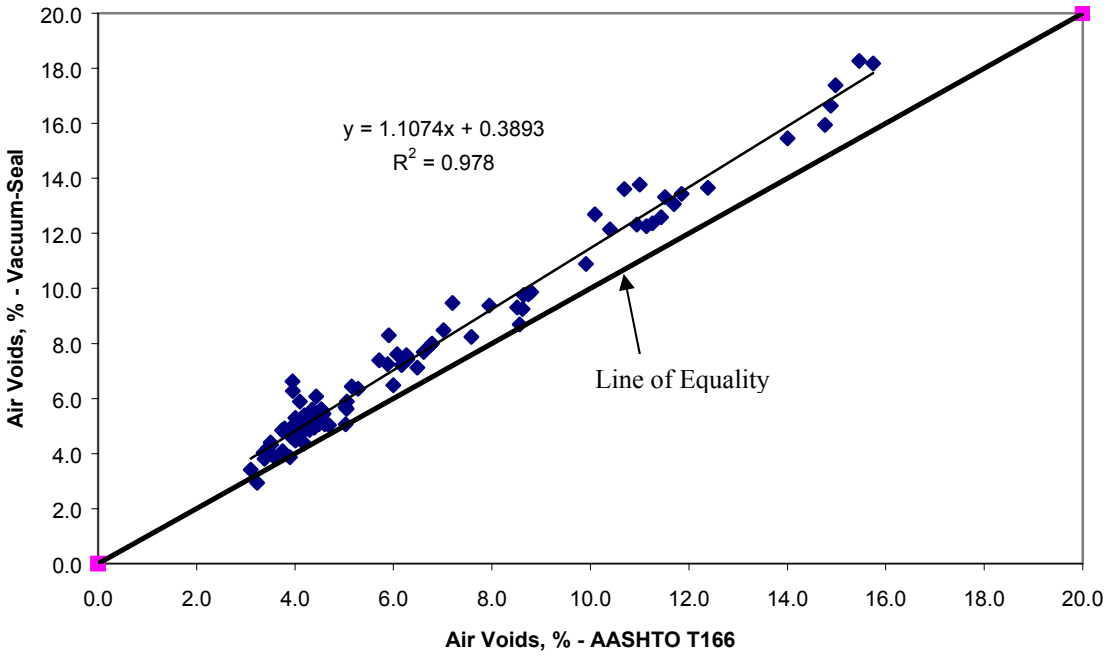

Figure 14: Relationship Between Air voids for TRZ Mixes

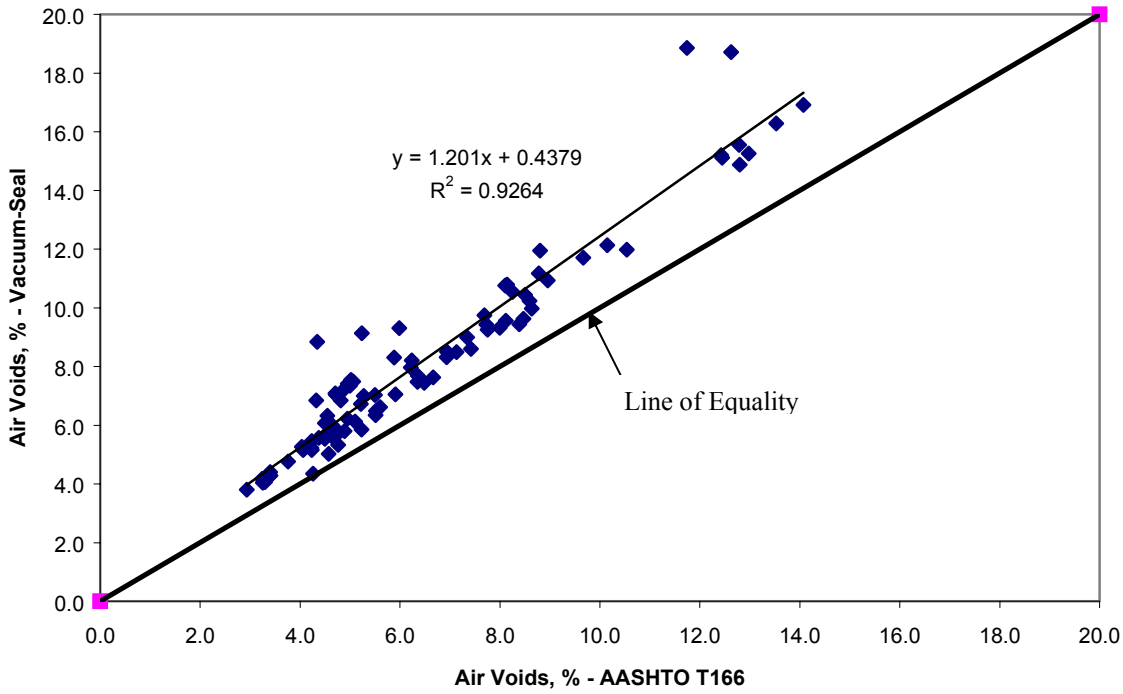

Figure 15: Relationship Between Air voids for BRZ Mixes

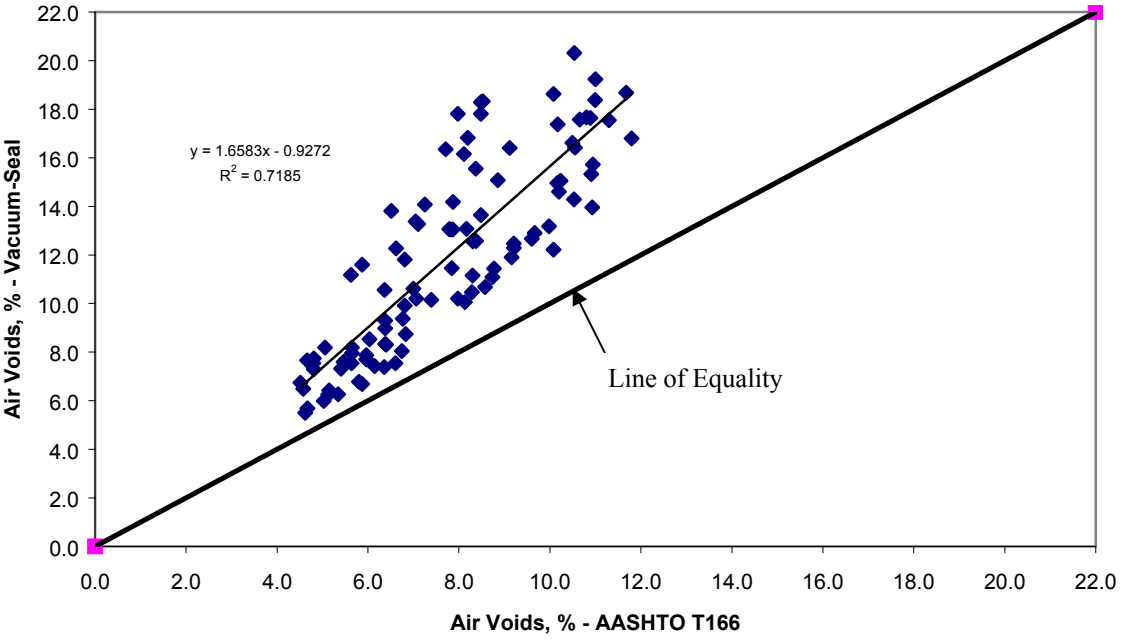

Figure 16: Relationship Between Air voids for SMA Mixes

An analysis of variance (ANOVA) was performed to determine which factors (aggregate type, NMAS, gradation shape, and t/NMAS) significantly affect the resulting air void contents. Since Superpave and SMA mixes are very different, an ANOVA was conducted for each mix type; the results are presented in Tables 15 and 16. Since this study was designed in an unbalanced manner where the t/NMASs used were not the same for each NMAS mix, the reduced degree of freedom (reduced DF) was used in the analysis. The results show all factors and all interactions have a significant effect on the air void contents except three-way interactions of NMAS*Grad*t/NMAS. T/NMAS has the greatest impact followed by NMAS, gradation, and aggregate type.

Figure 17 shows the impact of t/NMAS on the air voids. The plot indicates that as the t/NMAS increases the air voids decrease for a given NMAS. The impact of gradation on air voids for Superpave mixes is illustrated in Figure 18. The relationship is interesting in that the ARZ mixes had the lowest air voids compared to the TRZ and BRZ mixes for a given NMAS. This result could also suggest that fine-graded mixes are easier to compact compared to coarse-graded.

For the SMA mixes, the ANOVA results indicate that all factors and all interactions except the two-way interaction of t/NMAS*NMAS have a significant impact on the air voids. T/NMAS has the largest impact on the air voids followed by NMAS and aggregate type. Figure 19 illustrates the relationship between t/NMAS and air voids. The plot suggests that as t/NMAS increased the air voids decreased.

The main objective of this part of the study was to determine the minimum t/NMAS. To achieve this objective, relationships of average air voids for the three aggregate types versus t/NMAS with respect to NMAS and gradation were evaluated; the results are

Table 15: ANOVA of Air Voids for Superpave Mixes

Source	Reduced DF	Sum of Squares	Mean Squares	F-Statistic	F-Critical	Significant[1]
NMAS	2	711.33	355.67	1333.74	3.05	Yes
Gradation (Grad)	2	174.72	87.36	327.59	3.05	Yes
Aggregate Type (Agg)	2	61.32	30.66	114.98	3.05	Yes
Thickness/NMAS (tNMAS)	4	1802.00	450.50	1689.37	2.43	Yes
NMAS*Grad	4	37.30	9.33	34.97	2.43	Yes
NMAS*Agg	4	26.15	6.54	24.51	2.43	Yes
NMAS*tNMAS	3	88.60	29.53	110.75	2.66	Yes
Grad*Agg	4	32.30	8.08	30.28	2.43	Yes
Grad*tNMAS	8	36.80	4.60	17.25	2.00	Yes
Agg*tNMAS	8	13.50	1.69	6.33	2.00	Yes
NMAS*Grad*Agg	8	53.30	6.66	24.98	2.00	Yes
NMAS*Grad*tNMAS	6	3.30	0.55	2.06	2.16	No
NMAS*Agg*tNMAS	6	28.51	4.75	17.82	2.16	Yes
Grad*Agg*tNMAS	16	27.04	1.69	6.34	1.72	Yes
NMAS*Grad*Agg*tNMAS	12	16.90	1.41	5.28	1.81	Yes
Error	180	48.00	0.27	-	-	-
Total	269	-	-	-	-	-

[1]-Significance at 95 percent level of confidence

Table 16: ANOVA of Air Voids for SMA Mixes

Source	Reduced DF	Sum of Squares	Mean Squares	F-Statistic	F-Critical	Significant[1]
NMAS	2	89.61	44.81	105.69	3.05	Yes
Aggregate Type (Agg)	2	17.84	8.92	21.04	3.05	Yes
Thickness/NMAS (tNMAS)	4	1304.47	326.12	769.25	2.43	Yes
NMAS*Agg	4	36.50	9.13	21.53	2.43	Yes
NMAS*tNMAS	4	1.71	0.43	1.01	2.66	No
Agg*tNMAS	8	32.68	4.09	9.64	2.00	Yes
NMAS*Agg*tNMAS	8	18.01	2.25	5.31	2.16	Yes
Error	66	27.98	0.42			
Total	98					

[1]-Significance at 95 percent level of confidence

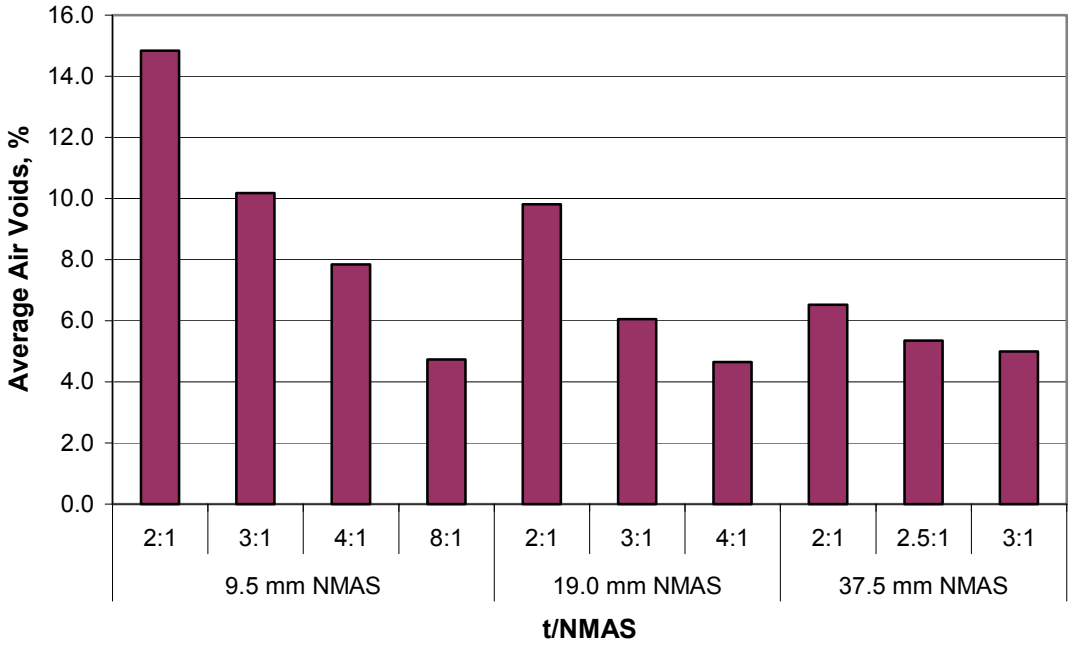

Figure 17: Relationships of t/NMAS and Air Voids for Superpave Mixes

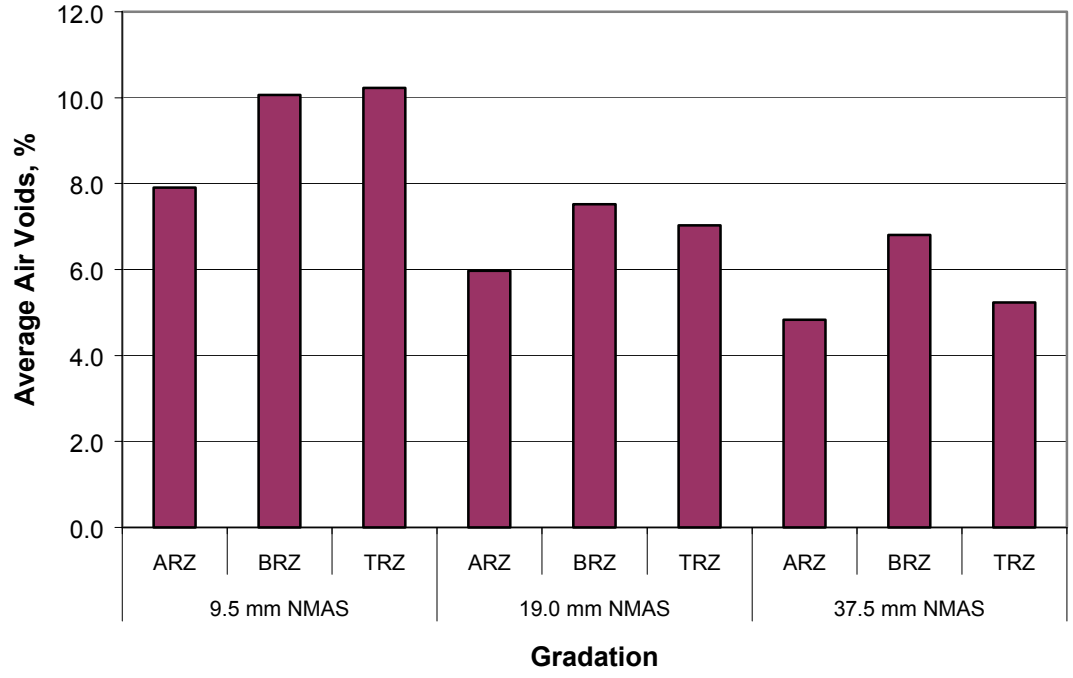

Figure 18: Relationships of Gradations and Air Voids for Superpave Mixes

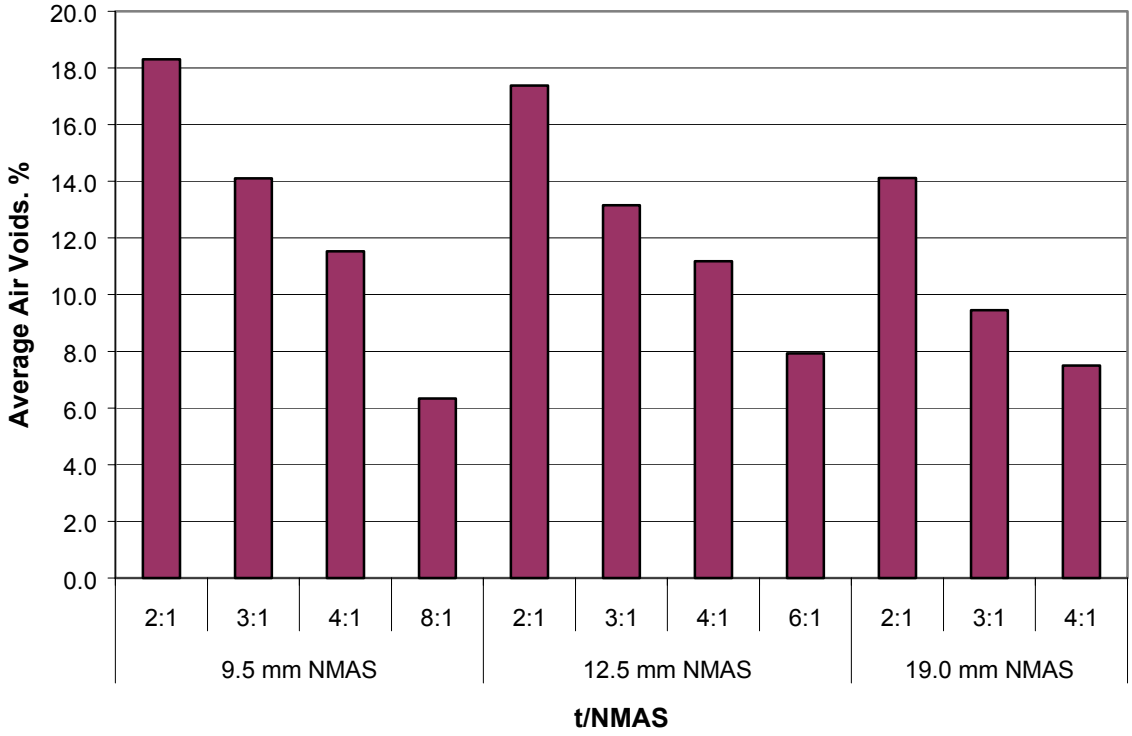

Figure 19: Relationships of t/NMAS and Air Voids for SMA Mixes

illustrated in Figures 20 through 25. Originally it was intended to determine the t/NMAS at which the air voids began to level out and to pick that t/NMAS level as the minimum level recommended to achieve satisfactory density without having to apply additional compactive effort. However much of the data in Figures 20 through 25 indicate that the air voids continue to drop (there is no clear minimum t/NMAS ratio for best density) with increasing t/NMAS up to and past typical t/NMAS values. This continued decrease in air voids with increase in t/NMAS did not provide a clear minimum t/NMAS. Hence an air void content of 7.0 percent was selected as the criteria to determine the minimum t/NMAS. This level of air voids was selected because compaction of most pavements in

the field is targeted at 92.0 to 94.0 percent of theoretical maximum density. This approach did not provide a sufficient comfort level for selecting a minimum t/NMAS, hence, it was decided to compact some samples with a laboratory vibratory compactor and when this data was not very conclusive it was further decided to compact some mixes in the field at various t/NMAS ratios during reconstruction of the NCAT test track. It was not originally planned to conduct tests with the laboratory vibratory compactor or with the field mixes but during the study it was determined that an adequate answer could not be determined from the Superpave gyratory compactor test plan so this additional work was performed to provide a better overall answer. These two efforts are discussed later in the report.

A characteristic of the Superpave gyratory compactor is that it applies a constant strain to the mix, and the force required to produce this strain varies as necessary depending on the stiffness of the mixture. This is not the approach that is observed in the field where the stress is constant and the strain varies. Hence, the Superpave gyratory compactor might not provide a reasonable answer since it differs from field compaction.

Figure 20 illustrates the plot of air voids versus t/NMAS for 9.5 mm Superpave mixes. The best fit lines indicate that as the t/NMAS increases the air voids decrease. A review of the data indicated that a power function provided the best fit. The coefficients of determination (R^2) values indicate strong relationships (0.98 to 1.0). The minimum t/NMAS values to provide 7.0 percent air voids are 3.9 for ARZ, 5.2 for BRZ, and 5.4 for TRZ mixes.

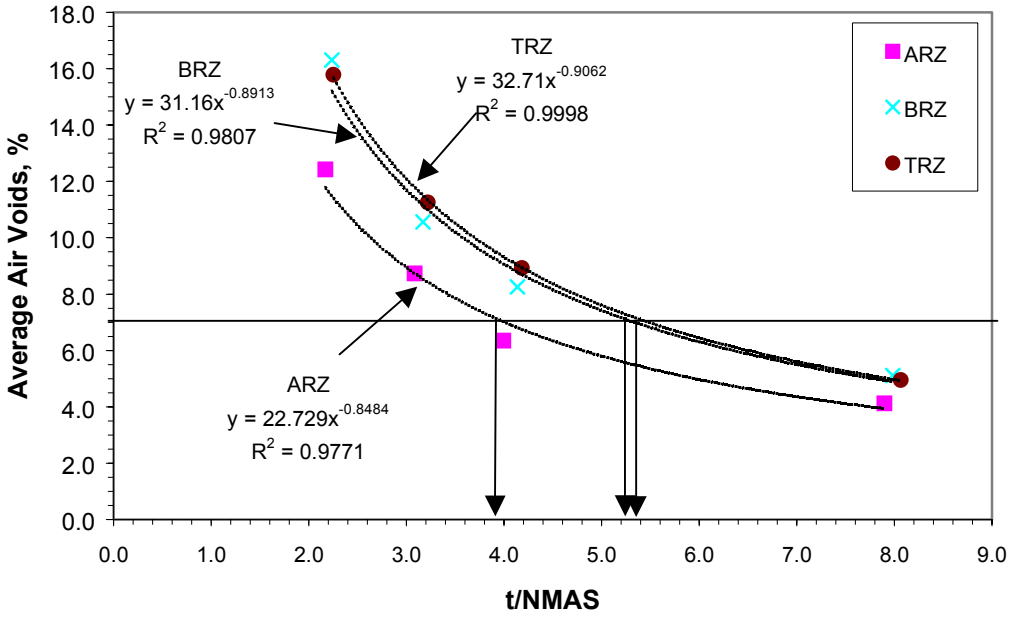

Figure 20: Relationships Between Air Voids and t/NMAS for 9.5 mm Superpave Mixes

Figure 21 illustrates the plot of average air voids versus t/NMAS for 19.0 mm Superpave mixes. The R^2 values suggest strong relationships (0.98 to 1.0). The minimum t/NMAS values determined from the plots are 2.4 for ARZ, 3.0 for BRZ, and 2.8 for TRZ mixes.

Relationships between average air voids and t/NMAS for 37.5 mm Superpave mixes are illustrated in Figure 22. From the plot, the minimum t/NMAS for BRZ is determined to be 2.4. The minimum t/NMAS values for ARZ and TRZ mixes are less than 2.0 based on the 7 percent air voids. Figure 22 seems to indicate that there is very little effect of t/NMAS on air voids for the TRZ and ARZ mixes. From the data, a ratio of 2.0 appears to be the appropriate ratio for these two mixtures. Hence, a ratio of 2.0 is selected as the point at which the density can be easily obtained in the Superpave

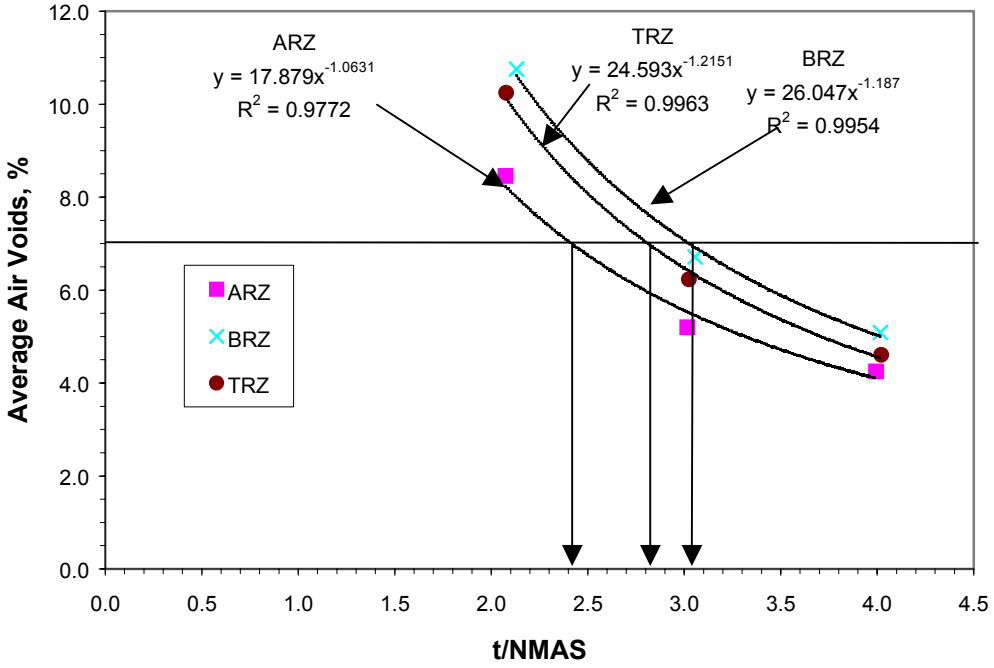

Figure 21: Relationships Between Air Voids and t/NMAS for 19.0 mm Superpave Mixes

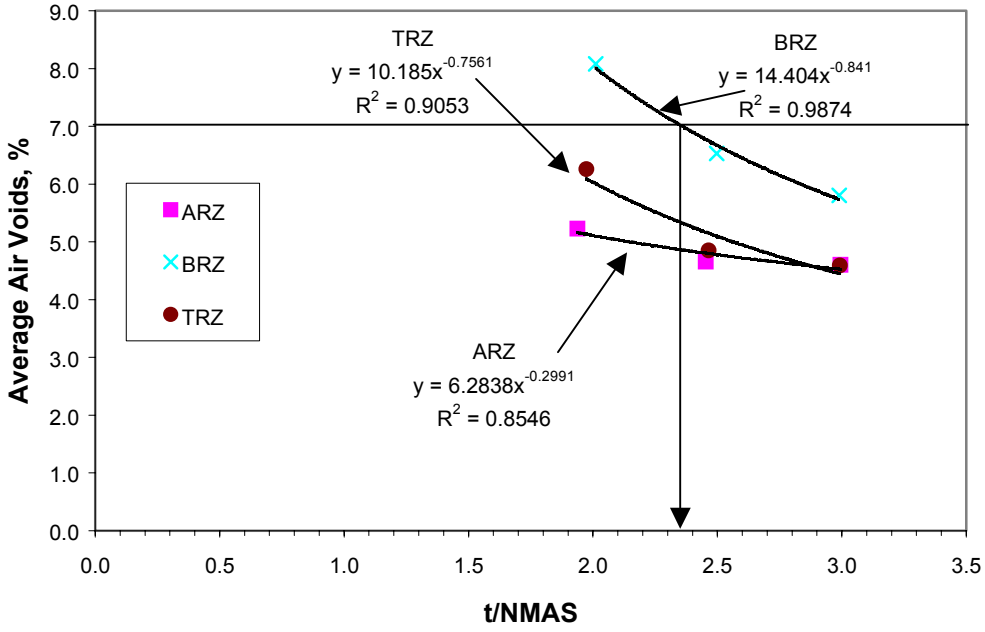

Figure 22: Relationships Between Air Voids and t/NMAS for 37.5 mm Superpave Mixes

gyratory compactor, however, this does not necessarily relate to field compaction. These numbers appear to be low and therefore, it seems that the results are not appropriate for setting the proper ratio for compaction.

Figures 23 through 25 illustrate the relationships between air voids and t/NMAS for 9.5 mm, 12.5 mm, and 19.0 mm NMAS SMA mixes, respectively. Using 7 percent air voids as a basis, the minimum t/NMAS values for 9.5 mm, 12.5 mm, and 19.0 mm are determined to be 7.3, 7.5, and 4.4, respectively. The summary of results is presented in Table 17. The results indicate that as the NMAS increases the minimum t/NMAS decreases and fine-graded mixes have lower desired t/NMAS values than the coarse-graded mixes.

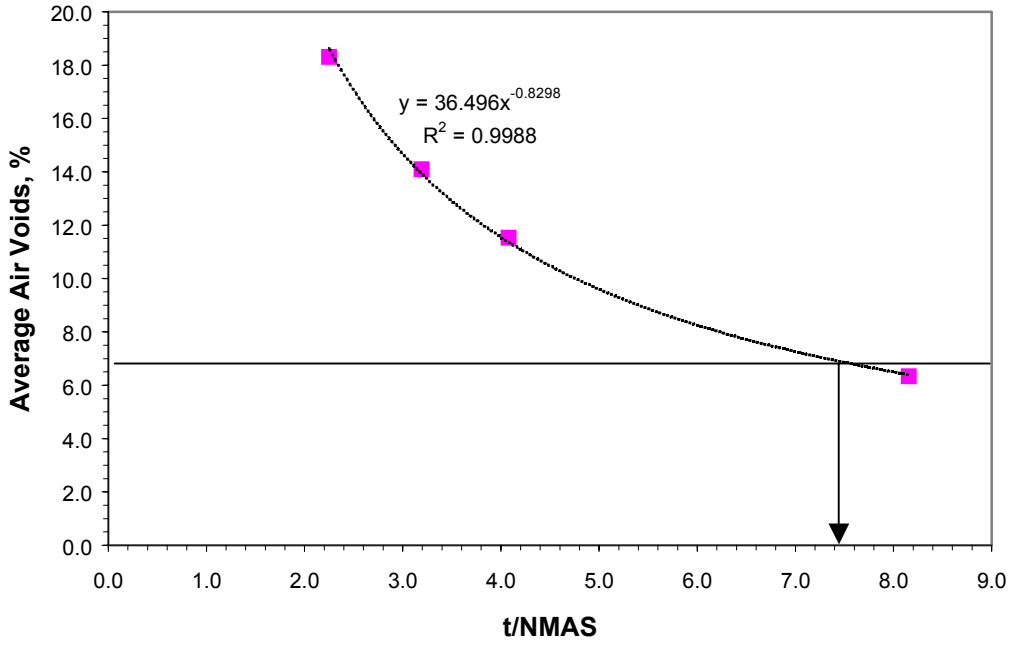

Figure 23: Relationships Between Air Voids and t/NMAS for 9.5 mm SMA Mixes

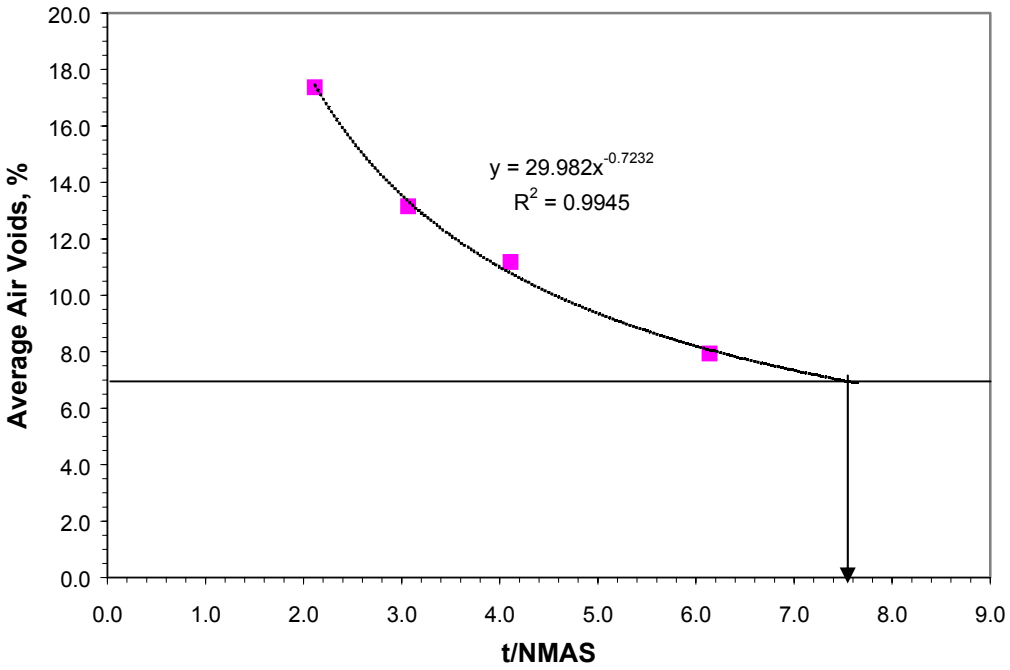

Figure 24: Relationships Between Air Voids and t/NMAS for 12.5 mm SMA Mixes

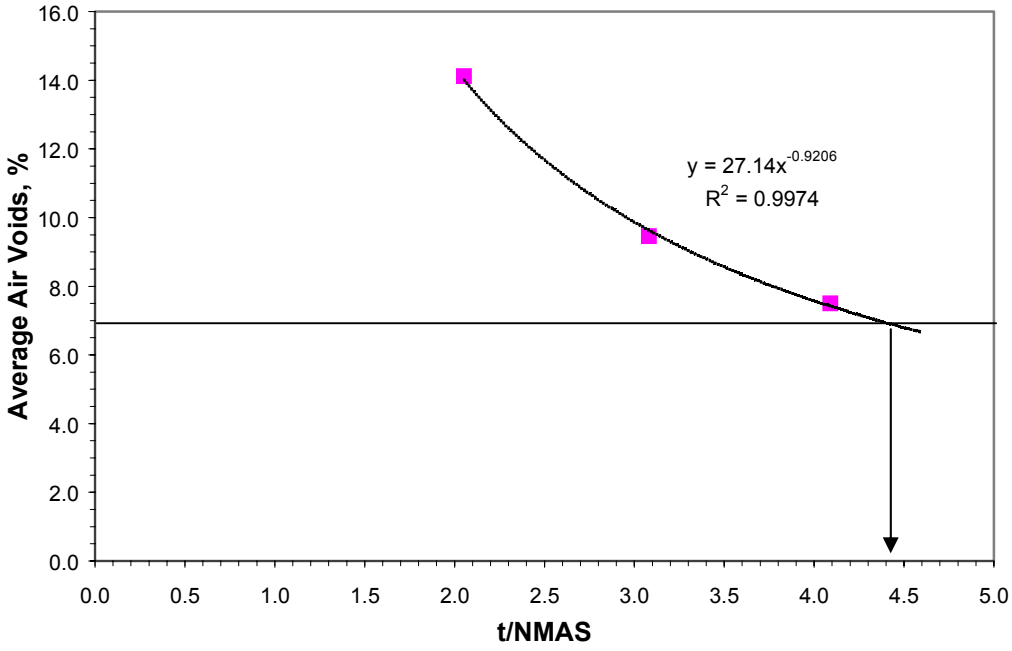

Figure 25: Relationships Between Air Voids and t/NMAS for 19.0 mm SMA Mixes

Table 17: Summary of Minimum t/NMAS to Provide 7 % Air Voids in Laboratory

Mix	Minimum t/NMAS	Minimum Thickness, mm
9.5 mm ARZ	3.9	37
9.5 mm BRZ	5.2	49
9.5 mm TRZ	5.4	51
19.0 mm ARZ	2.4	46
19.0 mm BRZ	3.0	57
19.0 mm TRZ	2.8	53
37.5 mm ARZ	2.0	75
37.5 mm BRZ	2.4	90
37.5 mm TRZ	2.0	75
9.5 mm SMA	7.3	69
12.5 mm SMA	7.5	94
19.0 mm SMA	4.4	84

The numbers developed for SMA are high and as discussed above are not considered to be reasonable. For that reason the gyratory data was considered to be unsuitable for use in setting the appropriate t/NMAS ratio and as a result it was decided to try a laboratory vibratory compactor to see if it would provide compacted mixtures with reasonable results.

5.3 Evaluation of Effect of t/NMAS on Density Using Vibratory Compactor

After obtaining the results for the Superpave gyratory compactor it was concluded that more tests were needed. It was decided to conduct tests with the vibratory compactor that may better simulate compaction in the field. Based on these results it was ultimately

decided to actually conduct field tests during reconstruction of the NCAT test track. The vibratory compactor was manufactured by Pavement Technology Inc. and was designed primarily to prepare samples for the wheel-tracking test. Results of the laboratory experiment using the vibratory compactor are presented in Tables 18 and 19. Results are presented for average air voids of the beams determined from the vacuum seal device and SSD methods and average water absorption for Superpave and SMA mixes for each aggregate type. For all mixes, there appears to be a difference between the air voids measured by SSD and the vacuum seal device. The variations become more significant for samples having higher air void contents that involved coarse–graded and SMA mixes at smaller t/NMAS ratios and at low compactive effort. The average water absorption values increase as the air void contents increase. The data from this experiment are included in Appendix C. Since this experiment was intended to check the results from the gyratory study, only the air voids determined from the vacuum seal device were utilized in the analysis.

An ANOVA was performed to evaluate the factors (compaction time, aggregate type, NMAS, gradation shape, and t/NMAS) significantly affecting the air void contents. The results are presented in Tables 20 and 21 for Superpave and SMA mixes, respectively. For Superpave mixes, all main factors have a significant impact on the air void contents. However, as shown in Table 20, three two-way interactions, six three-way interactions, and four four-way interactions do not have a significant effect on air voids. Compaction time was the most significant factor followed by gradation, t/NMAS, NMAS and aggregate type. For SMA mixes, all factors and all interactions have significant impacts on the air void contents. Compaction time has the most impact followed by

Table 18: Results of Air Voids for Limestone Superpave Mixes

NMAS mm	Grad.	T/NMAS	Compact. Time, s	Avg. SSD Air Voids, %	Avg. Vacuum Seal Air Voids, %	Avg.Water Abs., %
9.5	ARZ	2	30	7.7	8.2	0.3
			60	7.7	7.6	0.4
			90	5.7	7.0	0.1
		3	30	8.3	8.6	0.3
			60	7.0	7.1	0.2
			90	6.4	6.6	0.1
		4	30	6.4	7.2	0.2
			60	6.2	6.2	0.2
			90	3.9	4.0	0.2
9.5	BRZ	2	30	7.3	8.8	0.9
			60	6.1	7.2	0.9
			90	5.3	6.6	0.7
		3	30	8.3	8.9	0.6
			60	7.0	7.4	0.9
			90	4.8	5.7	0.2
		4	30	7.8	8.1	0.5
			60	6.7	7.8	0.3
			90	5.0	5.2	0.4
9.5	SMA	2	30	6.4	9.6	1.6
			60	5.2	5.8	0.9
			90	2.9	3.4	0.6
		3	30	6.6	8.5	0.9
			60	5.1	6.0	0.7
			90	3.5	3.8	0.5
		4	30	6.6	8.2	1.1
			60	4.4	5.0	0.6
			90	4.5	4.7	0.5
12.5	SMA	2	30	5.9	8.1	1.3
			60	5.7	7.6	1.0
			90	5.8	7.2	0.8
		3	30	6.8	7.6	0.9
			60	3.6	4.3	0.5
			90	2.9	3.2	0.3
		4	30	7.4	8.6	1.1
			60	6.4	6.9	0.8
			90	3.7	3.6	0.4
19	ARZ	2	30	7.7	7.9	0.4
			60	7.0	7.4	0.3
			90	4.4	4.4	0.2
		3	30	8.3	8.2	0.9
			60	7.1	6.8	0.5
			90	6.0	5.7	0.3
		4	30	8.2	8.2	1.1
			60	6.1	6.1	0.7
			90	5.7	5.4	0.5

Table 18 (cont.): Results of Air Voids for Limestone Mixes

NMAS mm	Grad.	T/NMAS	Compact. Time, s	Avg. SSD Air Voids, %	Avg. Vacuum Seal Air Voids, %	Avg. Water Abs., %
19	BRZ	2	30	7.9	9.6	1.0
			60	6.2	7.6	0.6
			90	3.6	4.8	0.3
		3	30	7.4	8.8	1.0
			60	6.0	7.1	0.6
			90	4.3	5.2	0.2
		4	30	7.8	8.5	0.8
			60	6.2	6.9	0.5
			90	6.1	6.6	0.4
19	SMA	2	30	4.4	6.7	0.7
			60	4.5	6.4	1.2
			90	3.7	4.9	0.6
		3	30	6.6	9.7	1.5
			60	5.3	7.5	0.6
			90	5.4	7.1	0.7
		4	30	7.3	10.0	1.8
			60	5.2	6.3	0.6
			90	4.9	6.0	0.6

Table 19: Results of Air Voids for Granite Mixes

NMAS mm	Grad.	T/NMAS	Compact. Time, s	Avg. SSD Air Voids, %	Avg. Vacuum Seal Air Voids, %	Avg. Water Abs., %
9.5	ARZ	2	30	6.3	6.5	0.2
			60	4.1	4.7	0.3
			90	3.8	4.5	0.3
		3	30	5.1	6.1	0.2
			60	5.3	5.1	0.2
			90	3.7	3.5	0.1
		4	30	5.6	5.2	0.2
			60	4.1	4.2	0.1
			90	3.8	3.4	0.1
9.5	BRZ	2	30	9.1	11.0	1.9
			60	6.4	8.2	0.9
			90	5.7	6.8	0.6
		3	30	8.5	10.1	1.7
			60	7.5	8.9	0.8
			90	6.4	7.1	0.4
		4	30	8.5	9.2	1.5
			60	7.7	8.1	0.8
			90	6.0	6.5	0.3

Table 19 (cont.): Results of Air Voids for Granite Mixes

NMAS mm	Grad.	T/NMAS	Compact. Time, s	Avg. SSD Air Voids, %	Avg. Vacuum Seal Air Voids, %	Water Abs., %
9.5	SMA	2	30	6.7	10.8	2.0
			60	6.7	9.2	2.1
			90	5.1	6.1	0.9
		3	30	8.5	10.4	2.5
			60	5.5	7.0	1.5
			90	3.4	4.5	0.5
		4	30	8.6	10.2	1.8
			60	5.3	6.0	0.6
			90	3.7	4.4	0.5
12.5	SMA	2	30	7.5	12.5	3.2
			60	5.7	9.0	1.3
			90	5.0	6.9	0.8
		3	30	7.7	10.8	2.6
			60	4.5	7.3	0.5
			90	4.2	5.0	0.5
		4	30	7.9	10.7	2.2
			60	7.3	8.7	2.0
			90	6.8	8.0	1.3
19	ARZ	2	30	8.2	9.1	2.2
			60	7.2	7.3	1.2
			90	5.5	5.4	0.6
		3	30	6.7	6.9	0.6
			60	5.1	5.7	0.8
			90	5.1	4.8	0.7
		4	30	8.3	7.9	1.5
			60	6.4	6.3	1.0
			90	3.8	4.5	0.5
19	BRZ	2	30	7.9	10.4	1.7
			60	7.5	9.7	1.2
			90	5.8	7.7	0.6
		3	30	8.1	11.4	1.6
			60	6.1	9.5	0.8
			90	5.7	7.3	0.7
		4	30	9.1	10.9	2.1
			60	6.5	8.9	1.0
			90	5.7	6.8	0.8
19	SMA	2	30	6.5	11.8	2.2
			60	5.5	7.7	0.9
			90	4.5	5.6	0.7
		3	30	7.2	11.3	1.9
			60	5.3	7.4	0.8
			90	4.7	5.8	0.5
		4	30	6.1	10.3	1.1
			60	5.6	8.1	0.9
			90	5.7	6.8	0.8

Table 20: ANOVA of air voids for Superpave mixes

Source	DF	Sum of Squares	Mean Squares	F-Stat	F-Critical	Significant[1]
Thickness/NMAS (t/NMAS)	2	11.18	5.59	28.76	3.13	Yes
Compaction Time (Comp)	2	206.25	103.13	530.55	3.13	Yes
NMAS	1	9.35	9.35	48.12	3.98	Yes
Aggregate (Agg)	1	1.19	1.19	6.13	3.98	Yes
Gradation (Grad)	1	119.72	119.72	615.92	3.98	Yes
t/NMAS*Comp	4	0.14	0.04	0.18	2.50	No
t/NMAS*NMAS	2	4.51	2.26	11.61	3.13	Yes
t/NMAS*Agg	2	0.53	0.27	1.37	3.13	No
t/NMAS*Grad	2	1.61	0.81	4.14	3.13	Yes
Comp*NMAS	2	2.96	1.48	7.62	3.13	Yes
Comp*Agg	2	0.41	0.20	1.04	3.13	No
Comp*Grad	2	3.52	1.76	9.05	3.13	Yes
NMAS*Agg	1	16.61	16.61	85.43	3.98	Yes
NMAS*Grad	1	1.02	1.02	5.23	3.98	Yes
Agg*Grad	1	66.02	66.02	339.63	3.98	Yes
t/NMAS*Comp*NMAS	4	5.45	1.36	7.01	2.50	Yes
t/NMAS*Comp*Agg	4	1.03	0.26	1.33	2.50	No
t/NMAS*Comp*Grad	4	1.58	0.40	2.03	2.50	No
t/NMAS*NMAS*Agg	2	1.51	0.76	3.89	3.13	Yes
t/NMAS*NMAS*Grad	2	0.94	0.47	2.41	3.13	No
t/NMAS*Agg*Grad	2	3.98	1.99	10.24	3.13	Yes
Comp*NMAS*Agg	2	0.24	0.12	0.61	3.13	No
Comp*NMAS*Grad	2	0.33	0.16	0.85	3.13	No
Comp*Agg*Grad	2	0.20	0.10	0.50	3.13	No
NMAS*Agg*Grad	1	2.64	2.64	13.59	3.98	Yes
t/NMAS*Comp*NMAS*Agg	4	6.74	1.69	8.67	2.50	Yes
t/NMAS*Comp*NMAS*Grad	4	1.50	0.37	1.93	2.50	No
t/NMAS*Comp*Agg*Grad	4	1.63	0.41	2.10	2.50	No
t/NMAS*NMAS*Agg*Grad	2	1.45	0.73	3.73	3.13	No
Comp*NMAS*Agg*Grad	2	0.25	0.13	0.64	3.13	No
t/NMAS*Comp*NMAS*Agg*Grad	4	1.95	0.49	2.51	2.50	Yes
Error	72	14.00	0.19			
Total	143					

[1]- Significance at 95 percent level of confidence

Table 21: ANOVA of air voids for SMA mixes

Source	DF	Sum of Squares	Mean Squares	F-Stat	F-Critical	Significant[1]
T/NMAS	2	7.77	3.89	24.18	3.13	Yes
Compaction Time (Comp)	2	351.63	175.82	1093.78	3.13	Yes
NMAS	2	16.18	8.09	50.33	3.13	Yes
Aggregate (Agg)	1	77.35	77.35	481.22	4.02	Yes
T/NMAS*Comp	4	3.65	0.91	5.68	2.55	Yes
tNMAS*NMAS	4	34.80	8.70	54.13	2.55	Yes
T/NMAS*Agg	2	4.08	2.04	12.69	3.13	Yes
Comp*NMAS	4	6.05	1.51	9.41	2.55	Yes
Comp*Agg	2	8.67	4.33	26.96	3.13	Yes
NMAS*Agg	2	7.24	3.62	22.51	3.13	Yes
T/NMAS*Comp*NMAS	8	6.37	0.80	4.96	2.01	Yes
T/NMAS*Comp*Agg	4	5.77	1.44	8.98	2.55	Yes
T/NMAS*NMAS*Agg	4	9.81	2.45	15.25	2.55	Yes
Comp*NMAS*Agg	4	3.24	0.81	5.03	2.55	Yes
T/NMAS*Comp*NMAS*Agg	8	21.81	2.73	16.96	2.12	Yes
Error	54	8.68	0.16			
Total	107					

[1]- Significance at 95 percent level of confidence

aggregate type, NMAS, and t/NMAS.

To determine the minimum t/NMAS, relationships between average air voids for the two types of aggregates and t/NMAS were plotted for each NMAS, compaction time, and gradation, as shown in Figures 26 through 32. Relationship between air voids and t/NMAS for 9.5 mm ARZ is shown in Figure 26. The results suggest that as t/NMAS and compaction time increase the air voids decrease. The relationships between density and t/NMAS for the three compactive efforts showed the same trend and at t/NMAS of 4.0 produced the highest density. Thus, the minimum t/NMAS of 4.0 was selected. Figure 27 illustrates the relationships between air voids and t/NMAS for 9.5 mm BRZ. The

results indicate that thickness did not have a great effect on compaction. For compaction time of 90 sec, the air voids at t/NMAS 2.0, 3.0, and 4.0 are approximately 6.0 percent whereas for compaction time 60 and 30 sec, the air voids are approximately 8.0 percent and 9.0 percent, respectively. Therefore, t/NMAS of 2.0 was selected as the minimum t/NMAS. Figures 26 and 27 suggest that the BRZ mix was more difficult to compact than ARZ mix for a given compactive effort. Figure 28 presents the relationship between air voids and t/NMAS for 19.0 mm ARZ. The results suggest that t/NMAS basically did not affect the compaction. A minimum t/NMAS of 2.0 was selected. Figure 29 illustrates the relationships between air voids and t/NMAS for 19.0 mm BRZ. The figure indicates that thickness did not affect compaction. Thus, a minimum t/NMAS of 2.0 was suggested. Again, the BRZ mix was more difficult to compact than ARZ, as shown in Figures 28 and 29.

The relationships between air voids and t/NMAS for 9.5 SMA is shown in Figure 30. The results indicate that t/NMAS affects the compaction at 60 sec compaction time and not at 30 and 90 sec. This is likely due to random variation in the test results. From the curve, the minimum t/NMAS was selected to be 3.0 Figure 31 shows the relationships between air voids and t/NMAS for 12.5 mm SMA. The trend of the curve is similar for the three compaction times. As the t/NMAS increased from 2.0 to 3.0 the air voids decreased and started to increase as the t/NMAS increased from 3.0 to 4.0. A minimum t/NMAS of 3.0 was suggested. Figures 30 and 31 also indicate that both 9.5 mm and 12.5 mm SMA mixes had about the same compactibility. The relationships between air voids and t/NMAS for 19.0 mm SMA is presented in Figure 32. The trend of the curves indicate that as t/NMAS increased from 2.0 to 3.0 the air voids increased and

leveled off at t/NMAS 3.0 and larger. Therefore, a minimum t/NMAS of 2.0 was selected. The summary of results is presented in Table 22.

The results with the vibratory compactor seem to disagree with those from the Superpave gyratory compactor. In most cases with the vibratory compactor there is very little difference between the different t/NMAS values. However, in a few cases there was a difference. Also, in many cases the best t/NMAS was 2.0 which is lower than that observed on many field projects. Typically, it was assumed that the coarse graded mixes would have a desired t/NMAS greater than fine graded mixes. This analysis did not always follow that trend. Again, it was believed that some fieldwork would be good to help validate the results with the Superpave gyratory compactor and with the vibratory compactor.

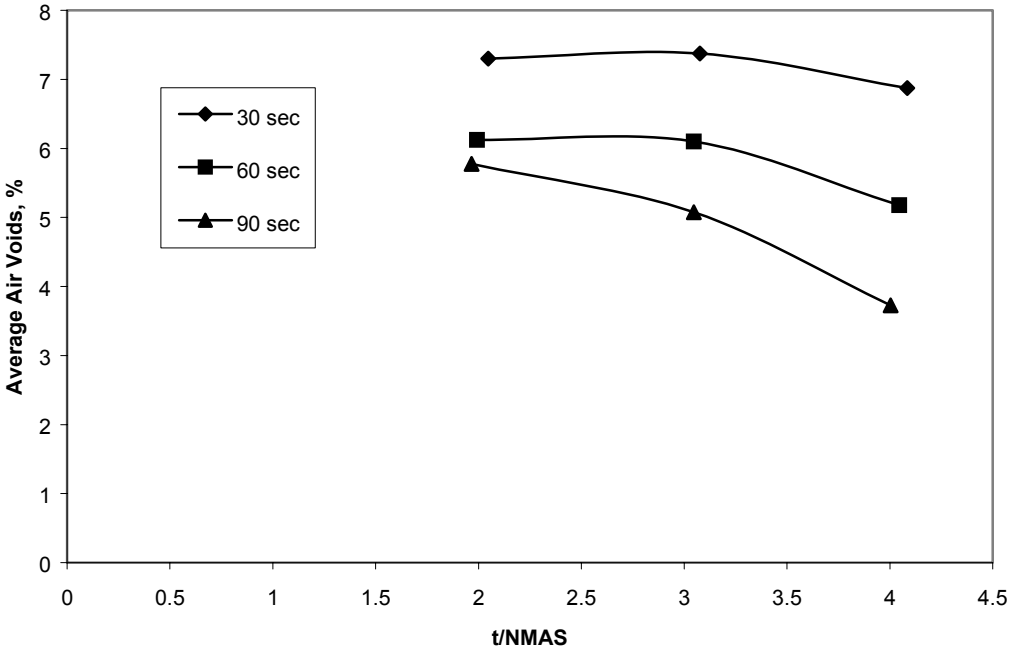

Figure 26: Relationship Between Air Voids and t/NMAS for 9.5 mm ARZ

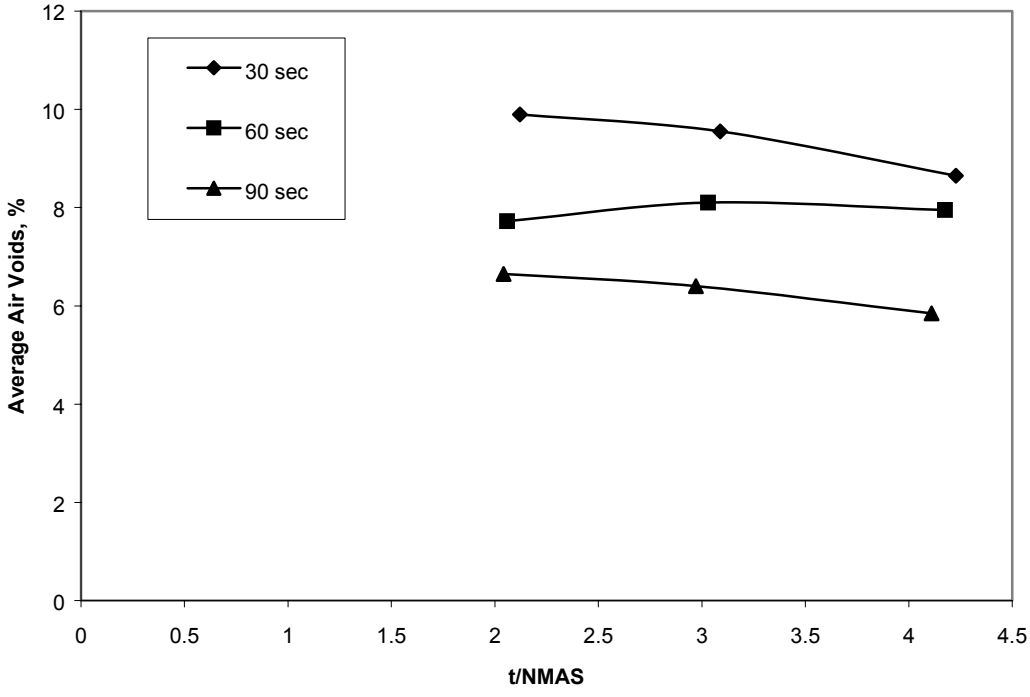

Figure 27: Relationship Between Air Voids and t/NMAS for 9.5 mm BRZ

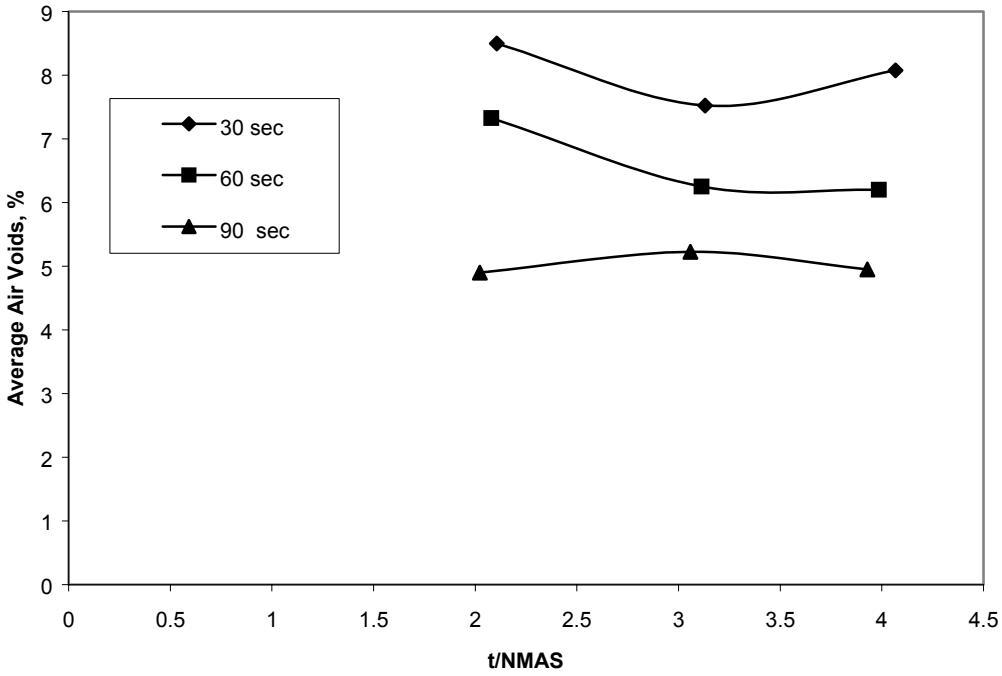

Figure 28: Relationship Between Air Voids and t/NMAS for 19.0 mm ARZ

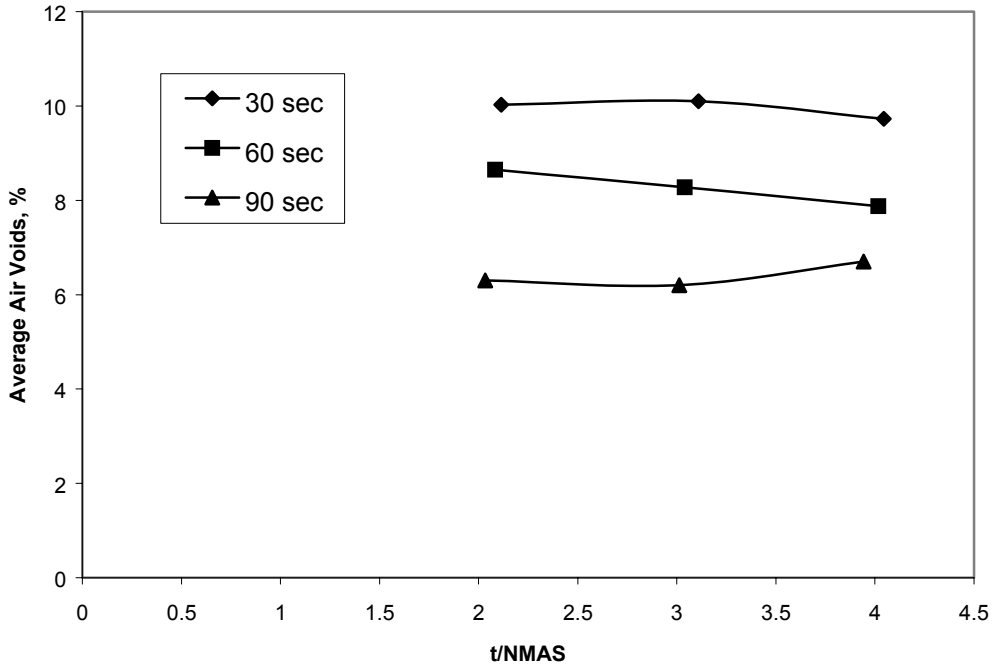

Figure 29: Relationship Between Air Voids and t/NMAS for 19.0 mm BRZ

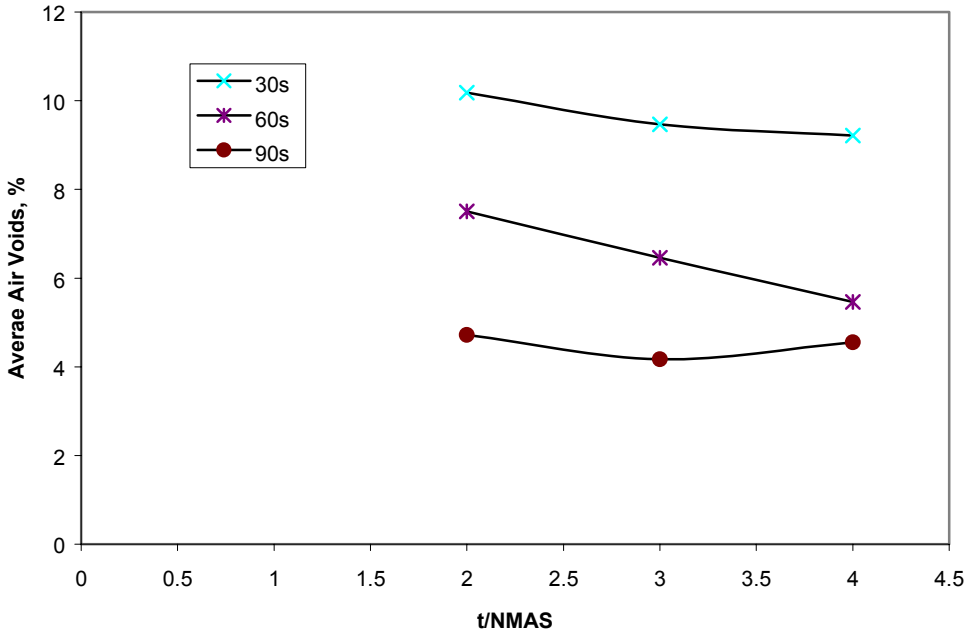

Figure 30: Relationship Between Air Voids and t/NMAS for 9.5 mm SMA

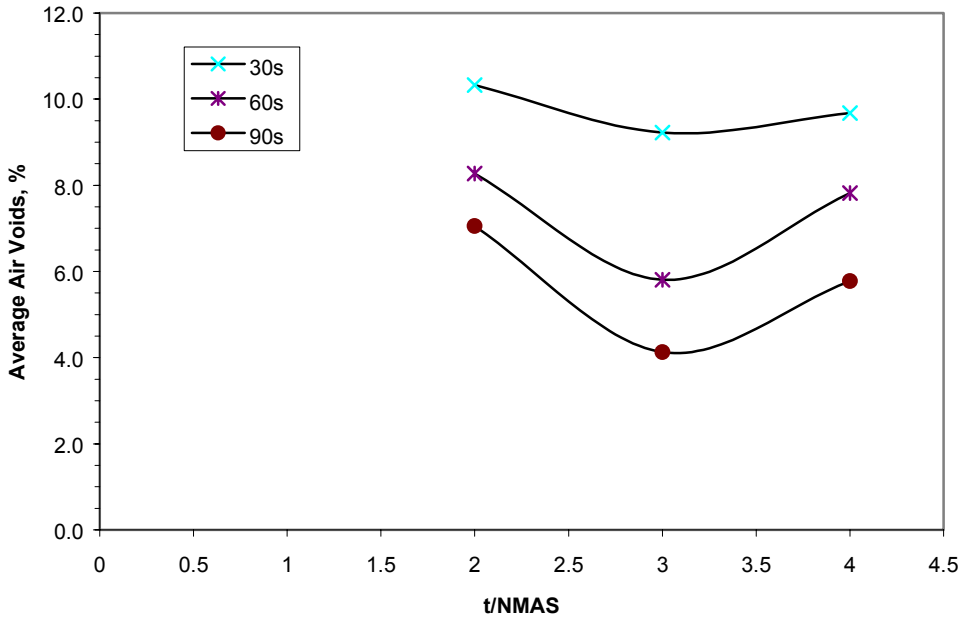

Figure 31: Relationship Between Air Voids and t/NMAS for 12.5 mm SMA

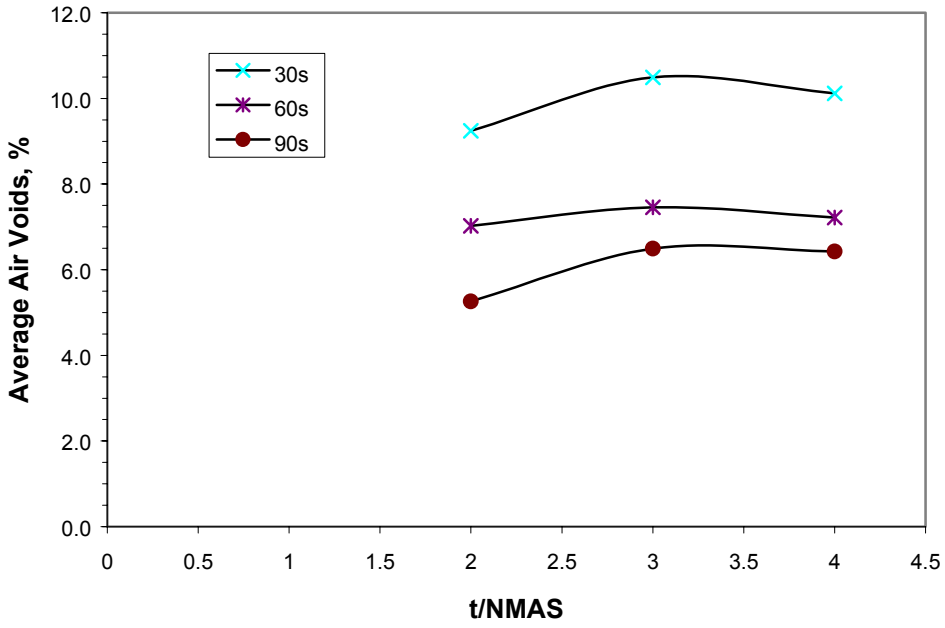

Figure 32: Relationship Between Air Voids and t/NMAS for 19.0 mm SMA

Table 22: Summary of Minimum t/NMAS Using Laboratory Vibratory Compactor

Mix	Minimum t/NMAS	Minimum Thickness, mm
9.5 mm ARZ	4.0	38
9.5 mm BRZ	2.0	19
19.0 mm ARZ	2.0	38
19.0 mm BRZ	2.0	38
9.5 mm SMA	3.0	28.5
12.5 mm SMA	3.0	37.5
19.0 mm SMA	2.0	38

5.4 Evaluation of Effect of t/NMAS on Density from Field Study

The field test sections consisted of seven mixes that were to be placed during the 2003 reconstruction of the NCAT test track. These mixes had to be field verified before they were placed. Hence, some of the mixes did not meet volumetrics and other requirements but they were judged to be sufficient for this part of the study since determining the desired thickness range was a relative value based on t/NMAS.

5.4.1 Section 1

Section 1 was constructed on July 18, 2003 and consisted of a t/NMAS that ranged from 2.0 to 5.0 and placed over an existing HMA layer. This construction was performed adjacent to the NCAT Test Track. The mix consisted of a 9.5 mm NMAS fine-graded mixture. The length of the section was about 40 m and the width was about 3.5 m. On some of the sections the placement began on the thick side and in some cases the rolling began on the thin side. This technique was used so that there would be no bias due to the placement of the HMA. On this section the paving began with the thicker portion of the section and the thickness was slowly decreased as the paver moved down the test lane. The desired mat thickness was achieved by gradually adjusting the screed depth crank of the paver during the paving operation. The weather conditions during the paving were 84^{o}F, overcast, with calm wind. The existing surface temperature was also 84^{o}F.

The roller utilized in this section was an 11 ton steel roller HYPAC C778B with 78 in. drum width that could operate in vibratory or static mode. The rubber tire roller available did not meet desired requirements for weight and tire pressure and thus the data

generated for the rubber tire roller compacted mixture was omitted from the analysis for this section. The breakdown rolling was performed with one pass of static mode on the mat having temperature of about 300^{o}F. This was followed by three passes of vibratory mode operated in low amplitude and high frequency (3800 vpm) and finished with one pass of static mode. It was determined that this rolling technique reached the peak density; hence, additional rolling was not performed.

A total of 16 cores were obtained from this section and the test results of the cores are presented in Table 23. The results include the thickness of cores, t/NMAS, the air voids determined from AASHTO T166 and vacuum-sealed methods and water absorption.

Table 23: Thickness, t/NMAS, Air Voids, and Water Absorption for Section 1

Core No.	Thickness, mm	t/NMAS	Voids SSD, %	Voids Vacuum Sealed, %	Water Abs., %
1	21.0	2.2	8.5	8.7	0.2
2	24.1	2.5	8.9	8.8	0.2
3	24.3	2.6	8.4	8.4	0.1
4	28.2	3.0	7.6	7.6	0.1
5	28.9	3.0	8.1	8.3	0.3
6	33.2	3.5	6.8	7.0	0.2
7	34.3	3.6	6.9	7.2	0.1
8	39.0	4.1	6.9	7.1	0.2
9	46.6	4.9	6.4	6.6	0.2
10	48.4	5.1	6.9	7.2	0.2
11	48.7	5.1	7.1	7.5	0.3
12	48.9	5.1	6.4	6.5	0.1
13	50.1	5.3	7.5	7.9	0.2
14	54.0	5.7	7.5	7.8	0.2
15	58.0	6.1	6.9	7.1	0.2
16	58.2	6.1	7.6	8.0	0.2

For all cores, there appears to be a slight difference between the air voids measured by SSD and vacuum-sealed device. Since the water absorption was small for each of the cores the difference was very small. Since the air voids determined from

vacuum-sealed device was used in the analysis for the previous part in this research, it was decided to utilize the air voids from vacuum sealed device in this analysis for consistency. This is assumed to be the most accurate measure of density. To determine the minimum t/NMAS for this mix, the relationship of air voids and thickness was evaluated and the result illustrated in Figure 33.

A review of the data indicated that a polynomial function provided the best fit. The best-fit line indicates that as the thickness increased the air voids decreased until a point where additional thickness resulted in an increase in air voids. The recommended thickness range was selected as the point(s) where the air voids increased by 0.5 %. This number is somewhat arbitrary but it is realistic. Therefore, as shown in Figure 33, the recommended thickness range for 9.5 mm fine-graded mix is 32 to 55 mm. This does not mean that compaction cannot be obtained when outside of these limits but it is an indication that more compactive effort would be needed. So this recommended range should only be used as a guide and should not be a rigid requirement. The effect of t/NMAS on the measured density was determined from Figure 33. Data in the figure indicates that the lowest air voids (7.0% air voids) occurred at t/NMAS of 4.4. At a ratio of 2 the void level was 2.5% higher, at a ratio of 3 the void level was 1.0% higher, at a ratio of 4 the void level was 0.1% higher and at a ratio of 5 the void level was 0.1% higher.

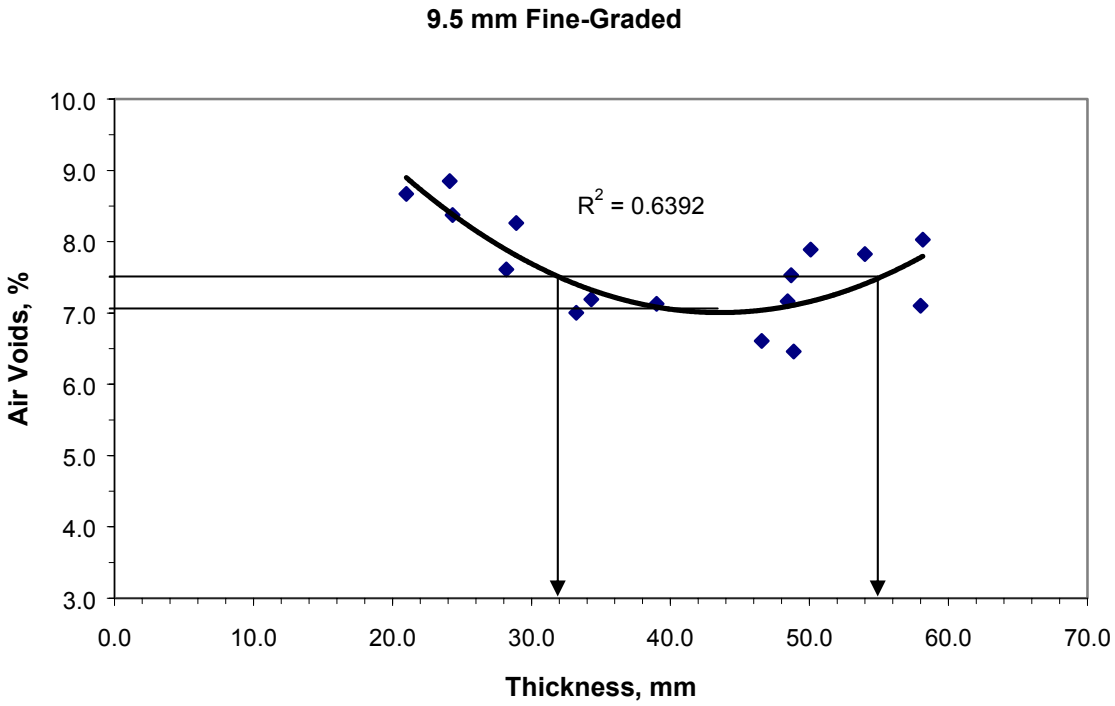

Figure 33: Relationship of Air Voids and Thickness for 9.5 mm Fine-Graded

5.4.2 Section 2

Section 2 was constructed on August 7, 2003 and consisted of a range of 2.0 to 5.0 t/NMAS overlay of an existing HMA layer. The mixture was a 9.5 mm NMAS coarse-graded mixture. The length of the section was about 40 m and the width was about 3.5 m. The paving started from the thick mat and progressed toward the thinner. The weather conditions during the paving were 82°F, overcast, with calm wind. The existing surface temperature was 96°F.

The roller utilized in this section was an 11-ton steel drum roller HYPAC C778B with 78 inch drum width that could operate in vibratory or static mode. The rubber tire roller was a 15-ton HYPAC C560B with a tire pressure of 90 psi. For the one side of the

mat utilizing only steel drum roller, the initial rolling was performed with four passes in the vibratory mode at low amplitude and high frequency (3800 vpm) at a mix temperature of about 300^{o}F. This was followed with four passes of static mode. For the other side of the mat that incorporated a rubber tire roller as an intermediate roller, the breakdown rolling was performed with four passes in the vibratory mode operated at low amplitude and high frequency (3800 vpm). This was followed with five passes of rubber tire roller and finished with one pass of the steel roller in the static mode.

A total of 15 cores were obtained from the side that utilized only a steel drum roller and 16 cores from the side that incorporated the rubber tire roller. The test results of the cores for each side are presented in Tables 24 and 25. The results include the thickness of cores, t/NMAS, the air voids determined from AASHTO T166 and vacuum seal methods, and water absorption. To determine the minimum t/NMAS for this mix, the relationship of air voids from the vacuum seal device and thickness was evaluated for each rolling pattern and the result illustrated in Figure 34.

A review of the data indicated that a polynomial function provided the best fit. The best-fit lines indicate that as the thickness increased the air voids decreased to at a point where additional thickness resulted in increased in air voids. The plots also suggest that the side utilizing only a steel drum compactor had better compaction. As shown in Figure 34, the desired thickness range for 9.5 mm coarse-graded mix is 33 to 56 mm for compaction with a steel wheel roller and 28 to 44 for compaction with the steel and rubber tire roller. The effect of t/NMAS on the measured density was determined from Figure 34. Data in the figure indicates that the lowest in-place air voids (10% air voids for the steel wheel roller only and 10.5% air voids for the steel and rubber tire rollers)

Table 24: Thickness, t/NMAS, Air Voids, and Water Absorption for Section 2 (Steel)

Core No.	Thickness, mm	t/NMAS	Voids SSD, %	Voids Vacuum Sealed, %	Water Abs., %
1	20.0	2.1	11.6	11.6	0.9
2	20.5	2.2	12.0	12.0	0.6
3	22.5	2.4	11.5	11.7	0.9
4	25.0	2.6	12.2	12.1	1.2
5	29.0	3.1	11.2	11.6	1.2
6	32.0	3.4	9.9	10.1	0.6
7	36.0	3.8	10.9	11.1	0.8
8	38.0	4.0	9.3	9.8	0.7
9	38.5	4.1	9.3	9.5	0.5
10	41.0	4.3	9.2	9.4	0.3
11	43.5	4.6	9.9	10.3	0.4
12	46.0	4.8	9.8	10.0	0.4
13	48.0	5.1	8.8	9.0	0.6
14	51.0	5.4	10.2	10.5	0.5
15	54.0	5.7	10.5	10.6	0.7

Table 25: Thickness, t/NMAS, Air Voids, and Water Absorption for Section 2 (Rubber Tire)

Core No.	Thickness, mm	t/NMAS	Voids SSD, %	Voids Vacuum Sealed, %	Water Abs., %
1	18.7	2.0	11.7	12.6	0.3
2	19.0	2.0	11.1	12.6	1.4
3	19.0	2.0	10.1	10.6	0.6
4	19.7	2.1	11.3	12.4	0.7
5	20.0	2.1	10.7	11.5	0.4
6	24.3	2.6	10.4	11.5	0.2
7	27.3	2.9	10.5	11.1	1.2
8	30.0	3.2	9.9	10.1	0.5
9	32.7	3.4	10.1	10.6	1.3
10	34.0	3.6	10.1	10.6	1.0
11	35.3	3.7	10.7	11.1	2.4
12	38.0	4.0	9.5	10.1	0.8
13	42.3	4.5	9.5	9.9	1.0
14	44.0	4.6	9.5	9.7	0.6
15	48.0	5.1	10.5	10.8	1.0
16	49.0	5.2	12.2	12.6	1.1

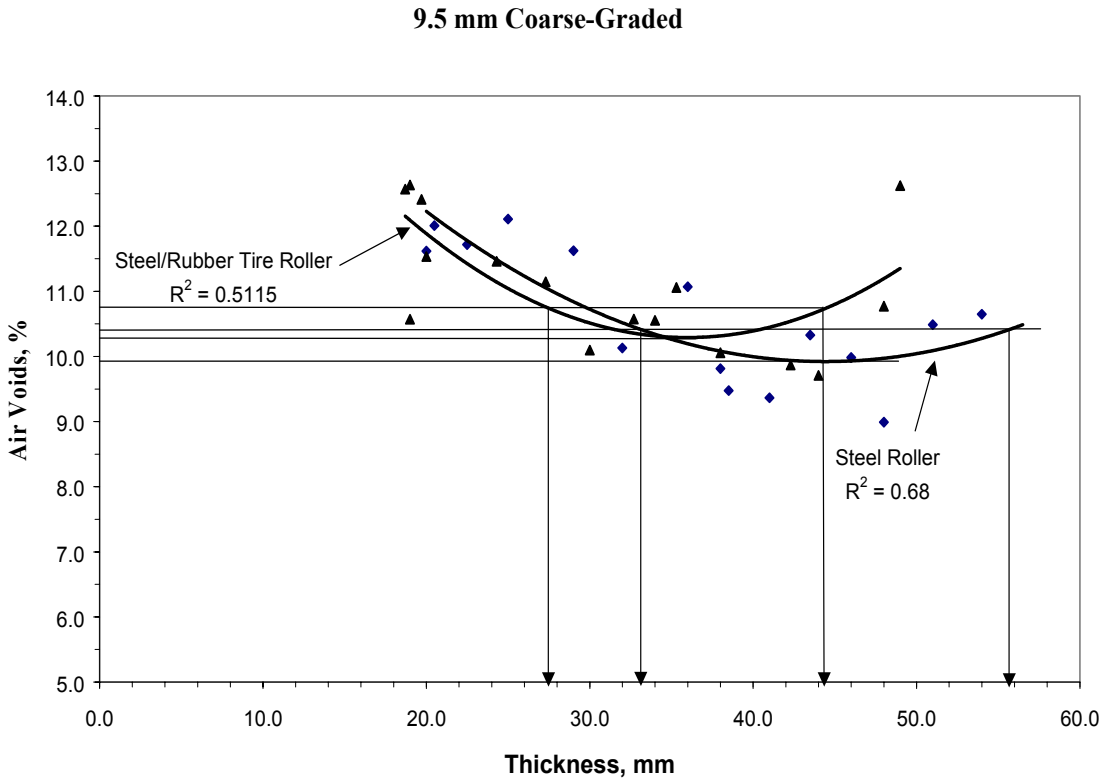

Figure 34: Relationship of Air Voids and Thickness for 9.5 mm Coarse-Graded

occurred at t/NMAS of 4.7 for the steel wheel roller and 3.8 for the rubber and steel wheel roller. For the compaction with a steel wheel roller, at a ratio of 2 the void level was 2.5% higher than the minimum, at a ratio of 3 the void level was 1.0% higher than the minimum, at a ratio of 4 the void level was 0.5% higher than the minimum, and at a ratio of 5 the void level was 0.0% higher. For the compaction with the steel and rubber tire rollers, at a ratio of 2 the void level was 2.0% higher than the minimum, at a ratio of 3 the void level was 0.5% higher than the minimum, at a ratio of 4 the void level was 0.0% higher than the minimum, and at a ratio of 5 the void level was 1.0% higher than the minimum.

5.4.3 Section 3

Section 3 was constructed on July 25, 2003 and ranged from a t/NMAS of 2.0 to 5.0 placed over an existing HMA layer. The mix was a 9.5 mm NMAS SMA. The length of the section was about 40 m and the width was about 3.5 m. The paving started from the thick mat and progressed to the thinner mat. The desired mat thickness was achieved by gradually adjusting the screed depth crank of the paver during the operation. The weather conditions during the paving were 95^{o}F, partly cloudy, with calm wind. The existing surface temperature was 115^{o}F.

The roller utilized in this section was an 11-ton steel drum roller HYPAC C778B with 78 in. wide drum that could operate in vibratory or static mode. The rubber tire roller was a 15-ton HYPAC C560B with a tire pressure of 90 psi. For the side of the mat utilizing only the steel drum roller, the initial rolling was performed with one pass of static rolling continued with five passes of vibratory mode operated in low amplitude and high frequency (3800 vpm) on the mat having temperature of about 320^{o}F. This was followed with two passes of static mode for the finish rolling. For the other side of the mat that incorporated a rubber tire roller as an intermediate roller, the breakdown rolling was performed with one pass of static and three passes of vibratory mode operated in low amplitude and high frequency (3800 vpm). This was followed with eight passes of rubber tire roller and finished with two passes of steel roller in static mode.

A total of 12 cores were obtained from the side that utilized only the steel drum roller and another 12 cores from the side that incorporated the rubber tire roller. The test results of the cores for each side are presented in Tables 26 and 27. The results include the thickness of cores, t/NMAS, the air voids determined from AASHTO T166 and

vacuum seal methods, and water absorption. To determine the range of recommended t/NMAS for this mix, the relationship of air voids from Vacuum seal device and thickness was evaluated for each rolling pattern and the results are illustrated in Figure 35.

A review of the data indicated that a polynomial function provided the best fit. The best-fit lines indicate that as the thickness increased the air voids decreased to a point where additional thickness resulted in increased air voids. The plots also suggest that the side utilizing only the steel drum compactor had better compaction. Rubber tire rollers are not used on SMA mixtures and this data confirms that there is no need to use the rubber tire roller. As shown in Figure 35, the recommended range for thickness for the 9.5 mm SMA mix is 36 to 50 mm for the compaction with a steel wheel roller and 25 to 48 mm for compaction with a steel and rubber tire roller. The effect of t/NMAS on the measured density was determined from Figure 35. Data in the figure indicates that the lowest in-place air voids (8.5% air voids for the steel wheel roller only and 10.3% air voids for the steel and rubber tire rollers) occurred at t/NMAS of 4.5 for the steel wheel roller and 3.8 for the rubber and steel wheel roller. For the compaction with a steel wheel roller, at a ratio of 2 the void level was 5.5% higher than the minimum, at a ratio of 3 the void level was 2.0% higher than the minimum, at a ratio of 4 the void level was 0.2% higher than the minimum, and at a ratio of 5 the void level was 0.2% higher than the minimum. For the compaction with the steel and rubber tire rollers, at a ratio of 2 the void level was 1.2% higher than the minimum, at a ratio of 3 the void level was 0.2% higher than the minimum, at a ratio of 4 the void level was 0.0% higher than the minimum, and at a ratio of 5 the void level was 0.5% higher than the minimum.

Table 26: Thickness, t/NMAS, Air Voids, and Water Absorption for Section 3 (Steel)

Core No.	Thickness, mm	t/NMAS	Voids SSD, %	Voids Vacuum Sealed, %	Water Abs., %
1	21.0	2.2	10.9	12.6	3.7
2	24.5	2.6	10.1	11.0	3.2
3	26.5	2.8	8.9	10.4	2.3
4	29.0	3.1	9.6	11.2	2.6
5	33.0	3.5	8.5	9.4	2.4
6	35.5	3.7	8.9	9.8	2.6
7	38.5	4.1	7.9	8.8	2.0
8	43.0	4.5	7.3	7.7	1.8
9	47.0	4.9	7.6	8.7	2.2
10	48.0	5.1	8.1	8.7	2.1
11	49.0	5.2	7.7	8.5	2.2
12	52.0	5.5	9.2	10.1	3.5

Table 27: Thickness, t/NMAS, Air Voids, and Water Absorption for Section 3 (RubberTire)

Core No.	Thickness, mm	t/NMAS	Voids SSD, %	Voids Vacuum Sealed, %	Water Abs., %
1	20.0	2.1	9.9	11.3	3.3
2	23.0	2.4	9.6	10.5	3.7
3	26.0	2.7	9.1	10.5	3.0
4	27.0	2.8	9.8	11.0	4.1
5	30.0	3.2	9.7	11.0	4.2
6	30.0	3.2	9.5	11.7	2.8
7	34.0	3.6	8.9	9.7	3.2
8	38.0	4.0	8.1	8.8	2.7
9	41.0	4.3	9.3	10.6	3.1
10	43.0	4.5	9.5	10.7	4.0
11	47.0	4.9	9.7	11.1	3.9
12	50.0	5.3	9.7	10.9	3.6

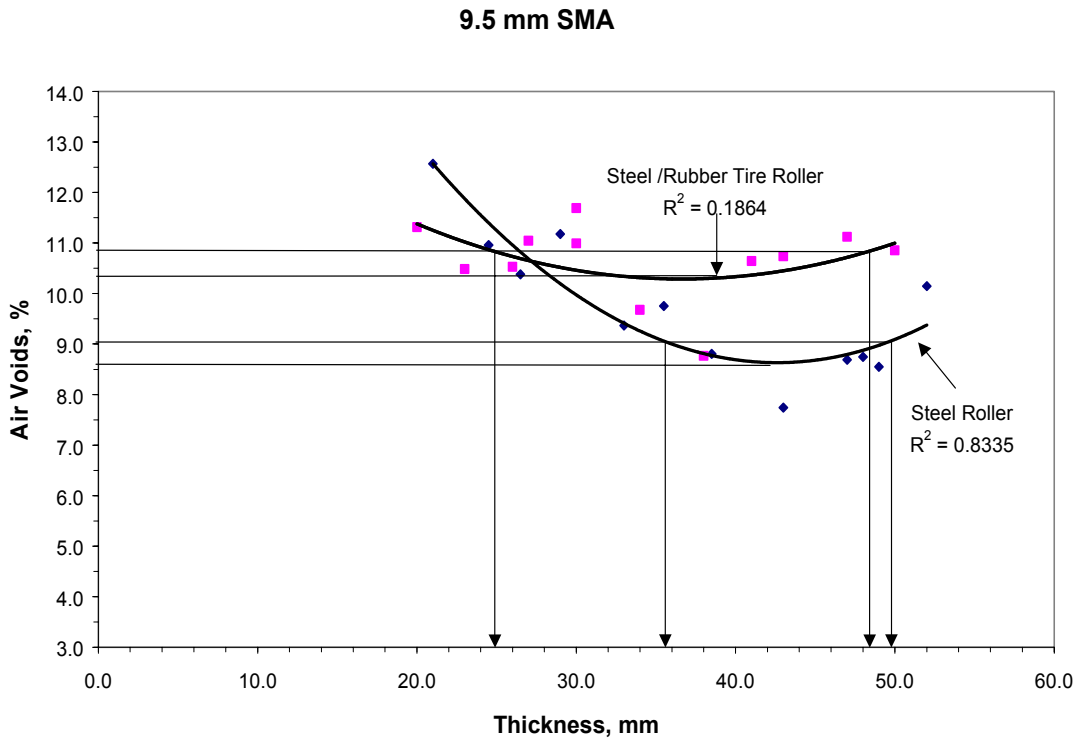

Figure 35: Relationship of Air Voids and Thickness for 9.5 mm SMA

5.4.4 Section 4

Section 4 was constructed on August 12, 2003 and consisted of a t/NMAS that ranged from 2.0 to 5.0 placed over an existing HMA layer. The mix was a 12.5 mm NMAS SMA. The length of the section was about 40 m and the width was about 3.5 m. The paving started from the thinner portion and proceeded toward the thicker portion of the mat. The desired mat thickness was achieved by gradually adjusting the screed depth crank of the paver during the operation. The weather conditions during the paving were 80^{o}F, overcast, with calm wind. The existing surface temperature was 85^{o}F.

The roller utilized in this section was an 11-ton steel drum roller HYPAC C778B with a 78 in. wide drum that could operate in vibratory or static mode. The rubber tire

roller was a 15-ton HYPAC C560B with a tire pressure of 90 psi. For the one side of the mat utilizing only steel drum roller, the initial rolling was performed with four passes in the vibratory mode operated at low amplitude and high frequency (3800 vpm). The mat temperature was approximately 320^{o}F. This was followed with three passes in the static mode including finish rolling. For the other side of the mat that incorporated a rubber tire roller as an intermediate roller, the initial rolling was performed with four passes in the vibratory mode operated at low amplitude and high frequency (3800 vpm). This was followed with four passes of the rubber tire roller and finished with one pass of steel roller in the static mode.

A total of 21 cores were obtained from the side that utilized only a steel drum roller and 21 cores from the side that incorporated the rubber tire roller. The test results of the cores for each side are presented in Tables 28 and 29. The results include the thickness of cores, n/NMAS, the air voids determined from AASHTO T166 and vacuum-sealed methods, and water absorption. To determine the recommended t/NMAS for this mix, the relationship of air voids from the vacuum sealed device and thickness was evaluated for each rolling pattern and the results were illustrated in Figure 36.

The best-fit lines indicate that as the thickness increased the air voids decreased until a point where excessive thickness resulted in increased air voids. The plots also suggest that the side utilizing only the steel drum compactor had better compaction. As shown in Figure 36, the suggested minimum thickness for 12.5 mm SMA mix is 48 for compaction with steel wheel roller and 57 for compaction with steel and rubber tire rollers. For these mixes the densification was still increasing as the t/NMAS was increasing even at the thicker portions. Also the curve did not fit the data as well as

desired so the plot of the points were actually used to select the suggested t/NMAS number. Note in the plots that the data points continue downward with increasing t/NMAS up to a point and then the data points remain relatively constant.

The effect of t/NMAS on the measured density was determined from Figure 36. Data in the figure indicates that the lowest in-place air voids (4.7% air voids for the steel wheel roller only and 7.5% air voids for the steel and rubber tire rollers) occurred at t/NMAS of 4.5 for the steel wheel roller and 4.8 for the rubber and steel wheel roller. For the compaction with a steel wheel roller, at a ratio of 2 the void level was 11.3% higher than the minimum, at a ratio of 3 the void level was 3.3% higher than the minimum, at a ratio of 4 the void level was 0.3% higher than the minimum, and at a ratio of 5 the void

Table 28: Thickness, t/NMAS, Air Voids, and Water Absorption for Section 4 (Steel)

Core No.	Thickness, mm	t/NMAS	Voids SSD, %	Voids Vacuum Sealed, %	Water Abs., %
1	25.0	2.0	12.4	17.9	6.8
2	27.3	2.2	10.3	13.7	6.3
3	28.3	2.3	9.8	11.0	4.7
4	34.7	2.8	7.9	9.7	2.7
5	37.7	3.0	6.2	7.4	1.6
6	37.7	3.0	6.7	8.5	2.1
7	38.0	3.0	7.4	7.6	2.7
8	38.7	3.1	6.3	6.4	2.4
9	40.3	3.2	5.4	5.5	1.2
10	42.3	3.4	5.0	6.7	1.2
11	44.0	3.5	5.1	5.1	1.0
12	47.0	3.8	5.0	5.7	0.9
13	49.0	3.9	5.5	5.6	1.3
14	52.0	4.2	4.9	6.6	0.7
15	52.3	4.2	5.3	6.0	1.1
16	52.7	4.2	5.6	5.7	1.5
17	54.3	4.3	5.0	5.6	0.7
18	58.0	4.6	4.5	5.2	0.6
19	61.0	4.9	4.9	5.2	0.8
20	63.0	5.0	4.5	5.1	0.6
21	65.0	5.2	4.0	4.1	0.4

Table 29: Thickness, t/NMAS Air Voids, and Water Absorption for Section 4 (Rubber Tire)

Core No.	Thickness, mm	t/NMAS	Voids SSD, %	Voids Vacuum Sealed, %	Water Abs., %
1	25.3	2.0	7.6	16.2	4.0
2	27.3	2.2	7.9	11.7	3.9
3	27.3	2.2	9.4	11.7	5.9
4	33.3	2.7	10.7	12.4	5.0
5	35.3	2.8	8.6	12.1	4.0
6	38.7	3.1	8.8	11.7	5.0
7	40.3	3.2	7.7	9.7	3.8
8	40.3	3.2	7.8	9.6	4.1
9	42.0	3.4	7.5	10.1	3.5
10	42.0	3.4	8.3	10.1	3.9
11	43.0	3.4	8.0	10.1	4.0
12	44.7	3.6	7.2	8.7	3.3
13	45.7	3.7	7.1	8.2	2.0
14	50.0	4.0	7.2	8.1	2.4
15	53.0	4.2	7.4	10.2	3.1
16	53.0	4.2	6.8	10.0	2.0
17	55.7	4.5	6.4	7.0	2.0
18	59.3	4.7	6.8	8.0	1.3
19	61.7	4.9	6.3	7.4	1.5
20	64.3	5.1	6.2	7.1	1.3
21	64.3	5.1	6.5	7.5	1.5

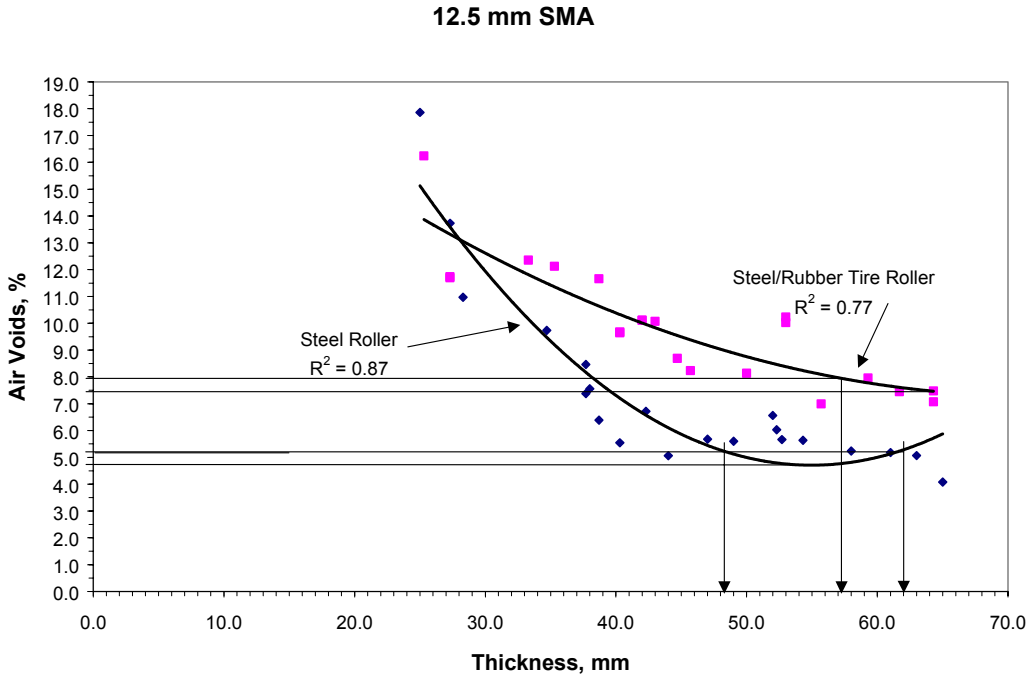

Figure 36: Relationship of Air Voids and Thickness for 12.5 mm SMA

level was 0.5% higher. For the compaction with the steel and rubber tire rollers, at a ratio of 2 the void level was 6.5% higher than the minimum, at a ratio of 3 the void level was 3.5% higher than the minimum, at a ratio of 4 the void level was 0.5% higher than the minimum, and at a ratio of 5 the void level was 0.0% higher than the minimum.

5.4.5 Section 5

Section 5 was constructed on July 16, 2003 and consisted of a t/NMAS that ranged from 2.0 to 5.0 placed over an existing HMA. The mix was a 19.0 mm NMAS fine-graded HMA. The length of the section was about 40 m and the width was about 3.5 m. The paving started on the thin end of the section and proceeded to the thicker mat. The desired mat thickness was achieved by gradually adjusting the screed depth crank of the paver during the operation. The weather conditions during the paving were 90^{o}F, clear, with calm wind. The existing surface temperature was 96^{o}F.

The roller utilized in this section was an 11 ton steel roller HYPAC C778B with 78 in. wide drum that operated in vibratory and static mode. The rubber tire roller available did not meet the tire pressure requirement and the results were omitted from the analysis for this section. The breakdown rolling was performed with four passes in the vibratory mode operated in low amplitude and high frequency (3800 vpm). The mat temperature was approximately 300^{o}F. Three passes of the roller in the static mode and one additional pass for finish rolling followed this initial rolling.

A total of 20 cores were obtained from this section and the test results of the cores are presented in Table 30. The results included the thickness of cores, t/NMAS, the air voids determined from AASHTO T166 and vacuum seal methods, and water absorption.

To determine the minimum t/NMAS for this mix, the relationship between air voids and thickness was evaluated and the result illustrated in Figure 37.

The best-fit line indicated that as the thickness increased the air voids decreased until a point where additional thickness resulted in increased air voids. As shown in Figure 37, the recommended thickness range for the 19.0 mm fine-graded mix is 59 to 87 mm. The effect of t/NMAS on the measured density was determined from Figure 37. Data in the figure indicates that the lowest in-place air voids (6.2% air voids) occurred at t/NMAS of 3.8. At a ratio of 2 the void level was 3.1% higher than the minimum, at a ratio of 3 the void level was 0.6% higher than the minimum, at a ratio of 4 the void level was 0.0% higher than the minimum, and at a ratio of 5 the void level was 1.3% higher than the minimum.

Table 30: Thickness, t/NMAS, Air Voids, and Water Absorption for Section 5

Core No.	Thickness, mm	t/NMAS	Voids SSD, %	Voids Vacuum Sealed, %	Water Abs., %
1	38.0	2.0	8.9	9.5	0.8
2	45.0	2.4	7.4	8.7	0.3
3	46.2	2.4	6.7	6.8	0.2
4	48.5	2.6	6.7	7.1	0.2
5	50.0	2.6	7.5	7.9	0.2
6	50.0	2.6	7.4	7.6	0.3
7	53.1	2.8	6.4	7.0	0.1
8	54.4	2.9	7.0	7.2	0.1
9	56.5	3.0	6.4	6.9	0.2
10	58.0	3.1	6.5	6.5	0.4
11	61.4	3.2	6.2	6.5	0.1
12	64.0	3.4	7.0	7.1	0.3
13	67.9	3.6	5.8	6.2	0.2
14	72.8	3.8	5.5	5.7	0.2
15	75.0	3.9	6.4	6.4	0.2
16	78.0	4.1	6.0	5.8	0.2
17	81.7	4.3	6.2	6.3	0.1
18	90.0	4.7	7.0	7.0	0.2
19	91.0	4.8	6.0	7.4	0.2
20	98.0	5.2	7.5	7.5	0.1

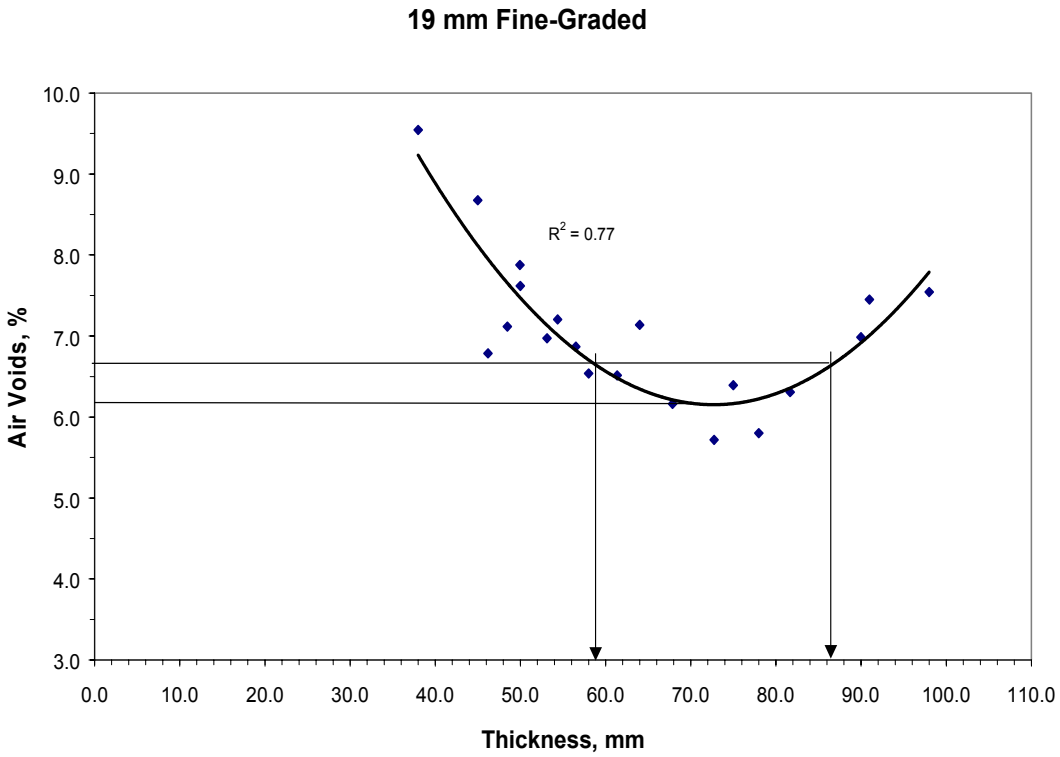

Figure 37: Relationship of Air Voids and Thickness for 19.0 mm Fine-Graded

5.4.6 Section 6

Section 6 was constructed on August 6, 2003 and consisted of a t/NMAS that ranged from 2.0 to 5.0 placed over an existing HMA. The mix was a 19.0 mm NMAS coarse-graded HMA. The length of the section was about 40 m and the width was about 3.5 m. The paving started from the thinner end and proceeded to the thicker end. The desired mat thickness was achieved by gradually adjusting the screed depth crank of the paver during the operation. The weather conditions during the paving were 79^{o}F, cloudy, with calm wind. The existing surface temperature was 84^{o}F.

The roller utilized in this section was an 11-ton steel drum roller HYPAC C778B with 78 in. wide drum that could operate in vibratory and static mode. The rubber tire

roller was a 15-ton HYPAC C560B with a tire pressure of 90 psi. For the one side of the mat utilizing only steel drum roller, the initial rolling was performed with four passes in the vibratory mode operated at low amplitude and high frequency (3800 vpm). The mat temperature was approximately 300^{o}F. This initial rolling was followed with six passes in the static mode. For the other side of the mat that incorporated a rubber tire roller as an intermediate roller, the initial rolling was performed with four passes in the vibratory mode operated in low amplitude and high frequency (3800 vpm). This initial rolling was followed with four passes of rubber tire roller two passes with a steel wheel roller in the static mode.

A total of 19 cores were obtained from the side that utilized only a steel drum roller and 17 cores from the side that incorporated the rubber tire roller. The test results of the cores for each side are presented in Tables 31 and 32. The results include the thickness of cores, t/NMAS, the air voids determined from AASHTO T166 and vacuum seal methods, and water absorption. There appears to be a slight difference between the air voids measured by SSD and vacuum seal device. To determine the minimum t/NMAS for this mix, the relationship between air voids from vacuum seal device and thickness was evaluated for each rolling pattern and the results are illustrated in Figure 38. The best-fit lines indicate that as the thickness increased the air voids decreased until a point where additional thickness resulted in increased air voids. The plots also suggest that the side utilizing the rubber tire roller had better compaction. As shown in Figure 38, the recommended minimum thickness for 19.0 mm coarse-graded mix is 60 mm for compaction with the steel and rubber tire rollers. There is too much scatter in the data to make a good selection of a recommended value for compaction with a steel wheel roller.

Table 31: Thickness, t/NMAS, Air Voids, and Water Absorption for Section 6

(Steel)

Core No.	Thickness, mm	t/NMAS	Voids SSD, %	Voids Vacuum Seal Method, %	Water Abs., %
1	40.0	2.1	7.0	8.0	1.1
2	44.0	2.3	5.8	7.7	1.3
3	48.0	2.5	6.0	6.8	0.8
4	50.7	2.7	7.5	8.9	1.7
5	52.3	2.8	6.3	7.4	1.0
6	54.0	2.8	4.9	5.5	0.8
7	56.0	2.9	8.0	8.4	2.7
8	60.0	3.2	8.0	9.1	3.4
9	61.0	3.2	9.0	9.8	3.6
10	62.7	3.3	8.2	9.6	2.9
11	66.3	3.5	7.1	8.7	3.2
12	67.0	3.5	8.4	9.0	2.9
13	72.0	3.8	6.6	7.0	2.5
14	77.0	4.1	6.8	7.2	2.4
15	79.0	4.2	5.5	5.9	1.4
16	83.0	4.4	6.9	7.9	2.5
17	86.0	4.5	5.3	5.8	1.1
18	87	4.6	4.3	5.3	0.9
19	96.0	5.1	5.5	6.2	1.9

Table 32: Thickness, t/NMAS, Air Voids, and Water Absorption for Section 6

(Rubber Tire)

Core No.	Thickness, mm	t/NMAS	Voids SSD, %	Voids Vacuum Seal Method, %	Water Abs., %
1	40.0	2.1	6.7	6.6	0.7
2	42.0	2.2	6.3	7.4	0.7
3	44.0	2.3	5.8	7.9	0.8
4	46.0	2.4	5.6	6.1	0.4
5	55.0	2.9	6.2	6.4	1.6
6	56.0	2.9	6.8	6.8	1.1
7	61.0	3.2	6.3	6.4	1.4
8	65.0	3.4	5.3	5.2	0.7
9	66.3	3.5	5.8	6.1	2.0
10	70.0	3.7	5.9	5.9	1.3
11	71.0	3.7	6.3	6.3	1.6
12	75.0	3.9	6.2	6.2	1.1
13	78.3	4.1	4.7	4.6	1.0
14	82.0	4.3	5.4	5.6	1.3
15	84.7	4.5	5.7	6.1	1.6
16	89.3	4.7	5.1	5.1	0.7
17	92.0	4.8	6.2	6.4	1.0

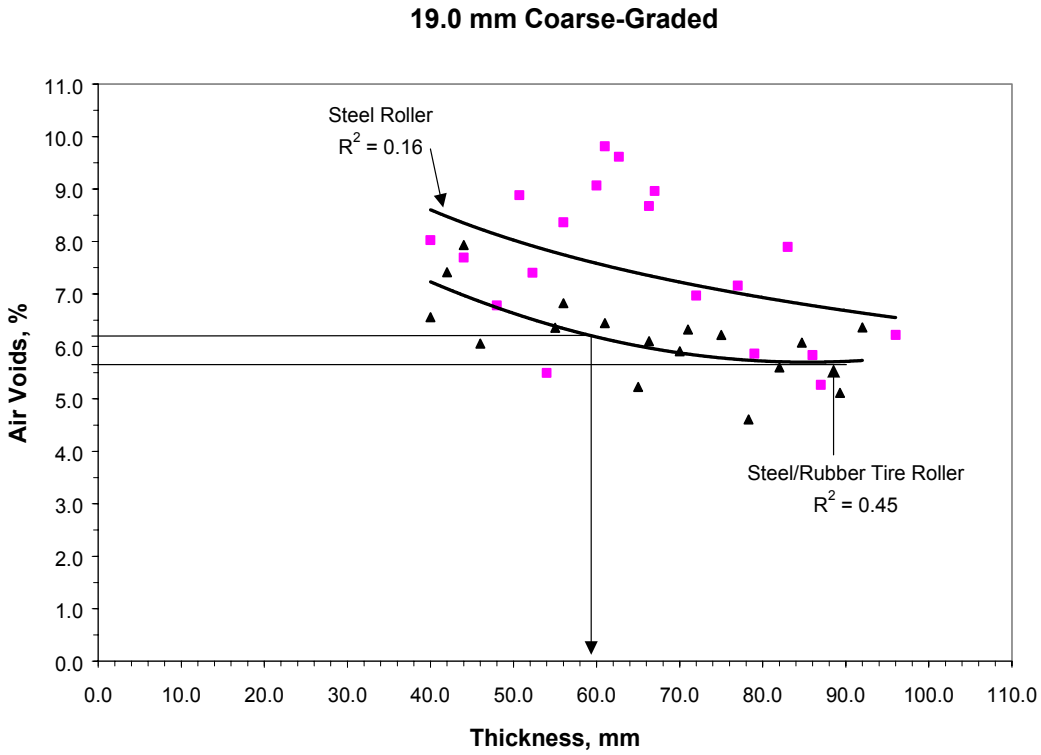

Figure 38: Relationship of Air Voids and Thickness for 19.0 mm Coarse-Graded

The effect of t/NMAS on the measured density was determined from Figure 38. Data in the figure indicates that the lowest in-place air voids (5.7% for the steel and rubber tire roller, the steel wheel roller alone was not used since it produced too much scatter in the data) occurred at t/NMAS of 4.5. At a ratio of 2 the void level was 1.8% higher than the minimum, at a ratio of 3 the void level was 0.6% higher than the minimum, at a ratio of 4 the void level was 0.1% higher than the minimum, and at a ratio of 5 the void level was 0.1% higher than the minimum.

5.4.7 Section 7

Section 7 was constructed on August 14, 2003 and consisted of a t/NMAS that ranged from 2.0 to 5.0 placed over an existing HMA. The mix consisted of a 19.0 mm

NMAS coarse-graded HMA and utilized modified asphalt. The length of the section was about 40 m and the width was about 3.5 m. The paving started from the thick portion and proceeded to the thinner. The desired mat thickness was achieved by gradually adjusting the screed depth crank of the paver during the operation. The weather conditions during the paving were 90^{o}F, clear, with calm wind. The existing surface temperature was 120^{o}F.

The roller utilized in this section was an 11-ton steel drum roller HYPAC C778B with 78 in. wide drum that could operate in vibratory or static mode. The rubber tire roller was a 15-ton HYPAC C560B with a tire pressure of 90 psi. For the one side of the mat utilizing only steel drum roller, the initial rolling was performed with four passes in the vibratory mode operated in low amplitude and high frequency (3800 vpm). The mat thickness had a temperature of about 330^{o}F. This was followed with another five passes in the vibratory mode operated at low amplitude and high frequency (3800 vpm). There was one additional pass with the steel wheel roller to finish the mat. For the other side of the mat that incorporated a rubber tire roller as an intermediate roller, the initial rolling was performed with two passes in the vibratory mode operated at low amplitude and high frequency (3800 vpm). This was followed with ten passes of rubber tire roller and finished with two passes of steel roller in the static mode.

A total of 23 cores were obtained from the side that utilized only the steel drum roller and 26 cores from the side that incorporated the rubber tire roller. The test results of the cores for each side are presented in Tables 33 and 34. The results include the thickness of cores, t/NMAS, the air voids determined from AASHTO T166 and vacuum seal methods, and water absorption. For all cores, there appears to be a difference

Table 33: Thickness, t/NMAS, Air Voids, and Water Absorption for Section 7 (Steel)

Core No.	Thickness, mm	t/NMAS	Voids SSD, %	Voids Vacuum Seal Method, %	Water Abs., %
1	37.3	2.0	10.0	11.8	4.9
2	42.0	2.2	8.8	10.9	4.3
3	45.0	2.4	6.6	6.9	1.5
4	45.7	2.4	7.4	8.2	2.7
5	47.0	2.5	7.9	8.7	1.3
6	50.7	2.7	6.0	6.4	1.7
7	51.7	2.7	6.4	6.8	1.9
8	55.7	2.9	6.7	7.2	2.1
9	58.7	3.1	6.3	7.1	2.0
10	59.7	3.1	6.4	6.8	2.0
11	59.7	3.1	6.3	7.1	1.8
12	60.3	3.2	5.7	6.3	1.0
13	63.3	3.3	5.7	6.0	0.8
14	63.7	3.4	5.4	5.9	1.0
15	67.3	3.5	4.7	4.8	0.4
16	72.3	3.8	6.3	7.2	2.1
17	76.3	4.0	5.4	6.0	1.4
18	82.7	4.4	5.7	6.3	1.3
19	85.7	4.5	6.0	6.7	1.7
20	90.7	4.8	5.6	6.3	1.2
21	96.3	5.1	4.8	5.4	1.1
22	99.3	5.2	4.9	5.4	1.2
23	99.7	5.2	6.0	8.0	1.9

between the air voids measured by SSD and vacuum seal device. To determine the minimum t/NMAS for this mix, the relationship of air voids from vacuum seal device and thickness was evaluated for each rolling pattern and the result illustrated in Figure 39.

The best-fit lines indicate that as the thickness increased the air voids decreased until a point where additional thickness resulted in an increase in air voids. The plots also suggested that the side utilizing only the steel drum compactor had better compaction. As shown in Figure 39, the minimum thickness range for 19.0 mm coarse-graded with modified asphalt mix is 65 to 92 mm. The effect of t/NMAS on the measured density was determined from Figure 39. Data in the figure indicates that the lowest in-

Table 34: Thickness, t/NMAS, Air Voids, and Water Absorption for Section 7 (Rubber Tire)

Core No.	Thickness, mm	t/NMAS	Voids SSD, %	Voids Vacuum Seal Method, %	Water Abs., %
1	36.3	1.9	12.5	15.2	6.1
2	38.7	2.0	9.5	13.7	4.0
3	38.7	2.0	10.2	13.0	5.2
4	38.7	2.0	10.1	13.9	5.3
5	45.3	2.4	8.9	10.3	3.5
6	47.3	2.5	8.1	9.7	2.6
7	48.3	2.5	11.0	12.9	5.3
8	54.7	2.9	9.4	11.1	5.0
9	58.7	3.1	8.9	9.7	2.3
10	60.7	3.2	8.1	9.0	1.8
11	64.3	3.4	8.7	11.2	4.1
12	66.0	3.5	8.0	9.6	3.3
13	66.0	3.5	8.8	10.5	4.7
14	69.7	3.7	8.0	8.7	3.2
15	72.7	3.8	7.0	7.5	1.7
16	72.7	3.8	7.7	8.1	2.9
17	77.3	4.1	6.7	7.6	1.9
18	81.0	4.3	7.7	8.7	2.6
19	85.0	4.5	6.4	6.9	1.6
20	89.0	4.7	6.9	7.5	1.7
21	91.0	4.8	6.3	7.1	1.3
22	98.0	5.2	7.1	9.1	2.6
23	110.7	5.8	6.6	6.9	1.8
24	113.7	6.0	7.0	9.4	1.9
25	113.7	6.0	6.3	7.4	1.8
26	116.0	6.1	6.8	7.2	1.6

place air voids (5.6% air voids for the steel wheel roller only and 7.4% air voids for the steel and rubber tire rollers) occurred at t/NMAS of 4.2 for the steel wheel roller and 5.3 for the rubber and steel wheel roller. For the compaction with a steel wheel roller, at a ratio of 2 the void level was 4.9% higher than the minimum, at a ratio of 3 the void level was 1.3% higher than the minimum, at a ratio of 4 the void level was 0.0% higher than the minimum, and at a ratio of 5 the void level was 0.8% higher. For the compaction with the steel and rubber tire rollers, at a ratio of 2 the void level was 6.1% higher than the minimum, at a ratio of 3 the void level was 3.4% higher than the minimum, at a ratio

of 4 the void level was 0.8% higher than the minimum, and at a ratio of 5 the void level was 0.0% higher than the minimum.

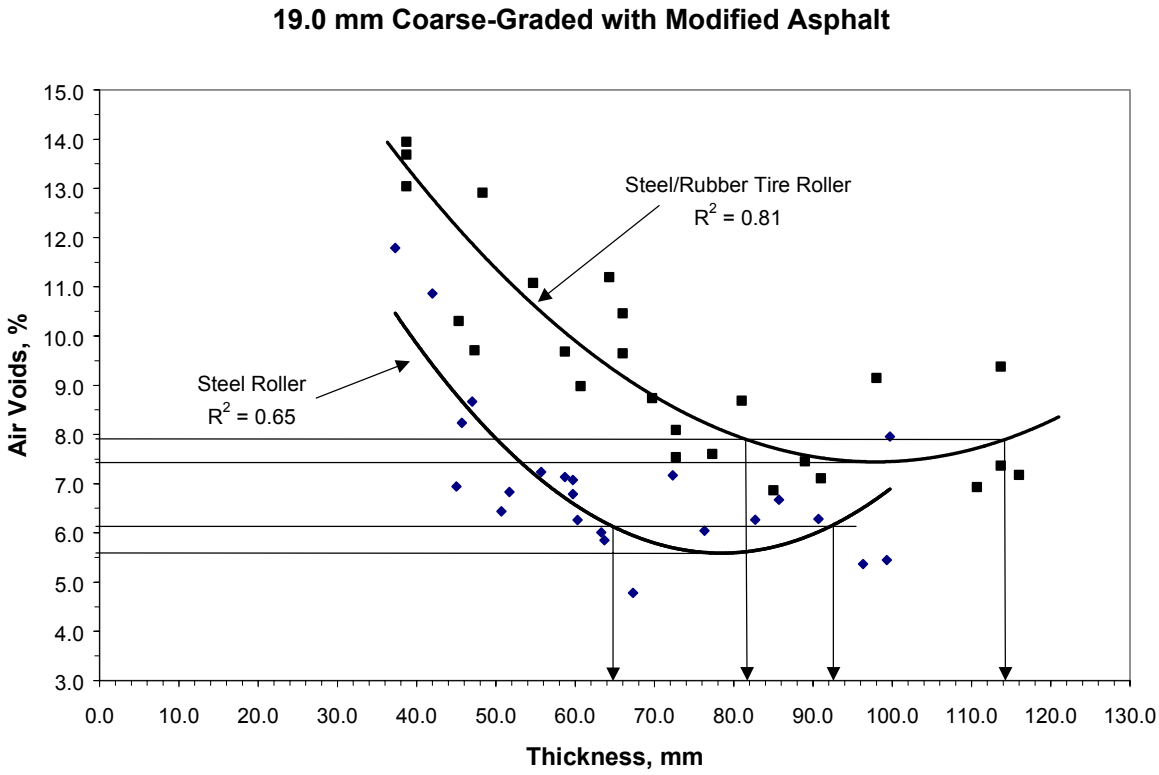

Figure 39: Relationship of Air Voids and Thickness for 19.0 mm Coarse-Graded with Modified Asphalt

5.5 Evaluation of the Effect of Temperatures on the Relationships Between Density and t/NMAS from the Field Experiment

Recall from the field experiment that three locations were selected for temperature measurements for each section; one near the beginning of the section, one near the middle, and one near the end of section. To determine the effect of temperature on the density, the temperature at 20 minutes after placement of mix at each location was selected (20 minutes was selected since this provides a reasonable compaction time).

Since the mixes in this study used two different types of asphalt binder, (PG 67-22 and PG 76-22), the temperatures at 20 minutes were normalized by subtracting the high temperature grade of the asphalt type from the temperatures at 20 minutes. Table 35 presents the t/NMAS, the average temperature readings at 20 minutes, the asphalt high temperature grade, and the difference between mix temperature and high temperature grade. The differences in temperature were plotted against the t/NMAS together with the core densities for each section as shown in Figures 40 through 46.

Table 35: T/NMAS, Temperature at 20 min., Asphalt High Temperature Grade, and Difference in Temperature

Section/Mix	t/NMAS	Temp. at 20 min., °C	Asphalt Grade, PG	Difference
1	2.5	60	67	-7
9.5mmFG	3.6	82	67	15
	5.1	95	67	28
2	2.1	64	67	-3
9.5mmCG	2.4	72	67	5
	5.1	105	67	38
3	2.2	65	76	-11
9.5mmSMA	3.7	100	76	24
	5.2	112	76	36
4	2.2	72	76	-4
12.5mmSMA	3.1	118	76	42
	3.8	120	76	44
5	2.6	124	67	57
19mmFG	3.0	122	67	55
	5.2	130	67	63
6	2.1	82	67	15
19mmCG	3.2	120	67	53
	5.1	118	67	51
7	2.7	86	76	10
19mmCG	3.8	120	76	44
	5.2	142	76	66

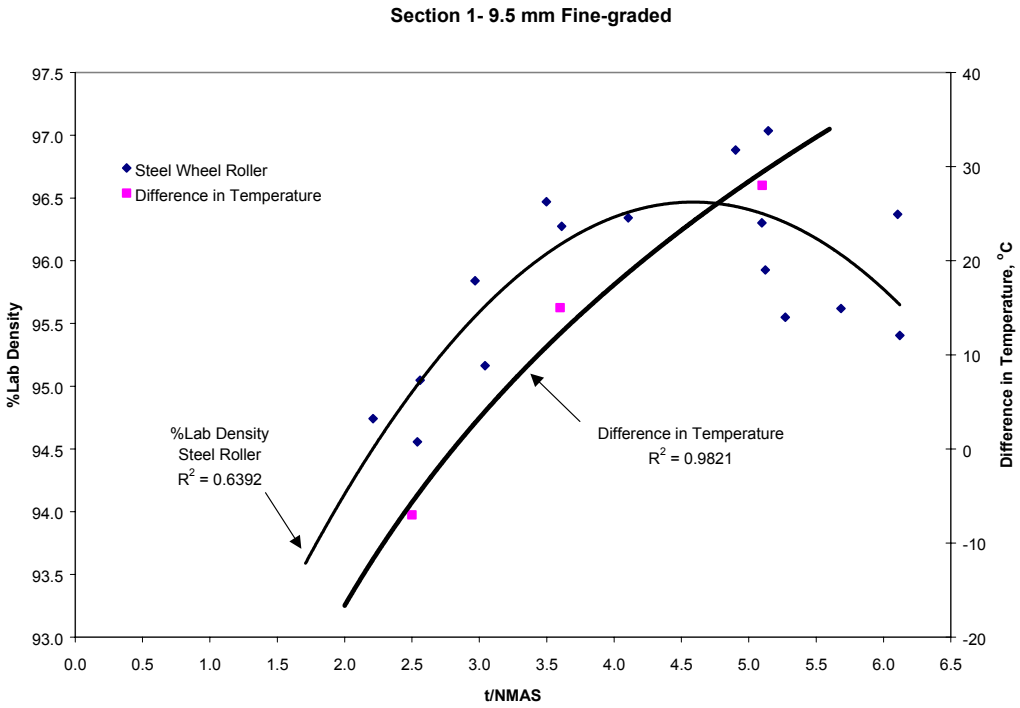

Figure 40: Relationships Between Density, t/NMAS and Temperature for Section 1

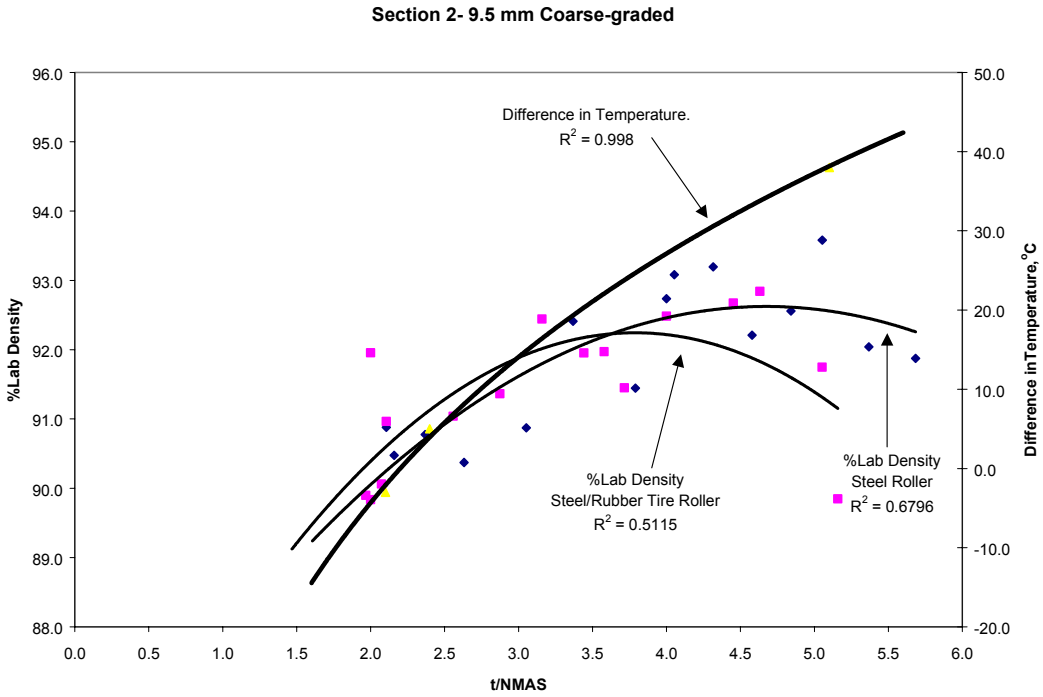

Figure 41: Relationships Between Density, t/NMAS and Temperature for Section 2

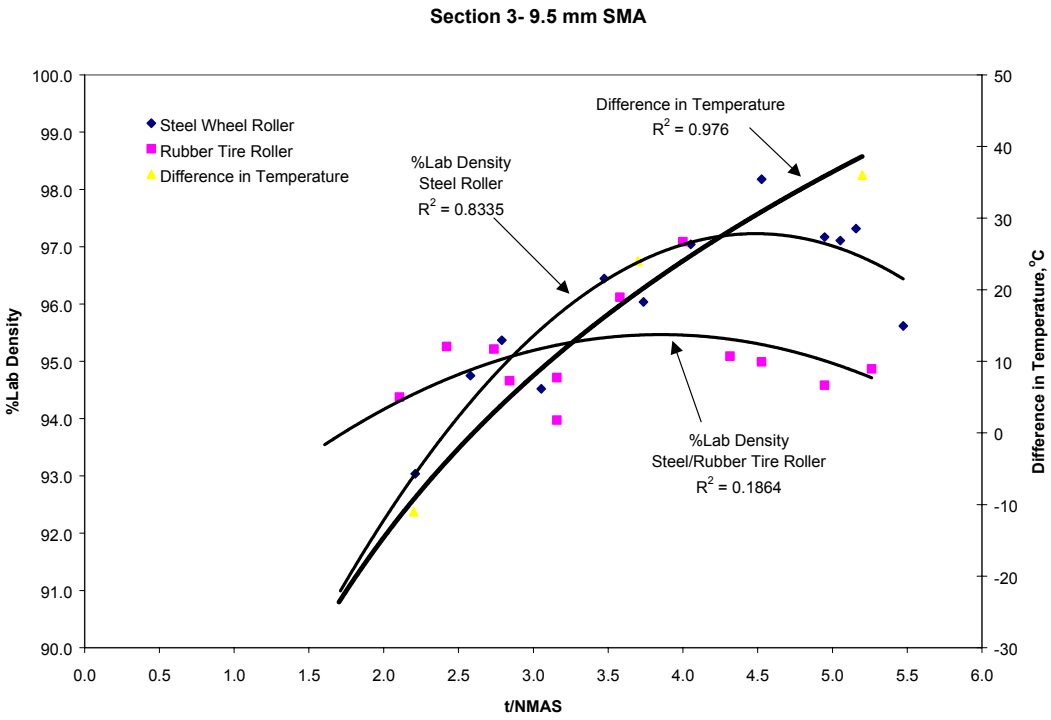

Figure 42: Relationships Between Density, t/NMAS and Temperature for Section 3

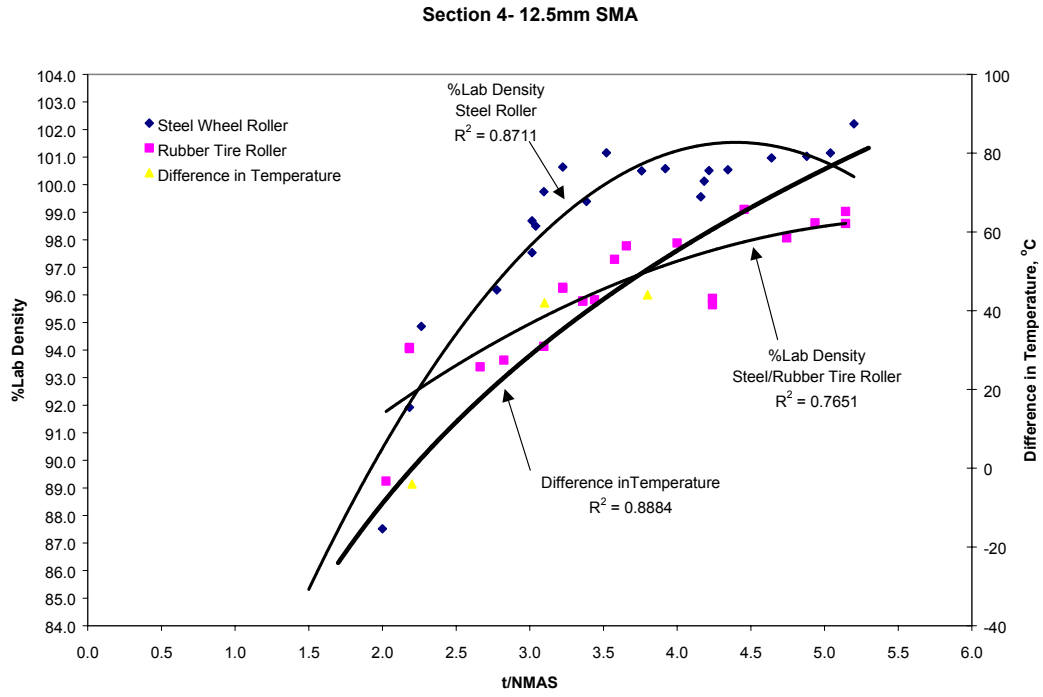

Figure 43: Relationships Between Density, t/NMAS and Temperature for Section 4

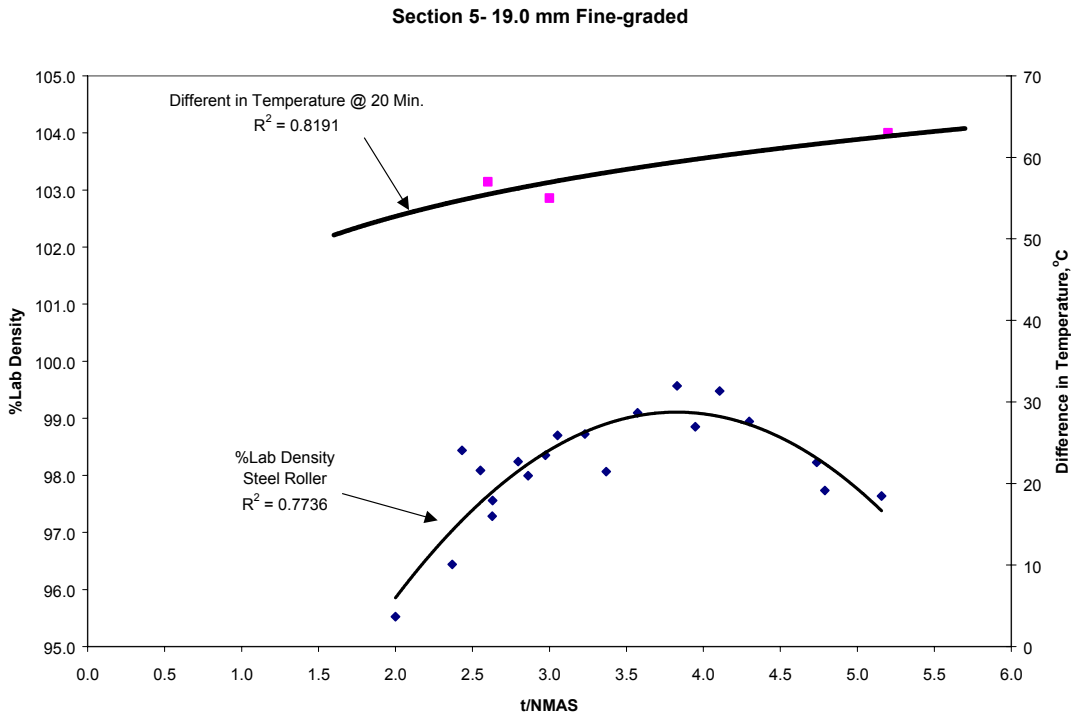

Figure 44: Relationships Between Density, t/NMAS and Temperature for Section 5

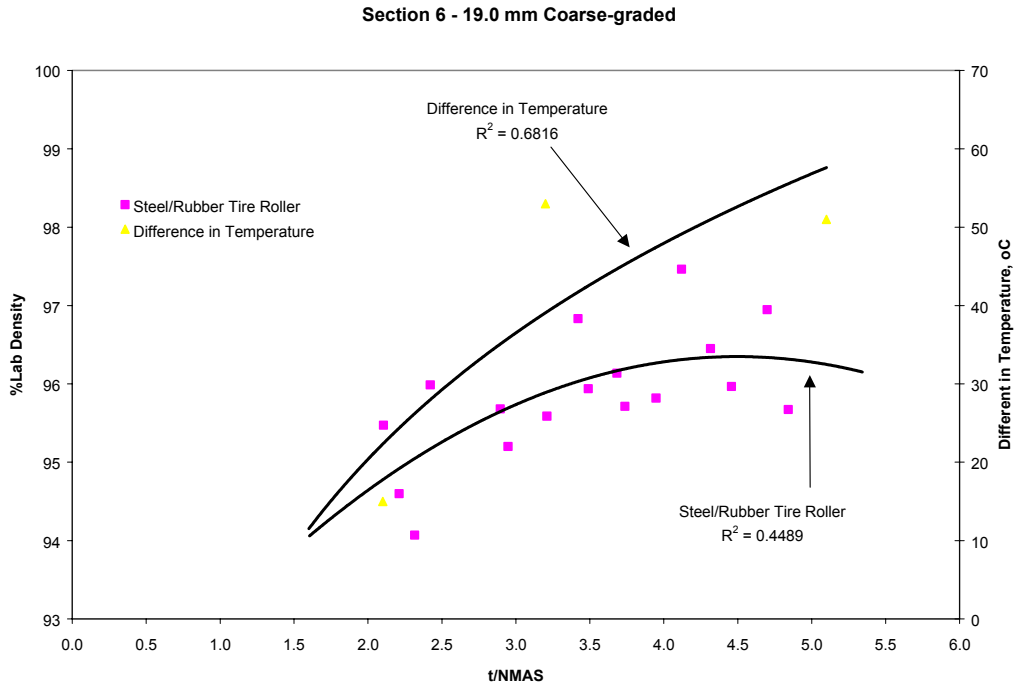

Figure 45: Relationships Between Density, t/NMAS and Temperature for Section 6

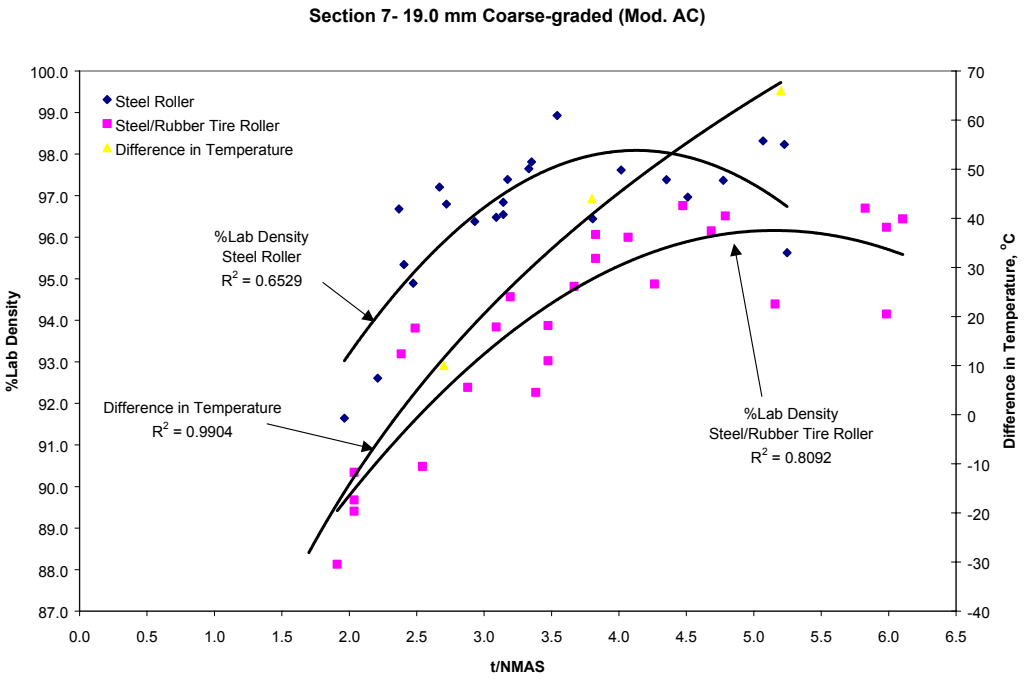

Figure 46: Relationships Between Density, t/NMAS and Temperature for Section 7

The relationship between density and t/NMAS for all data is shown in Figure 47. The best-fit line has an R^2 of 0.26 and indicates that as the thickness increased the density increased until a point where additional thickness resulted in a decrease in density. The effect of the layer thickness and cooling time on mix temperature is provided in Figure 48. The data was obtained from the thermocouples installed in the pavement. This plot indicates that during hot weather compaction time for a layer thickness of 1.5 inches is approximately twice that for a one-inch layer. This clearly shows that one of the problems in obtaining density is layer thickness regardless of the t/NMAS. If the amount of compaction time is reduced by 50% it may be very difficult to compact the mixture to an adequate density. To place the same amount of compactive effort on an HMA mixture prior to cooling to some defined temperature will take twice as many rollers at a 1-inch

thickness as that required for a 1.5-inch surface. Generally speaking it is likely to be significantly more difficult to compact a 1-inch layer than to compact a 1.5-inch layer.

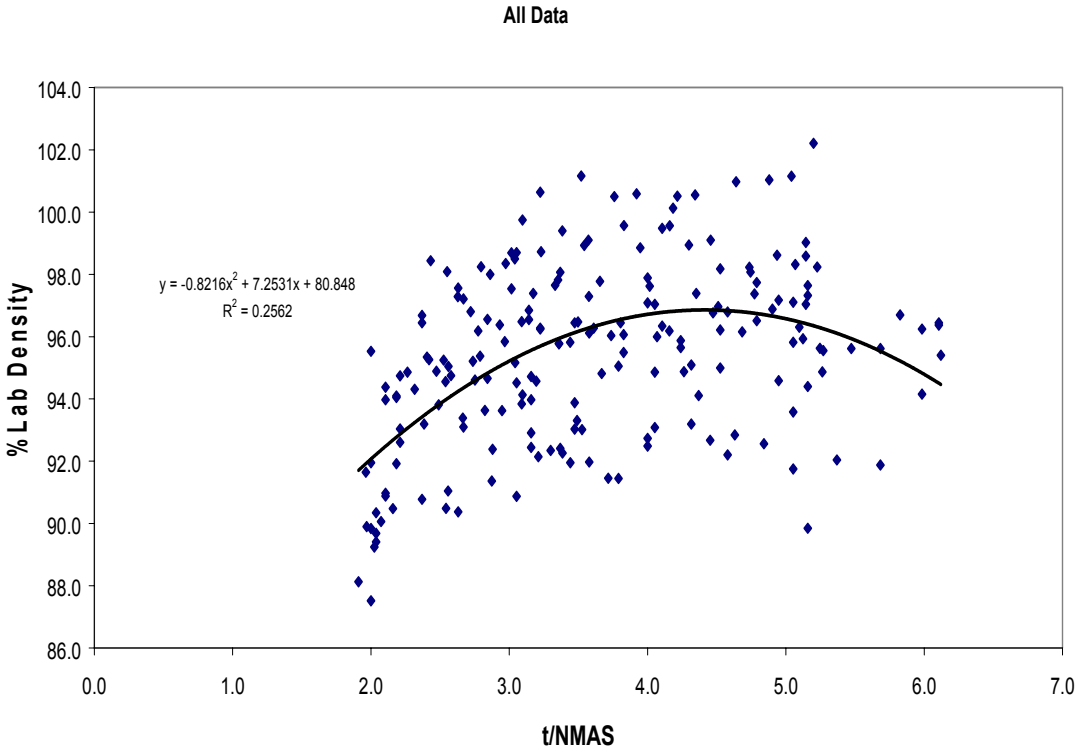

Figure 47: Relationships Between Density and t/NMAS for All Sections

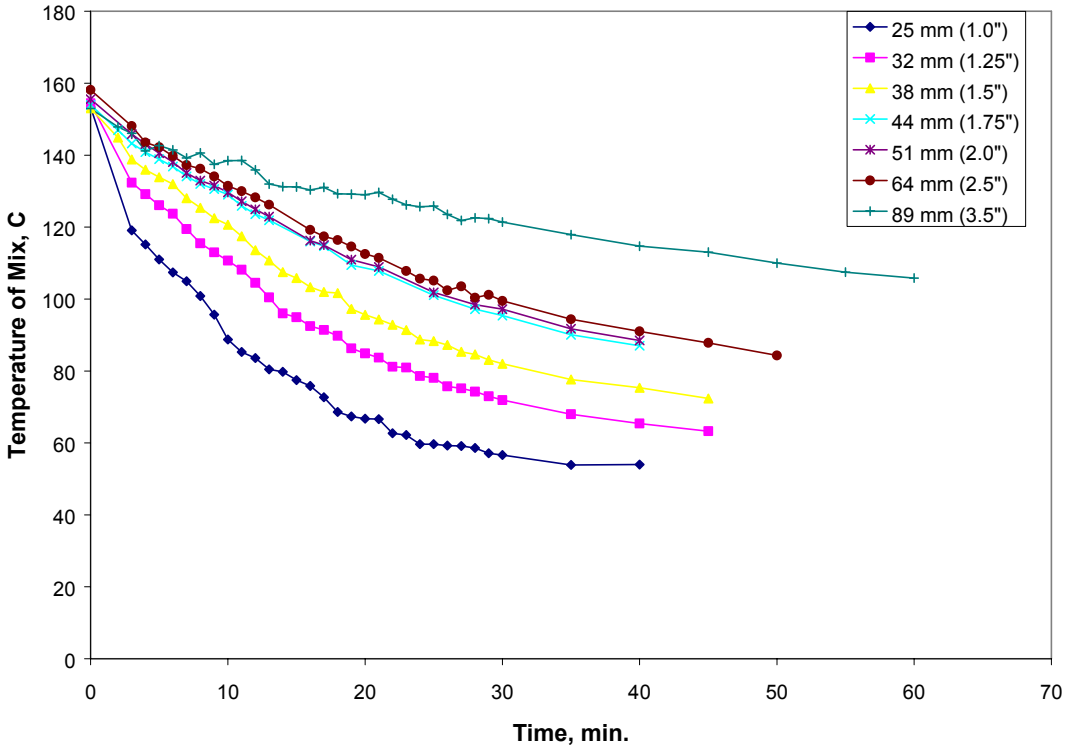

Figure 48: The Effect of Layer Thickness and Cooling Time on Mix Temperature

5.6 Evaluation of Effect of t/NMAS on Permeability Using the Gyratory Compacted Specimen Experiment

In this study specimens were compacted to 7.0 ± 1.0 percent air void content at t/NMAS of 2.0, 3.0 and 4.0. For some mixes the target air voids could not be achieved even at 300 gyrations. Permeability testing was only performed on specimens that met the desired air voids. The data from this experiment are presented in Appendix D. The results, as presented in Table 36, suggest that in most cases, granite mixes were more permeable than limestone mixes. The results also indicate that as the gradations became coarser, the permeability increased.

Table 36: Results of Permeability Testing Using Gyratory Compacted Specimens

NMAS	Gradation	T/NMAS	Limestone Mix		Granite Mix	
			Average Air Voids, %	Average Permeability, $10x^{-5}$ cm/sec	Average Air Voids, %	Average Permeability, $10x^{-5}$ cm/sec
9.5	ARZ	2	13.5	-	12.4	-
		3	9.4	-	9.4	-
		4	6.7	3	6.4	1
9.5	BRZ	2	14.7	-	16.1	-
		3	12.1	-	10.8	-
		4	7.2	19	7.7	33
9.5	SMA	2	14.4	-	18.3	-
		3	10.5	-	12.8	-
		4	8.5	-	9.5	-
12.5	SMA	2	16.7	-	16.7	-
		3	14.3	-	14.3	-
		4	10.6	-	10.6	-
19	ARZ	2	10.5	-	6.9	58
		3	7.4	4	7.8	1
		4	6.9	3	7.1	11
19	BRZ	2	9.7	-	10.0	-
		3	6.3	109	8.3	-
		4	7.7	147	6.2	191
19	SMA	2	14.4	-	11.8	-
		3	8.3	-	8.5	-
		4	6.8	116	7.5	344

- No measured permeability for specimens that did not achieve 7.0 ± 1.0 % air voids

Coarse-graded mixes with larger NMAS were more permeable than smaller NMAS mixes at 7.0 percent air voids. For 19.0 mm NMAS BRZ mix at t/NMAS of 4.0, the average permeability for granite mix was 191 x 10^{-5} cm/sec and for the limestone mix it was 147 x 10^{-5} cm/sec. This exceeded the maximum allowable permeability 125 x 10^{-5} cm/sec suggested by Florida Department of Transportation (4). The 19.0 mm NMAS SMA granite mix at t/NMAS of 4.0 also failed to meet the limiting value with an average permeability of 344 x 10^{-5} cm/sec. Hence, the mixes with more coarse aggregate and

larger nominal maximum size had higher permeabilities. There is no evidence that the thickness of the compacted specimens affected the measured permeability.

5.7 Evaluation of Effect of t/NMAS on Permeability Using Laboratory Vibratory Compacted Specimen

All specimens compacted at t/NMAS of 2.0, 3.0 and 4.0 achieved the target air void content of 7 ± 1.0 percent. The permeability test results for mixes using limestone and granite aggregate are shown in Table 37. Data from this experiment are presented in Appendix D. Figure 49 shows the relationship between average permeability for the two aggregate types and t/NMAS. In general, the permeability decreased as t/NMAS increased. Most of the mixes had permeability values of less than 50 x 10^{-5} cm/sec. However, at t/NMAS equal to 2.0, the 9.5 mm and 12.5 mm NMAS SMA mixes had average permeability values of 173 x 10^{-5} cm/sec and 196 x 10^{-5} cm/sec, respectively. These values for the SMA exceed the maximum permeability value of 125 x 10^{-5} cm/sec. It appears from this data that a specification requirement of 7 percent air voids would be acceptable for all of the mixes if the t/NMAS was 3 or greater.

5.8 Evaluation of Effect of t/NMAS on Permeability from Field Study

Permeability tests were conducted on the seven HMA sections that were evaluated in the field. These tests were conducted in-place with the field permeameter and in the laboratory with the lab permeability test. Cores were taken from the in-place pavement for measurement of density and for measurement of field permeability.

Table 37: Results of Permeability Testing Using Vibratory Compactor

NMAS	Gradation	T/NMAS	Limestone Mix		Granite Mix	
			Average Air Voids, %	Average Permeability, $10x^{-5}$ cm/sec	Average Air Voids, %	Average Permeability, $10x^{-5}$ cm/sec
9.5	ARZ	2	8.0	12	6.4	18
		3	7.5	28	6.1	3
		4	6.7	14	7.5	10
9.5	BRZ	2	6.7	61	7.6	43
		3	7.0	27	7.7	1
		4	7.1	0	7.9	1
9.5	SMA	2	6.1	108	7.0	237
		3	7.0	76	6.9	51
		4	6.9	6	7.6	39
12.5	SMA	2	7.1	44	7.3	348
		3	6.2	2	6.1	0
		4	6.4	9	6.9	53
19	ARZ	2	7.4	37	7.3	0
		3	7.9	21	6.0	0
		4	6.7	12	6.7	0
19	BRZ	2	6.5	0	6.9	65
		3	6.1	9	7.5	87
		4	6.4	0	7.2	43
19	SMA	2	6.0	0	7.4	0
		3	6.5	0	7.2	25
		4	6.2	0	7.5	0

5.8.1 Section 1 – 9.5 mm Fine-Graded HMA

The test results for the 9.5 mm fine-graded HMA is provided in Table 38. A review of the results indicates that the permeability was not very high for any of the specimens. It is interesting to note that the sections that are the thickest had the higher permeability. However, the permeability was not significant for any of the cores so it is not reasonable to make comparisons for such low numbers.

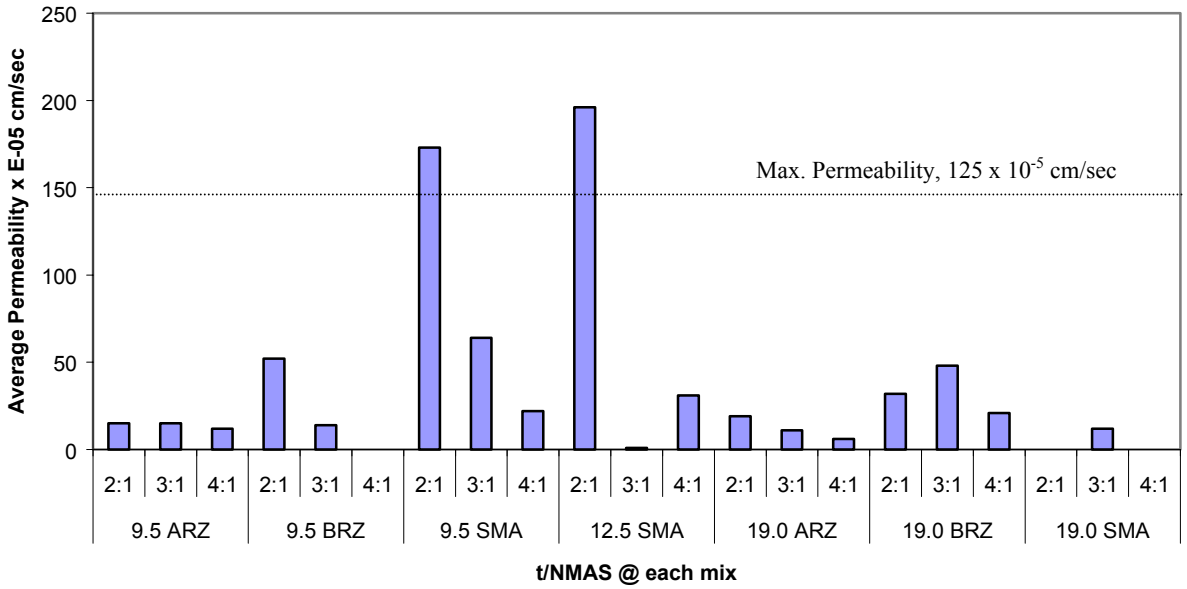

Figure 49: Relationship Between Permeability and t/NMAS

Table 38: Permeability Results for 9.5 mm Fine-Graded HMA (Steel Roller only)

Core No.	Thickness, mm	Voids Vacuum Sealed, %	Field Perm., 10^{-5} cm/sec	Lab. Perm, 10^{-5} cm/sec
1	21.0	8.7	4	1
2	24.1	8.8	3	7
3	24.3	8.4	1	3
4	28.2	7.6	1	4
5	28.9	8.3	4	6
6	33.2	7.0	3	1
7	34.3	7.2	5	3
8	39.0	7.1	5	4
9	46.6	6.6	5	1
10	48.4	7.2	13	1
11	48.7	7.5	26	5
12	48.9	6.5	10	3
13	50.1	7.9	22	2
14	54.0	7.8	28	35
15	58.0	7.1	17	21
16	58.2	8.0	24	2

The data from Table 38 is plotted in Figure 50. The field permeability appears to be affected by layer thickness while the laboratory-measured permeability did not appear to be affected by the layer thickness. Figure 51 shows the effect of air voids on permeability. Since the permeability was so low there was very little relationship with air voids.

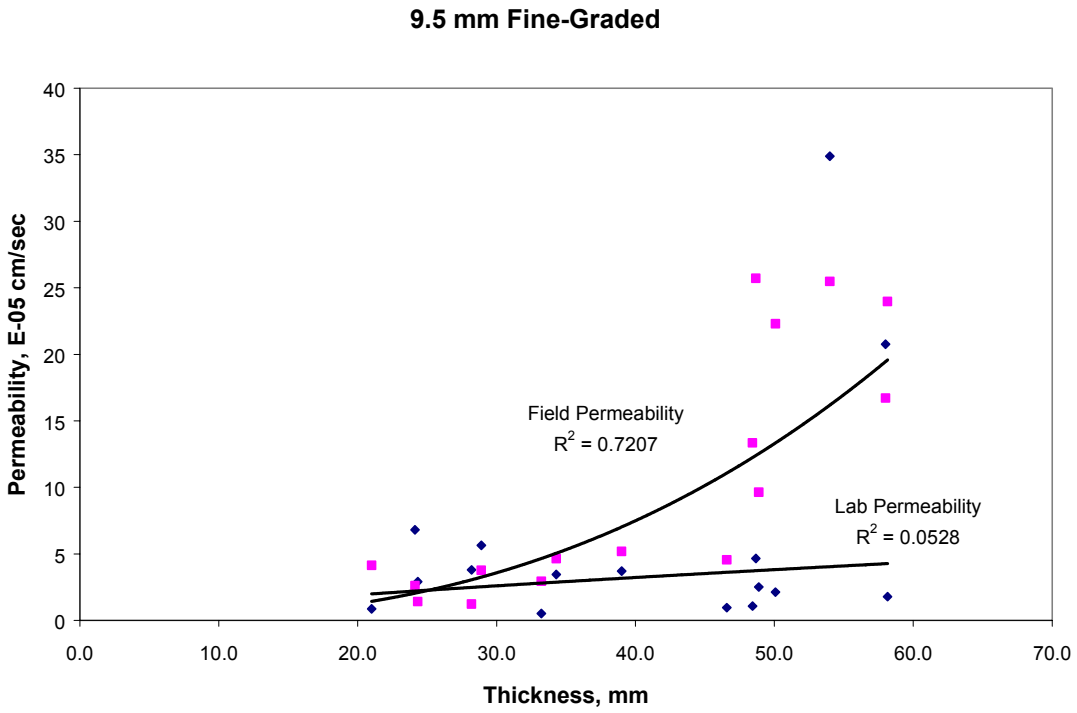

Figure 50: Permeability of 9.5 mm Fine-Graded HMA Mixtures and Thickness.

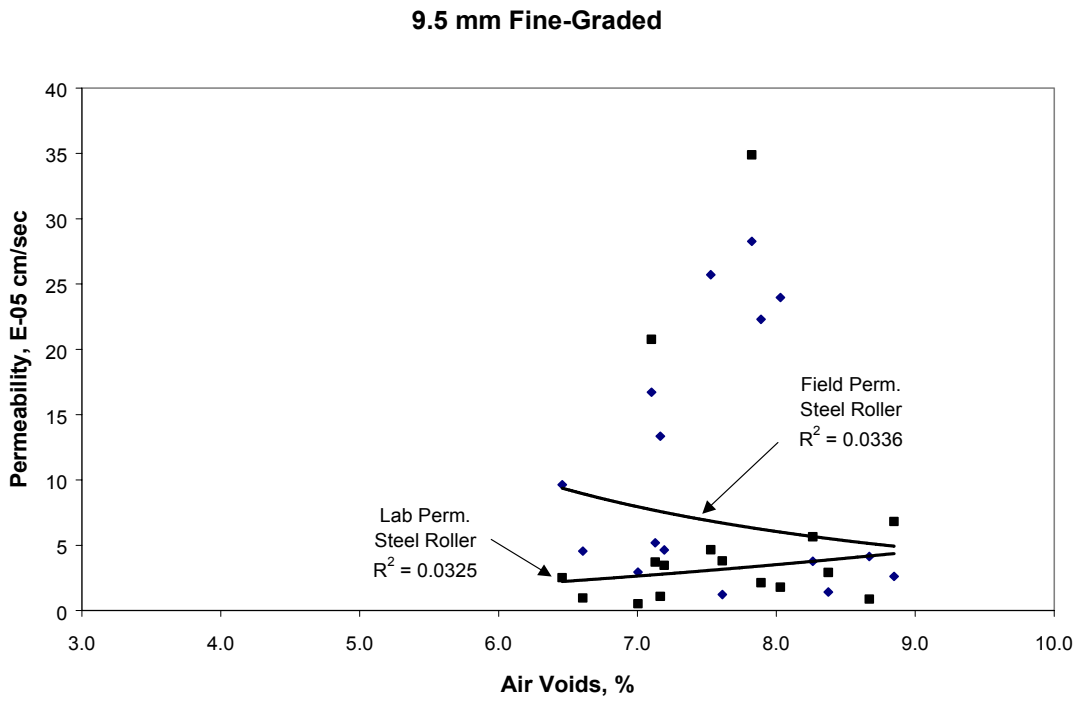

Figure 51: Permeability of 9.5 mm Fine-Graded HMA Mixtures and Air Voids

5.8.2 Section 2 – 9.5 mm Coarse-Graded HMA

The permeability results for Section 2 for compaction with the steel wheel roller only are shown in Table 39. The results are higher for Section 2 than for Section 1, however the in-place voids are also higher. The results for the portion compacted with the steel wheel and rubber tire rollers are provided in Table 40. It appears that the lab permeability for the portion compacted with the rubber tire roller is somewhat lower than that for the portion compacted with the steel wheel only. It has long been believed that one advantage of using a rubber tire roller is that it tends to reduce permeability due to the kneading action of the rubber tires. These data seems to support this concept. The results are plotted in Figure 52 as a function of layer thickness. The results are plotted as

a function of voids in Figure 53.

Table 39: Permeability Results for 9.5mm Coarse-Graded Mixes (steel wheel roller only)

Core No.	Thickness, mm	Voids Vacuum Sealed, %	Field Perm., 10^{-5} cm/sec	Lab. Perm, 10^{-5} cm/sec
1	20.0	11.6	22	292
2	20.5	12.0	29	291
3	22.5	11.7	135	713
4	25.0	12.1	113	871
5	29.0	11.6	97	618
6	32.0	10.1	64	434
7	36.0	11.1	71	658
8	38.0	9.8	146	258
9	38.5	9.5	76	275
10	41.0	9.4	234	264
11	43.5	10.3	223	453
12	46.0	10.0	289	433
13	48.0	9.0	347	234
14	51.0	10.5	489	494
15	54.0	10.6	532	577

Table 40: Permeability Results for 9.5 mm Coarse-Graded HMA using Steel/Rubber Tire

Core No.	Thickness, mm	Voids Vacuum Sealed, %	Field Perm., 10^{-5} cm/sec	Lab. Perm, 10^{-5} cm/sec
1	18.7	12.6	33	521
2	19.0	12.6	44	435
3	19.0	10.6	14	296
4	19.7	12.4	26	382
5	20.0	11.5	62	115
6	24.3	11.5	72	107
7	27.3	11.1	83	163
8	30.0	10.1	151	417
9	32.7	10.6	197	233
10	34.0	10.6	150	254
11	35.3	11.1	130	356
12	38.0	10.1	131	355
13	42.3	9.9	97	256
14	44.0	9.7	101	330
15	48.0	10.8	352	693
16	49.0	12.6	632	1070

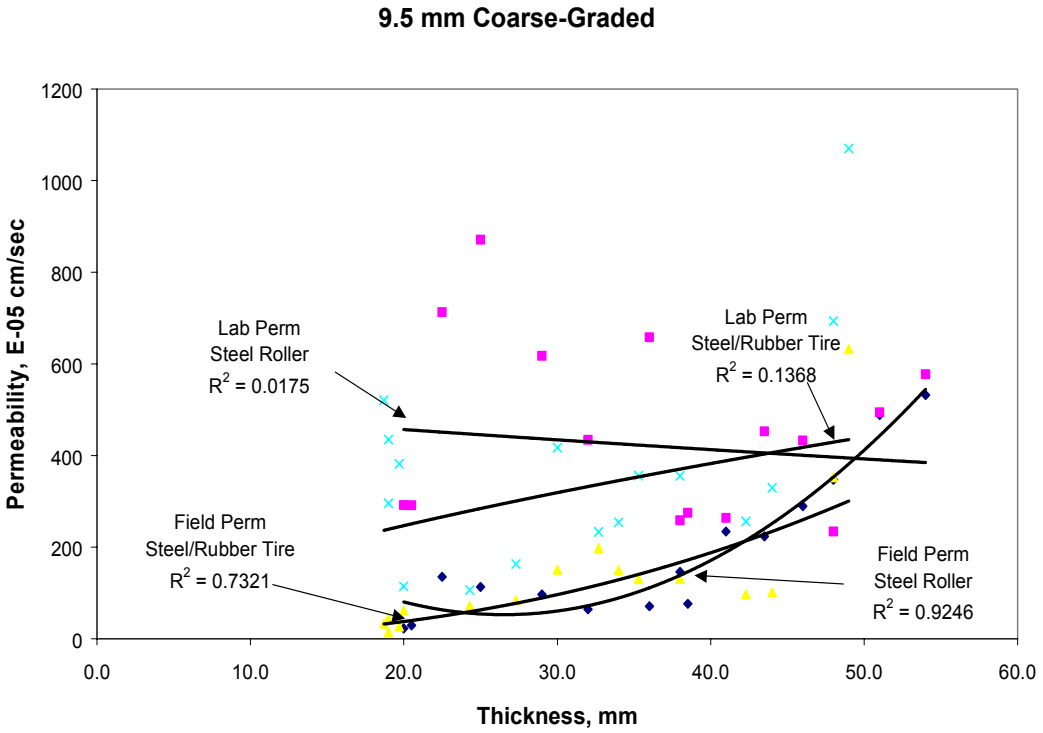

Figure 52: Permeability of 9.5 mm Coarse-Graded HMA Mixtures and Thickness.

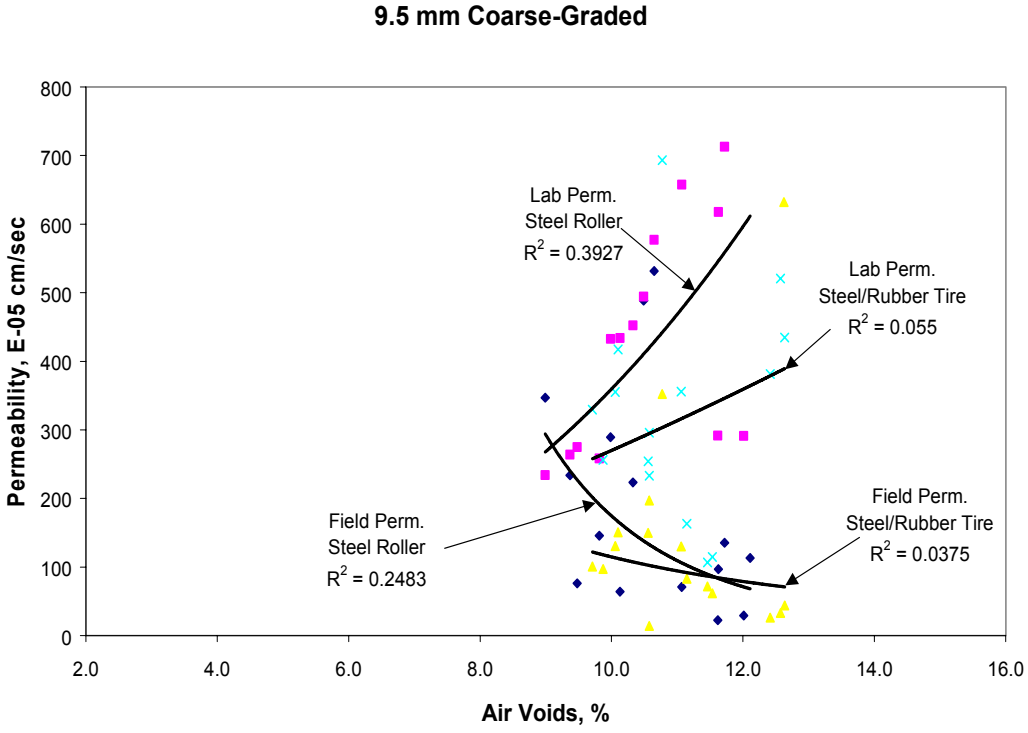

Figure 53: Permeability of 9.5 mm Coarse-Graded HMA Mixtures and Air Voids

5.8.3 Section 3 – 9.5 mm SMA

The permeability for the Section 3 mix is provided in Table 41 for the data that represents the mixture compacted with only the steel wheel roller. These data indicate that the measured field permeability is considerably higher than the lab permeability. The permeability results for the section using the steel wheel and steel/rubber tire roller are provided in Tables 41 and 42. Plots of the data are shown in Figures 54 and 55. These data also indicate that the measured field permeability is considerably higher than the lab permeability. Part of the reason for this difference may be the texture of the SMA mixtures. Rougher texture may result in some error in the field permeability if a good seal is not obtained between the permeameter and the HMA surface. The air voids are relatively high for each of the locations tested.

Table 41: Permeability of 9.5 mm SMA Mix Compacted with Steel Wheel Roller.

Core No.	Thickness, mm	Voids Vacuum Sealed, %	Field Perm., 10^{-5} cm/sec	Lab. Perm, 10^{-5} cm/sec
1	21.0	12.6	139	124
2	24.5	11.0	184	81
3	26.5	10.4	110	59
4	29.0	11.2	145	67
5	33.0	9.4	204	48
6	35.5	9.8	379	49
7	38.5	8.8	243	31
8	43.0	7.7	213	31
9	47.0	8.7	218	30
10	48.0	8.7	247	31
11	49.0	8.5	303	29
12	52.0	10.1	441	44

Table 42: Permeability of 9.5 SMA Mix Compacted with Steel/Rubber Tire Roller

Core No.	Thickness, mm	Voids Vacuum Sealed, %	Field Perm., 10^{-5} cm/sec	Lab. Perm, 10^{-5} cm/sec
1	20.0	11.3	214	41
2	23.0	10.5	135	90
3	26.0	10.5	142	51
4	27.0	11.0	234	37
5	30.0	11.0	323	63
6	30.0	11.7	285	90
7	34.0	9.7	323	66
8	38.0	8.8	168	19
9	41.0	10.6	307	92
10	43.0	10.7	425	151
11	47.0	11.1	506	77
12	50.0	10.9	651	168

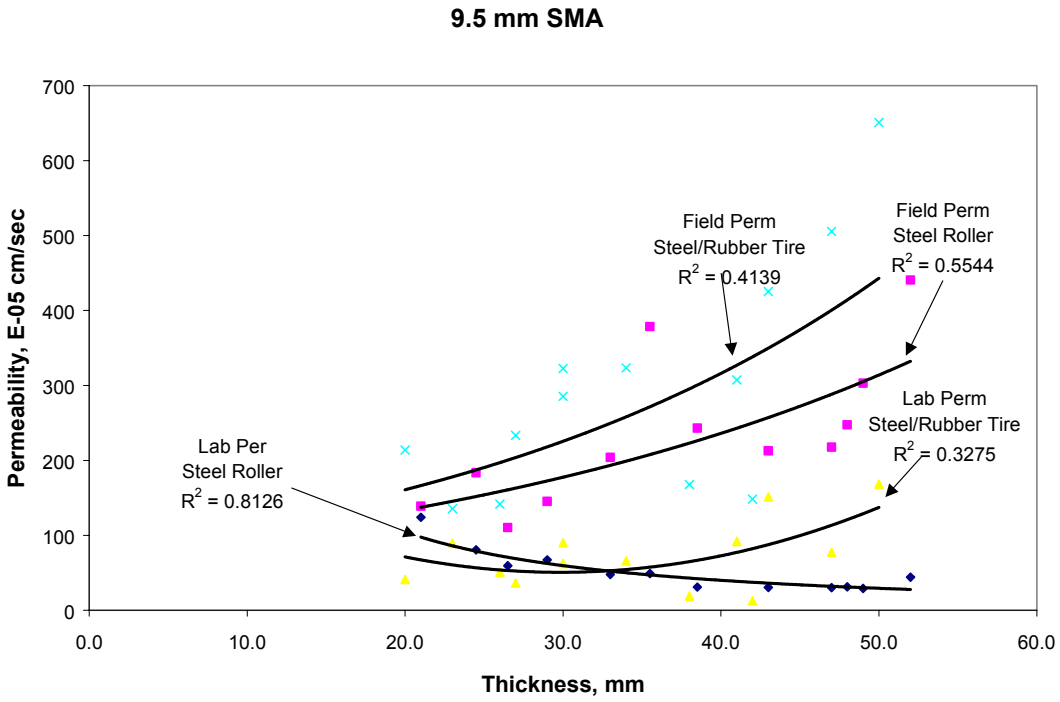

Figure 54: Permeability of 9.5 SMA Mixtures and Thickness.

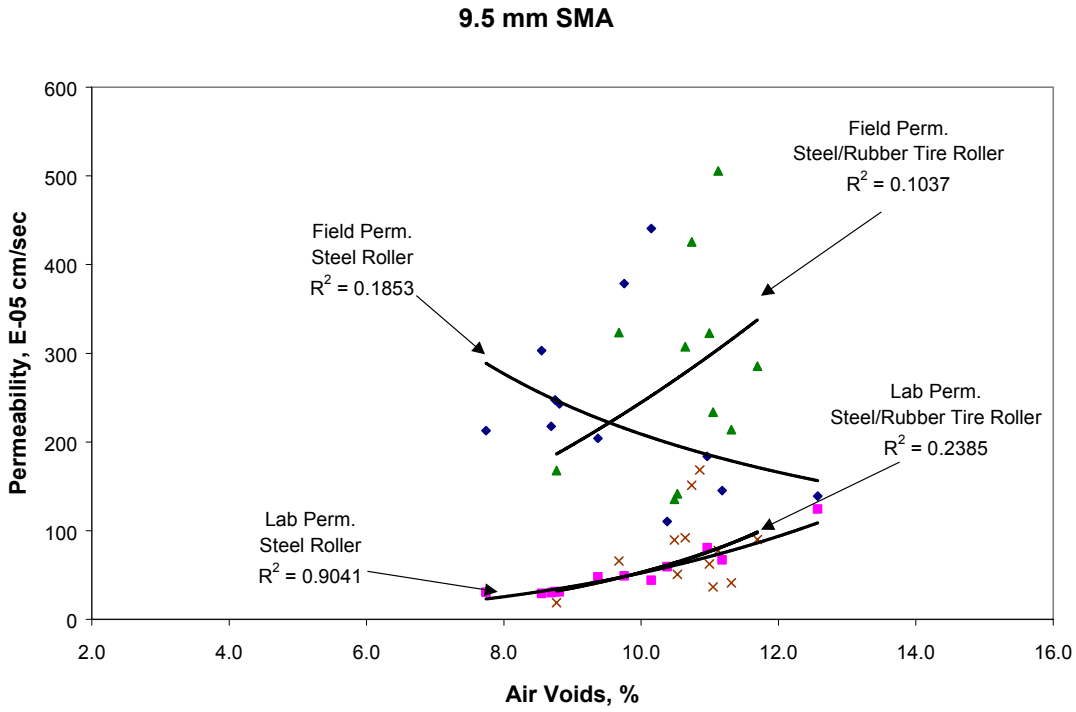

Figure 55: Permeability of 9.5 SMA Mixtures and Air Voids.

5.8.4 Section 4 – 12.5 mm SMA

The permeability for mixes from Section 4 is provided in Tables 43 and 44. The data indicate that the permeability is very high for some of the higher void levels which are sometimes approximately 15% or greater. Not all of the cores were tested for permeability in the laboratory; NA is noted for the cores that were not tested. Sufficient tests were conducted to show the range of permeability for the various thicknesses.

Table 43: Permeability of 12.5 mm SMA Mix Compacted with Steel Roller

Core No.	Thickness, mm	Voids Vacuum Sealed, %	Field Perm., 10^{-5} cm/sec	Lab. Perm, 10^{-5} cm/sec
1	25.0	17.9	1455	NA
2	27.3	13.7	425	2807
3	28.3	11.0	386	1271
4	34.7	9.7	385	362
5	37.7	7.4	408	NA
6	37.7	8.5	49	NA
7	38.0	7.6	296	300
8	38.7	6.4	27	NA
9	40.3	5.5	13	NA
10	42.3	6.7	81	95
11	44.0	5.1	3	NA
12	47.0	5.7	35	17
13	49.0	5.6	36	40
14	52.0	6.6	41	17
15	52.3	6.0	49	NA
16	52.7	5.7	28	NA
17	54.3	5.6	92	10
18	58.0	5.2	98	0.1
19	61.0	5.2	13	0.1
20	63.0	5.1	14	0.1
21	65.0	4.1	6	NA

Table 44: Permeability of 12.5 mm SMA Mix Compacted with Steel/Rubber Tire Roller

Core No.	Thickness, mm	Voids Vacuum Sealed, %	Field Perm., 10^{-5} cm/sec	Lab. Perm, 10^{-5} cm/sec
1	25.3	16.2	1963	5850
2	27.3	11.7	745	NA
3	27.3	11.7	745	586
4	33.3	12.4	908	1392
5	35.3	12.1	963	NA
6	38.7	11.7	1407	1341
7	40.3	9.7	1443	NA
8	40.3	9.6	647	NA
9	42.0	10.1	1778	NA
10	42.0	10.1	1629	NA
11	43.0	10.1	1283	1529
12	44.7	8.7	478	NA
13	45.7	8.2	364	344
14	50.0	8.1	786	485
15	53.0	10.2	656	1049
16	53.0	10.0	325	NA
17	55.7	7.0	534	270
18	59.3	8.0	262	113
19	61.7	7.4	50	267
20	64.3	7.1	112	164
21	64.3	7.5	240	NA

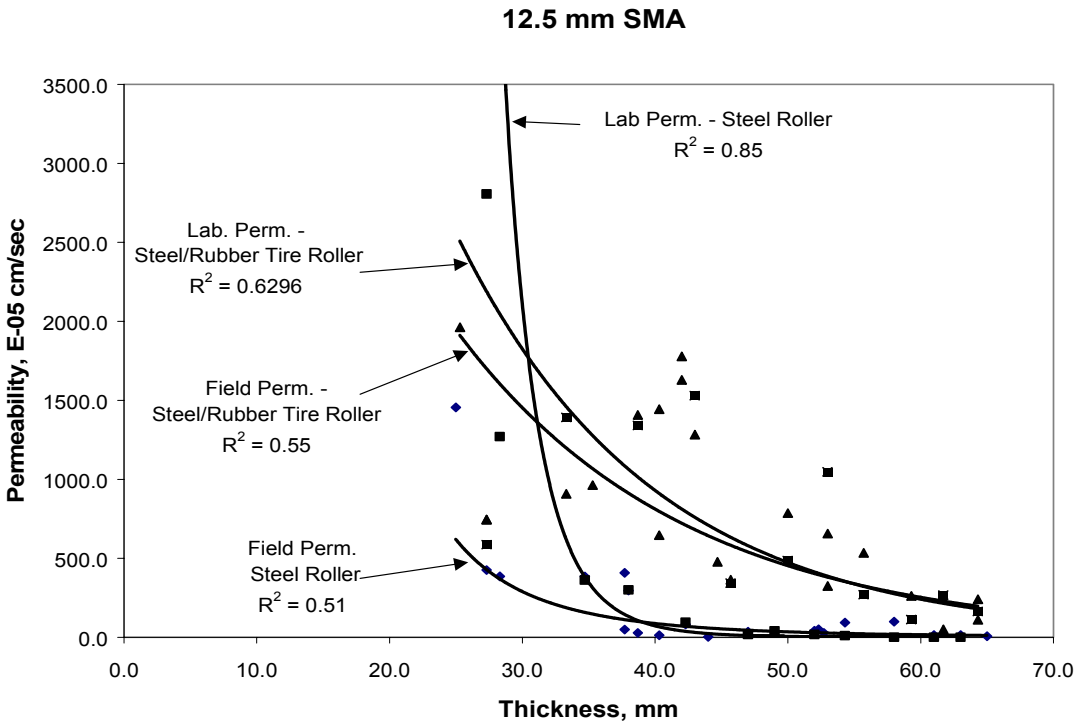

Figure 56: Permeability of 12.5 mm SMA Mixture and Thickness.

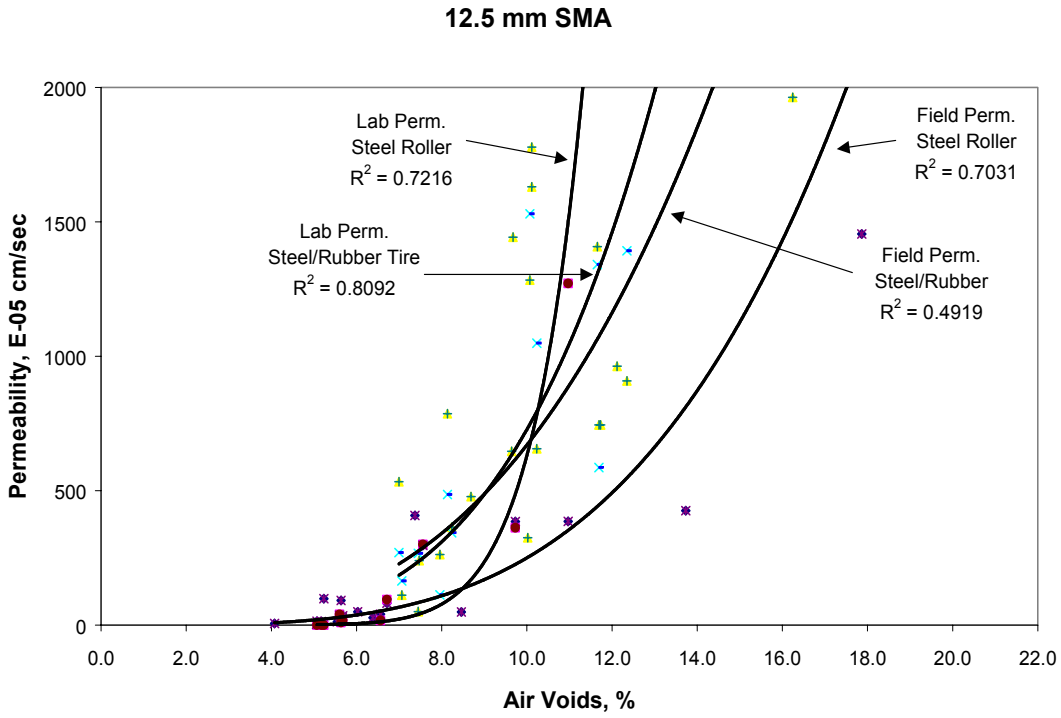

Figure 57: Permeability of 12.5 mm SMA Mixture and Air Voids

5.8.5 Section 5 – 19.0 mm Fine-Graded

The permeability of specimens in Section 5 is provided in Table 45. The results indicate that the lab permeability was below the 125 x 10^{-5} cm/s that is often recommended as a cutoff for acceptable permeability. The results are plotted in Figures 58 and 59. The data clearly show that the field permeability was always significantly higher than the laboratory measured permeability.

Table 45: Permeability of 19.0 mm Fine-Graded Mix Compacted with Steel Roller

Core No.	Thickness, mm	Voids Vacuum Sealed, %	Field Perm., 10^{-5} cm/sec	Lab. Perm, 10^{-5} cm/sec
1	38.0	9.5	105	77
2	45.0	8.7	73	9
3	46.2	6.8	57	3
4	48.5	7.1	140	27
5	50.0	7.9	59	5
6	50.0	7.6	152	15
7	53.1	7.0	47	5
8	54.4	7.2	54	7
9	56.5	6.9	38	5
10	58.0	6.5	42	12
11	61.4	6.5	71	2
12	64.0	7.1	93	3
13	67.9	6.2	51	2
14	72.8	5.7	48	1
15	75.0	6.4	128	3
16	78.0	5.8	97	3
17	81.7	6.3	71	1
18	90.0	7.0	89	4
19	91.0	7.4	110	30
20	98.0	7.5	161	12

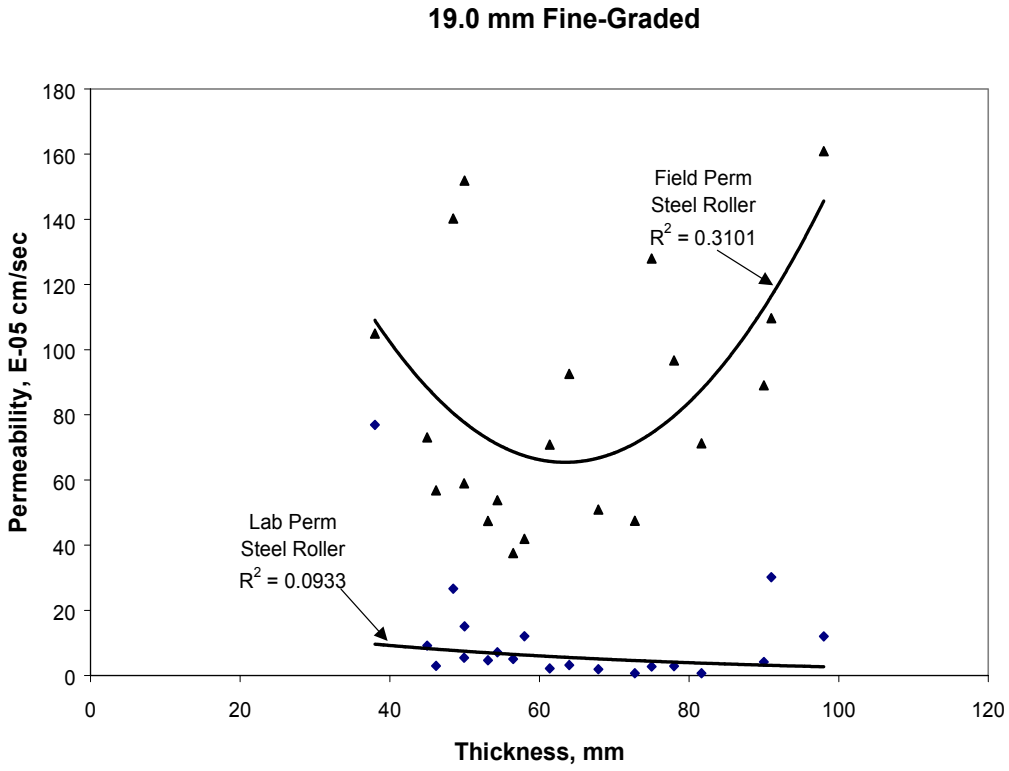

Figure 58: Permeability of 19.0 mm Fine-Graded HMA and Thickness

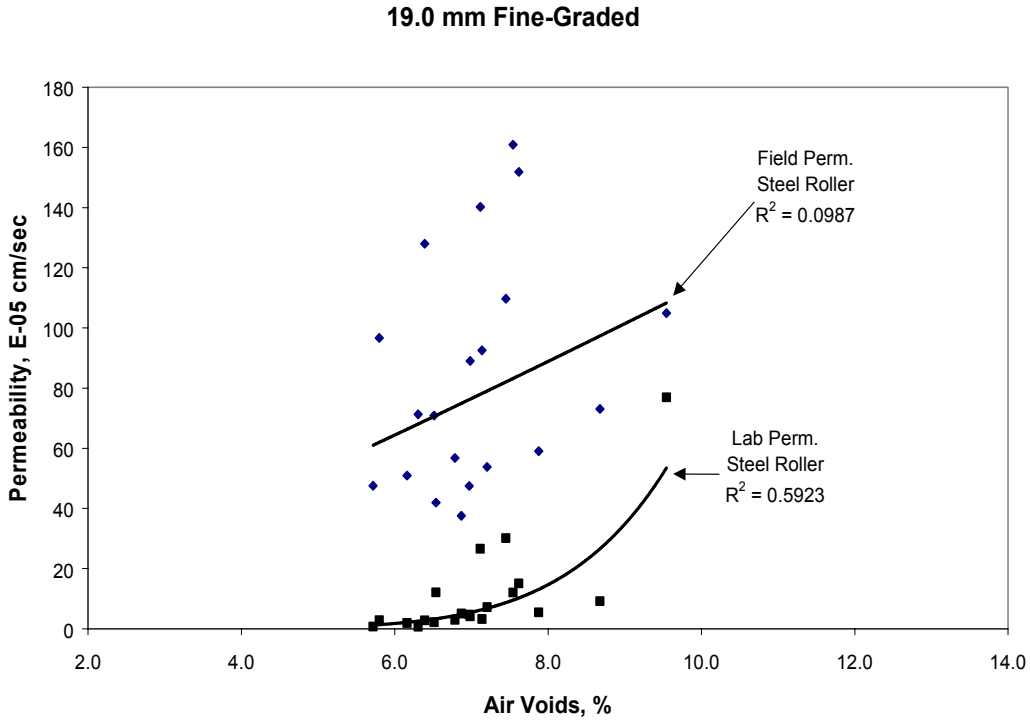

Figure 59: Permeability of 19.0 mm Fine-Graded HMA and Air Voids

5.8.6 Section 6 – 19.0 mm Coarse-Graded

The permeability results for Section 6 are provided in Tables 46 and 47. The measured lab permeability results are considerably lower than the field permeability results. It also appears that the permeability of the mix compacted with a rubber tire roller was significantly lower than that compacted with steel wheel only. The results are plotted in Figures 60 and 61.

Table 46: Permeability of 19.0 mm NMAS Coarse-Graded HMA Compacted with Steel Roller

Core No.	Thickness, mm	Voids Vacuum Sealed, %	Field Perm., 10^{-5} cm/sec	Lab. Perm, 10^{-5} cm/sec
1	40.0	8.0	230	41
2	44.0	7.7	136	92
3	48.0	6.8	166	NA
4	50.7	8.9	137	96
5	52.3	7.4	290	NA
6	54.0	5.5	33	NA
7	56.0	8.4	56	36
8	60.0	9.1	218	98
9	61.0	9.8	444	NA
10	62.7	9.6	651	NA
11	66.3	8.7	552	141
12	67.0	9.0	860	NA
13	72.0	7.0	204	64
14	77.0	7.2	700	34
15	79.0	5.9	718	35
16	83.0	7.9	604	NA
17	86.0	5.8	1540	118
18	87	5.3	949	53
19	96.0	6.2	1760	33

Table 47: Permeability of 19.0 mm NMAS Coarse-Graded HMA Compacted with Steel/Rubber Tire

Core No.	Thickness, mm	Voids Vacuum Sealed, %	Field Perm., 10^{-5} cm/sec	Lab. Perm, 10^{-5} cm/sec
1	40.0	6.6	172	14
2	42.0	7.4	65	4
3	44.0	7.9	60	1
4	46.0	6.1	56	2
5	55.0	6.4	48	2
6	56.0	6.8	10	2
7	61.0	6.4	18	NA
8	65.0	5.2	71	2
9	66.3	6.1	34	3
10	70.0	5.9	65	5
11	71.0	6.3	135	NA
12	75.0	6.2	104	NA
13	78.3	4.6	101	1
14	82.0	5.6	463	2
15	84.7	6.1	170	1
16	89.3	5.1	179	NA
17	92.0	6.4	1057	NA

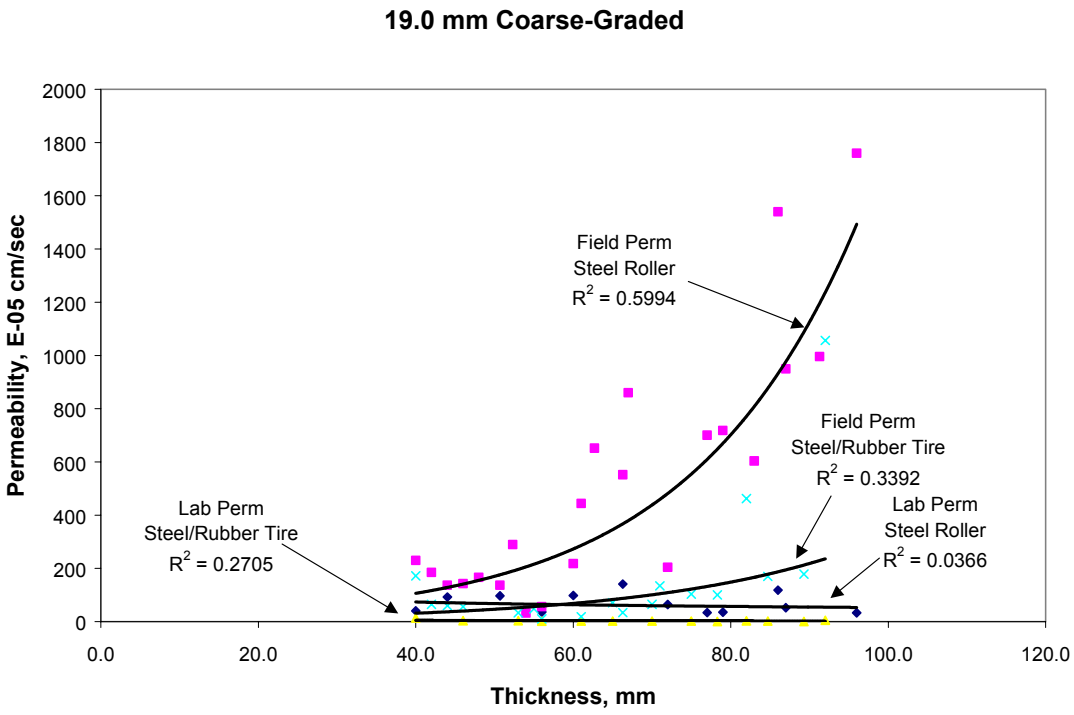

Figure 60: Permeability of 19.0 mm Coarse-Graded HMA and Thickness

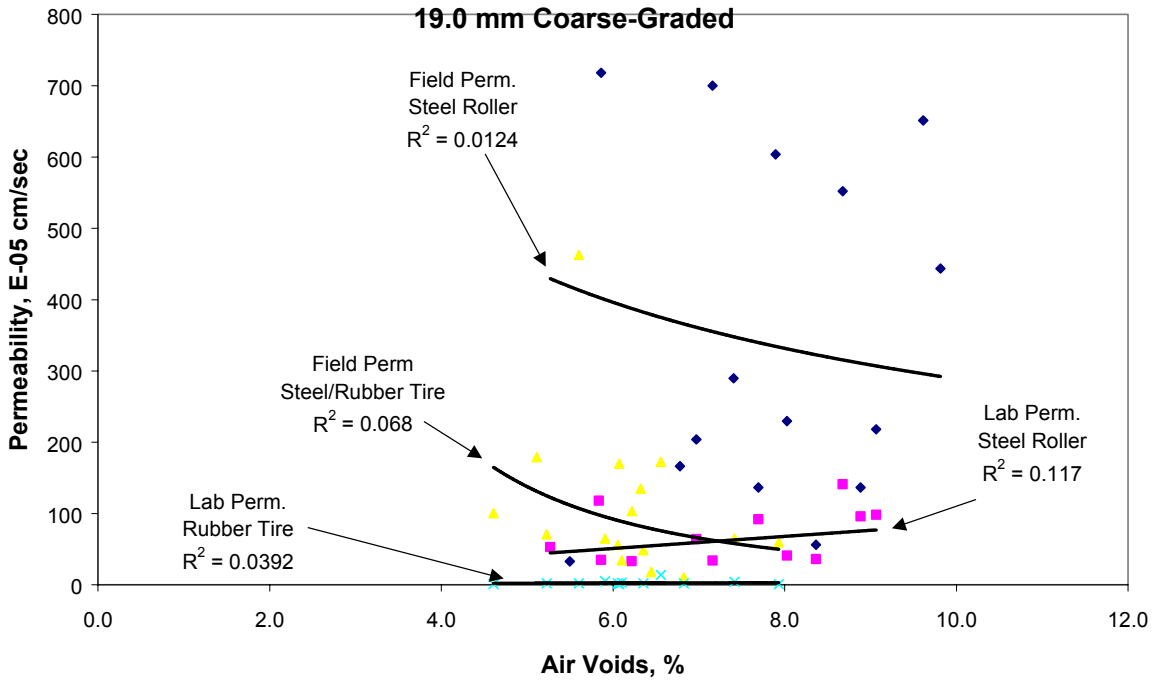

Figure 61: Permeability of 19.0 m Coarse-Graded HMA and Air Voids

5.8.7 Section 7 – 19.0 mm Coarse-Graded with Modified Asphalt

The permeability of the mix in Section 7 is provided in Tables 48 and 49. The results are plotted in Figures 62 and 63. The air void levels are clearly lower for the mixture compacted with the steel wheel roller.

Table 48: Permeability of 19.0 mm Coarse-Graded HMA with Modified Asphalt Compacted with Steel Wheel Roller.

Core No.	Thickness, mm	Voids Vacuum Sealed, %	Field Perm., 10^{-5} cm/sec	Lab. Perm, 10^{-5} cm/sec
1	37.3	11.8	468	1203
2	42.0	10.9	420	679
3	45.0	6.9	113	NA
4	45.7	8.2	282	NA
5	47.0	8.7	311	273
6	50.7	6.4	121	NA
7	51.7	6.8	103	63
8	55.7	7.2	124	79
9	58.7	7.1	126	NA
10	59.7	6.8	121	NA
11	59.7	7.1	153	NA
12	60.3	6.3	109	29
13	63.3	6.0	72	NA
14	63.7	5.9	83	0
15	67.3	4.8	130	0
16	72.3	7.2	94	44
17	76.3	6.0	135	10
18	82.7	6.3	177	2
19	85.7	6.7	437	1
20	90.7	6.3	528	10
21	96.3	5.4	653	0
22	99.3	5.4	1030	2
23	99.7	8.0	952	NA

Table 49: Permeability of 19.0 mm Coarse-Graded HMA with Modified Asphalt Compacted with Steel/Rubber Tire Roller.

Core No.	Thickness, mm	Voids Vacuum Sealed, %	Field Perm., 10^{-5} cm/sec	Lab. Perm, 10^{-5} cm/sec
1	36.3	15.2	1897	NA
2	38.7	13.7	706	1
3	38.7	13.0	832	NA
4	38.7	13.9	1199	NA
5	45.3	10.3	1183	43
6	47.3	9.7	746	NA
7	48.3	12.9	876	146
8	54.7	11.1	810	304
9	58.7	9.7	920	NA
10	60.7	9.0	797	51
11	64.3	11.2	888	119
12	66.0	9.6	664	NA
13	66.0	10.5	1002	NA
14	69.7	8.7	897	0
15	72.7	7.5	611	NA
16	72.7	8.1	1101	12
17	77.3	7.6	749	10
18	81.0	8.7	683	18
19	85.0	6.9	738	4
20	89.0	7.5	812	NA
21	91.0	7.1	1130	0
22	98.0	9.1	1658	4
23	110.7	6.9	2599	1
24	113.7	9.4	2331	NA
25	113.7	7.4	3030	NA
26	116.0	7.2	2177	NA

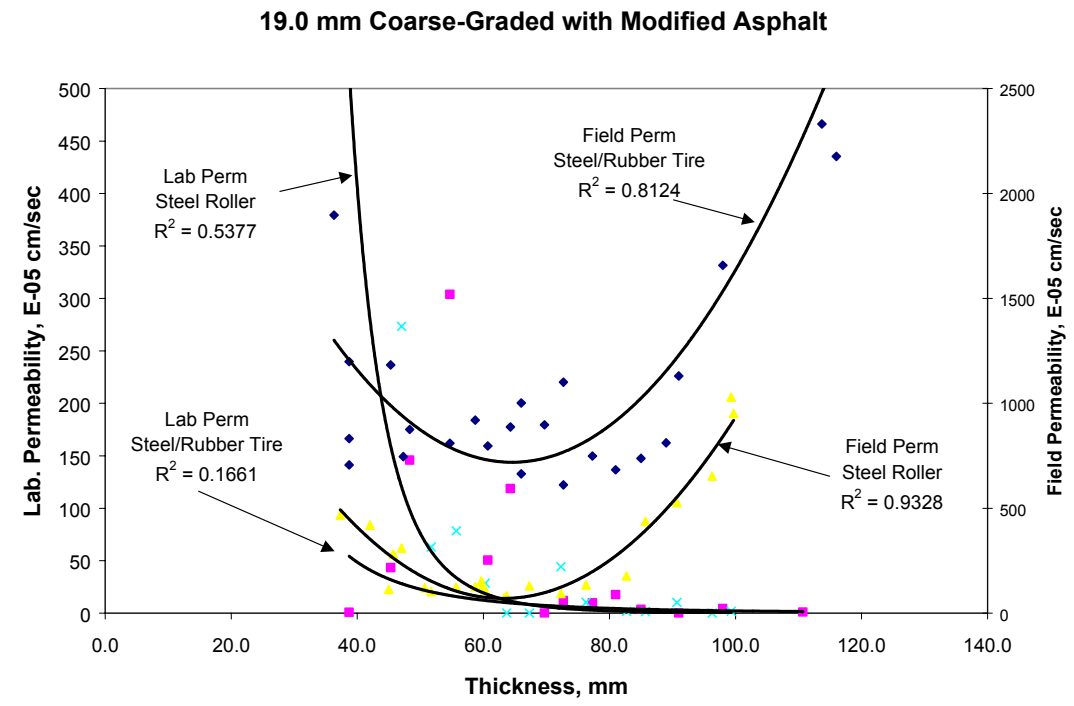

Figure 62: Permeability of 19.0 mm Coarse-Graded with Modified Asphalt and Thickness

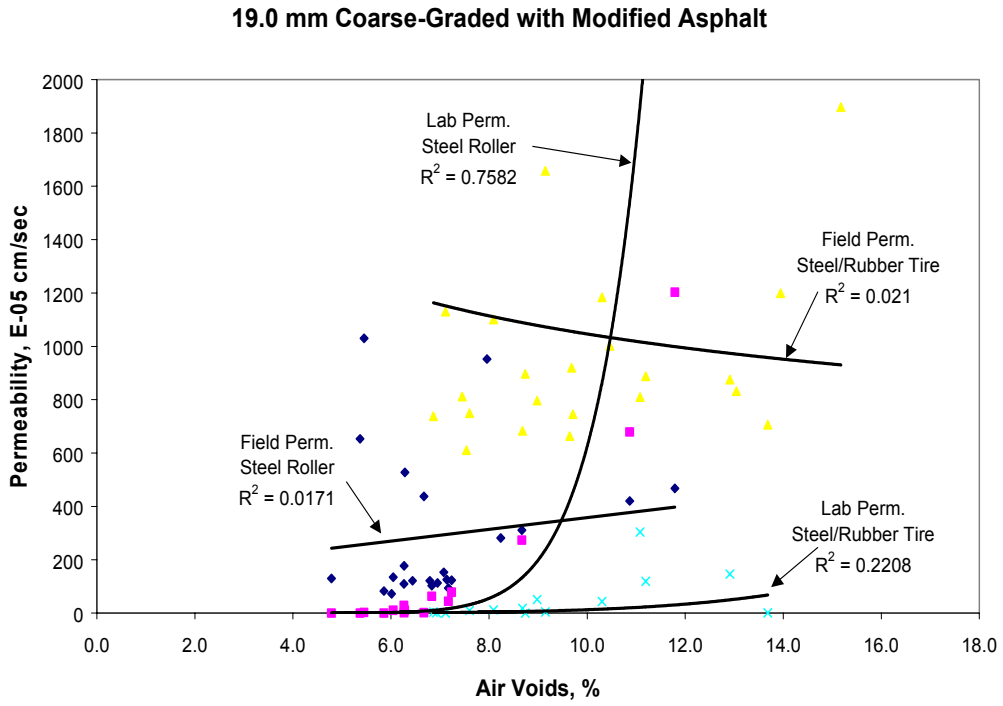

Figure 63: Permeability of 19.0 mm Coarse-Graded with Modified Asphalt and Air Voids.

5.9 Part 2– Evaluation of Relationship of Laboratory Permeability, Density and Lift Thickness of Field Compacted Cores

Table 50 provides the average thickness of the cores obtained from NCHRP 9-9(1) projects, the average air void content by the SSD method, the average air void content by the vacuum sealed method, the average water absorption from SSD testing, and the average laboratory permeability values. Based on the discussion in the first part of this research that compared the SSD method and the vacuum sealed method, it was decided to use the air voids determined from vacuum sealed method in the analysis.

Figure 64 illustrates the relationship between in-place air voids and permeability for all cores. The R^2 value for this figure is relatively high (0.66) and the relationship is significant (p-value = 0.000). In this figure, the y-axis was reduced to show a clearer relationship. Of the 287 data points, 18 data points having permeability values larger than 1000 x 10^{-5} cm/sec are not shown in the figure. The largest permeability value was 12,800 x 10^{-5} cm/s. The data shows that as the in-place air voids increased, permeability also increased. Based on the trend line, permeability is very low at air void content less than 6 to 8 percent. The permeability starts to increase at a greater rate with changes in in-place air voids above 8 percent.

The relationship between in-place air voids and permeability for the 9.5 mm NMAS mix is illustrated in Figure 65. The R^2 values for both coarse-graded and fine-graded mixes were relatively high (0.70 and 0.86, respectively) and both relationships are significant (p-value = 0.000). For both gradation types, the permeability begins to

increase at greater rate at approximately 8.0 percent air voids. At this air void content, the pavement is expected to have a permeability of 60 x 10^{-5} cm/sec for coarse-graded mix

Table 50: Average Air Voids, Water Absorption and Permeability for Field Projects

Project No.	NMAS, mm	Gradation	Ndes	Average Thickness mm	Average In-place Voids, T 166, %	Average In-place Voids, Vacuum Sealed, %	Average Water Absorption, %	Average Lab. Permeability 10^{-5}cm/sec
1	9.5	Coarse	86	34.3	8.1	8.1	0.4	74
2	9.5	Coarse	90	40.5	9.5	11.8	1.2	468
3	9.5	Coarse	90	44.5	9.1	10.7	1.0	214
4	9.5	Coarse	105	45.7	8.3	9.9	0.9	242
5	9.5	Coarse	50	31.2	16.3	17.0	1.7	2198
6	9.5	Coarse	100	33.9	8.4	8.6	0.4	108
7	9.5	Coarse	125	34.9	7.6	8.1	0.3	130
8	9.5	Coarse	100	44.1	9.9	11.1	1.5	606
9	9.5	Coarse	100	22.3	9.7	10.4	0.7	339
10	9.5	Fine	75	40.5	7.1	7.3	0.2	6
11	9.5	Fine	75	32.4	10.4	11.3	0.4	385
12	12.5	Coarse	106	39.9	11.6	13.1	1.7	453
13	12.5	Coarse	100	42.4	12.5	16.9	2.4	5656
14	12.5	Coarse	100	38.0	10.6	12.3	0.8	420
15	12.5	Coarse	75	33.7	10.4	11.7	0.6	279
16	12.5	Coarse	125	53.5	8.1	9.3	2.2	346
17	12.5	Coarse	125	51.0	11.3	12.5	3.3	2379
18	12.5	Coarse	125	52.8	8.8	9.9	1.2	238
19	12.5	Coarse	125	56.8	9.6	10.8	1.1	361
20	12.5	Coarse	109	50.6	6.9	7.7	0.2	39
21	12.5	Coarse	86	47.6	6.3	7.0	0.7	92
22	12.5	Coarse	100	44.1	5.3	5.8	0.2	2
23	12.5	Coarse	125	51.1	7.3	9.1	0.4	260
24	12.5	Coarse	100	78.8	8.6	9.3	1.3	59
25	12.5	Coarse	125	48.4	6.5	8.1	0.3	30
26	12.5	Coarse	100	36.3	7.7	7.7	0.2	43
27	12.5	Fine	86	53.3	5.3	6.2	0.2	9
28	12.5	Fine	86	44.3	8.6	9.0	0.8	133
29	12.5	Fine	125	45.8	10.3	10.4	0.3	86
30	12.5	Fine	68	39.8	8.1	8.3	0.3	19
31	12.5	Fine	76	51.2	9.2	10.3	0.5	124
32	12.5	Fine	109	55.2	7.9	8.2	0.4	78
33	12.5	Fine	100	34.8	9.6	10.4	0.8	318
34	12.5	Fine	75	38.7	8.5	8.5	0.4	144
35	19	Fine	95	33.0	8.4	8.4	0.4	12
36	19	Fine	68	49.6	6.6	6.5	0.2	38
37	19	Fine	96	48.7	7.0	7.0	0.1	12

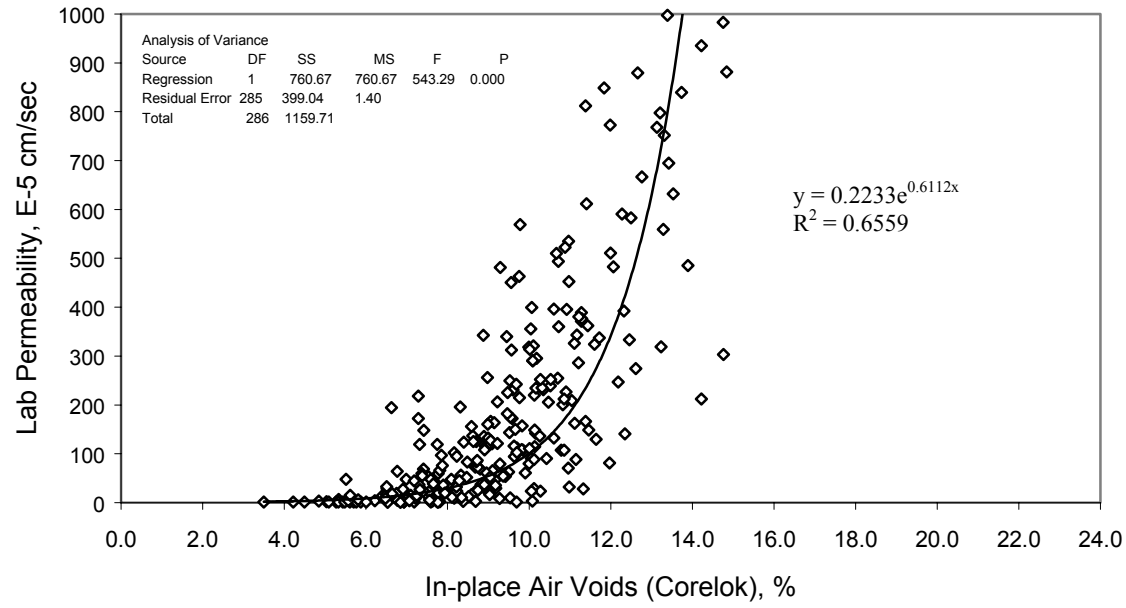

Figure 64: Plot of Laboratory Permeability versus In-place Air Voids-All Data

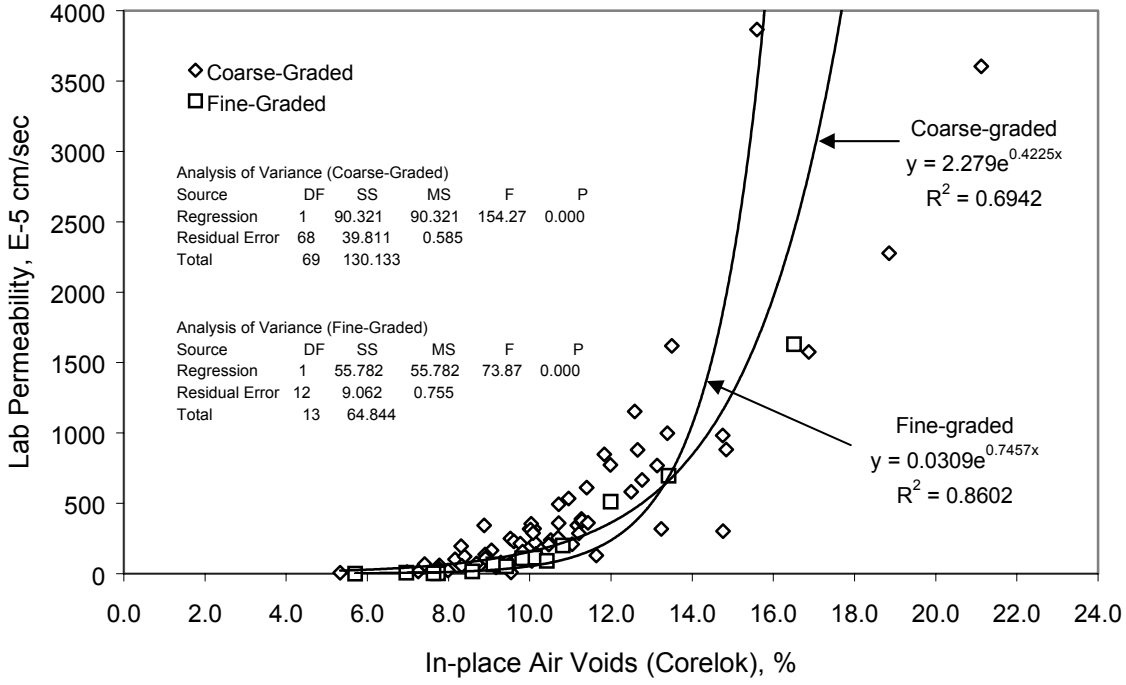

Figure 65: Plot of Permeability versus In-place Air Voids for 9.5 mm NMAS Mixes.

and 10 x 10^{-5} cm/sec for fine-graded mix. Since there are only a couple of data points for fine-graded mix above approximately 10 percent air voids, this model should not be used to predict permeability at these higher void levels. So at lower void levels the coarse-graded mixes are more permeable. It is also observed from the plot that a void level of approximately 8 percent or lower will result in a permeability of less than 125 x 10-5 cm/sec.

The relationships for the coarse-graded and fine-graded 12.5 mm NMAS mixes are shown in Figure 66. There is no significant difference between fine and coarse-graded mixes. The relationships between in-place air voids and permeability for both gradation types were reasonable and significant with an R^2 of 0.61 for coarse-graded mixes (p-value = 0.000) and 0.58 for fine-graded mixes (p-value = 0.000). As shown by the best-fitted lines, the permeability values for both gradation types were basically the same at a given air void content. The permeability starts to increase at a greater rate at approximately 8.0 percent air voids. The permeability at 8.0 percent air voids for coarse-graded and fine-graded mixes was approximately 30 x 10^{-5} cm/sec. The correlation between voids and permeability varies depending on the mixture. To be sure that the 12.5mm mixture is not permeable the air voids should be at approximately 7 percent or lower.

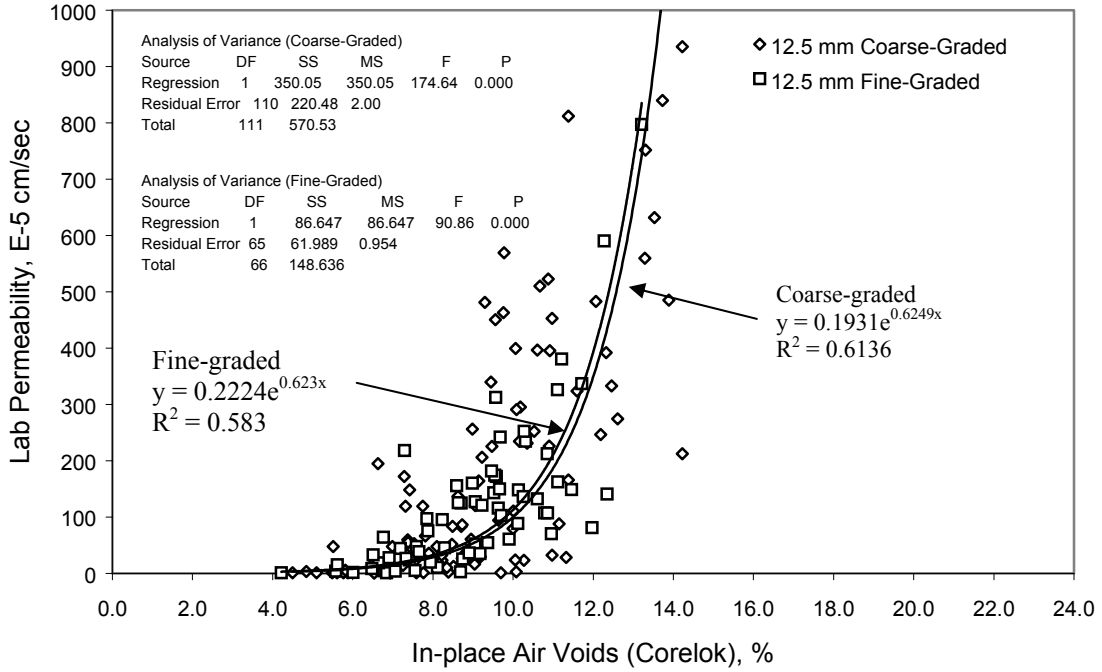

Figure 66: Plot of Permeability versus In-place Air Voids for 12.5 mm NMAS Mixes.

Figure 67 illustrates the relationship between in-place air voids and permeability for fine-graded 19.0 mm NMAS mixes. The R^2 value for this figure is 0.59 and the relationship is significant (p-value = 0.000). Based on the trend line, permeability is very low at air void contents less than 8.0 percent. At air void contents above 8.0 percent, the permeability begins to increase rapidly with a small increase in in-place air void content. At 8.0 percent air voids, the fine- graded 19.0 mm NMAS mix has a permeability value of 16 x 10^{-5} cm/sec.

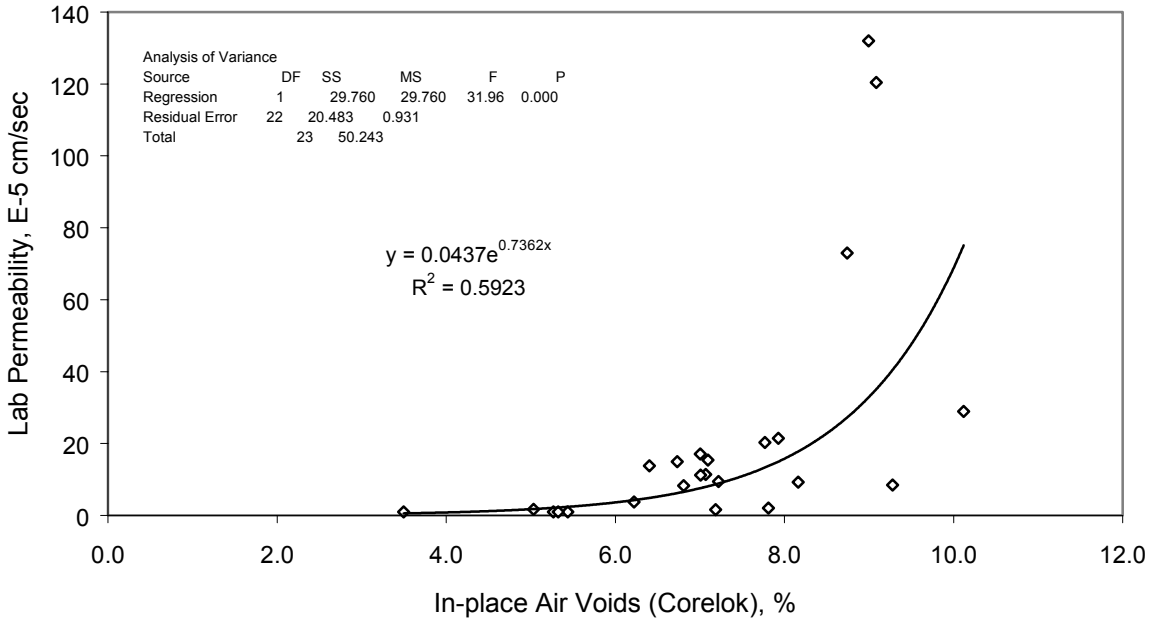

Figure 67: Plot of Permeability versus In-place Air Voids for 19.0 mm Fine-Graded NMAS mix.

In order to evaluate the factors affecting permeability, a multiple linear regression (MLR) was performed. This procedure was conducted to identify factors most affecting permeability. A best subsets regression was utilized to evaluate all independent variables and select the variables that provided the most significant relationship with the dependent variable (permeability). The best subsets regression procedure allows the user to input numerous factors that have the potential to impact the dependent parameter. For this analysis, the natural log of permeability was selected as the response, while natural log of in-place air voids based on vacuum sealed method, NMAS, sample thickness, natural log of voids in mineral aggregates (VMA), and coarse aggregate ratio were included as the predictors. The coarse aggregate ratio was defined as the percent retained on a sieve, three sizes lower than the NMAS divided by the percent passing that particular sieve.

Therefore, for NMAS of 19.0 mm, 12.5 mm, and 9.5 mm the associated sieve sizes were 4.75 mm, 2.36 mm, and 1.18 mm, respectively. The coarse aggregate ratio indicated whether a gradation was coarse or fine-graded.

Of the 287 core samples, only 226 cores had the VMA values available. Thus, the MLR was performed based on results of the 226 core samples and the best subsets regression analysis is presented in Table 51. Based on the C-p and R^2 values, the best model that could predict permeability was a combination of the natural log of air voids, coarse aggregate ratio, and the natural log of VMA. The three identified factors were then regressed versus the natural log of permeability and the following regression equation was obtained.

$$Ln(k) = -2.20 + 6.75Ln(CL) + 0.316(CAratio) - 3.05Ln(VMA)$$

Where,

Ln (k) = natural log of permeability

Ln (CL) = natural log of air voids from vacuum sealed device

CAratio = coarse aggregate ratio

Ln(VMA) = natural log of voids in mineral aggregate

Table 51: Best Subsets Regression on Factors Affecting Permeability

No. of Variables	R-Sq	R-Sq(adj)	C-p	NMAS	Thickness	Ln (CL)	CAratio	Ln (VMA)
1	68.5	68.4	31.3			X		
1	43.2	42.9	235.1					X
2	71.6	71.4	8.2			X	X	
2	70.2	69.9	19.8			X		X
3	72.5	72.2	3.1			X	X	X
3	71.8	71.5	8.5	X		X		X
4	72.6	72.1	4.1		X	X	X	X
4	72.5	72	4.9	X		X	X	X
5	72.7	72	6	X	X	X	X	X

There was a good correlation for the above equation with an R^2 of 0.72. The equation indicated that permeability increased as the air voids increased. The illustrations of this relationship are presented in the previous figures. The permeability also increased as the coarse aggregate ratio increased. The coarser the gradations, the larger the individual air voids leading to higher potential for interconnected air voids. The equation also suggested that the permeability increased as the VMA decreased. Lower VMA suggests less room for asphalt cement in a mix, which results in higher potential for interconnected air voids.

6.0 DISCUSSION OF RESULTS

6.1 Determination of the Minimum t/NMAS

The minimum t/NMAS determined from both gyratory and vibratory compactors was discussed earlier. Neither of these methods appeared to provide a clear approach for selecting the minimum t/NMAS. The results that provided the clearest answer to the minimum t/NMAS were obtained from the HMA sections constructed at the NCAT test track. For these sections the thickness was varied from relatively thin to relatively thick and a reasonable compactive effort with conventional rollers was applied. The results from these 7 mixtures appeared to provide suitable numbers that could be used to provide guidance on selecting minimum t/NMAS ratios. The data determined from this part of the study are summarized and presented in Table 52.

The results shown in Table 52 indicate that t/NMAS clearly has an effect on the compactibility of HMA mixes. This table shows the effect of changing the t/NMAS. The numbers presented indicate the difference between the air voids at the t/NMAS indicated and the lowest air voids at optimum t/NMAS.

Table 52: Effect of t/NMAS on Compactibility of HMA

Description of Mix	Difference from Minimum Air Voids for t/NMAS=2	Difference from Minimum Air Voids for t/NMAS=3	Difference from Minimum Air Voids for t/NMAS=4	Difference from Minimum Air Voids for t/NMAS=5
Section 1-9.5mm Fine Graded—Steel Roller	2.5%	1.0%	0.1%	0.1%
Section 2-9.5mm Coarse Graded-Steel Roller	2.5%	1.0%	0.5%	0.0%
Section 2-9.5mm Coarse Graded-Steel and Rubber Roller	2.0%	0.5%	0.0%	1.0%
Section 3-9.5mm SMA(mod AC) Steel Roller	5.5%	2.0%	0.2%	0.2%
Section 3-9.5mm SMA(Mod AC) Steel & Rubber Roller	1.2%	0.2%	0.0%	0.5%
Section 4-12.5mm SMA (mod AC) Steel Roller	11.3%	3.3%	0.3%	0.5%
Section 4-12.5mm SMA (mod AC) Steel & Rubber Roller	6.5%	3.5%	0.5%	0.0%
Section 5-19mm Fine Graded Steel Roller	3.1%	0.6%	0.0%	1.3%
Section 6-19mm Coarse Graded Steel and Rubber Roller	1.8%	0.6%	0.1%	0.1%
Section 7-19mm Coarse Graded (mod AC) Steel Roller	4.9%	1.3%	0.0%	0.8%
Section 7-19mm Coarse Graded (mod AC) Steel & Rubber Roller	6.1%	3.4%	0.8%	0.0%

A t/NMAS of 4 seems to be about optimum however a closer look is needed since there are a number of different mix types. The data suggest that there is a greater than 2 percent difference in air voids between the results at a ratio of 3 and the ratio that gives the lowest air voids. This signifies that for a given compactive effort the air voids at a t/NMAS ratio of 3 will generally be about 2% higher than the optimum t/NMAS. However, this finding is for a constant compactive effort. Increasing the compactive effort will allow an adequate density to be obtained in many cases even when the t/NMAS is not optimum.

In all cases a t/NMAS of 2 provided air voids more than 1% greater than the air voids obtained at optimum t/NMAS. In most cases the difference in density between t/NMAS of 2 and optimum exceeded 2.5%. This indicates that one would expect to see approximately 2.5% higher air voids when the t/NMAS was 2 than when it was close to optimum.

For fine-graded mixes it appears that the desired minimum t/NMAS is 3. There were only 2 fine-graded mixes evaluated and both were within 1 percent of the optimum voids at a t/NMAS equal to 3. There were 3 coarse-graded mixes evaluated and 2 of the 3 mixes had air voids within 1 percent of optimum at a t/NMAS equal to 3. The SMA mixes appeared to deviate even more from optimum at a t/NMAS of 3. However, a t/NMAS looks satisfactory for SMA mixtures. The results are all very consistent: a t/NMAS of 4 nearly always appeared to be about optimum. In three cases a t/NMAS of 5 was closer to the lowest air voids but the air voids difference at t/NMAS of 4 was still very low. In summary the data indicates that a minimum thickness t/NMAS of 4 is preferred for coarse-graded mixes and SMA mixes. For fine-graded mixes this minimum

t/NMAS can be reduced to 3 without adversely affecting the compactibility of the mixtures.

6.2 Effect of Mix Temperature on Compaction

When looking at the effect of t/NMAS on density one must also look at the effect of mat thickness and cooling rate. One of the reasons that lower t/NMAS ratios are difficult to compact is the effect of cooling. A thin section regardless of the t/NMAS will cool quickly and therefore be difficult to compact. When large NMAS aggregate is used the rate of cooling is relatively low even when the t/NMAS is low. There was some indication that the t/NMAS could be smaller for larger NMAS and the cooling rate is likely the reason. A 19mm mix placed at a t/NMAS of 2 is still 38mm thick which will hold the heat for a reasonable period of time. However, a 9.5mm mix placed at a t/NMAS of 2 is only 19mm thick and will cool very quickly.

The temperature data collected from the test sections showed that for the conditions during the tests a 25mm layer thickness cooled at about twice the rate as a 37.5mm layer thickness. Hence it would require twice as many rollers to roll the 25mm layer the same number of passes at the same speed over the same temperature range. So care must be used when selecting the layer thickness to ensure adequate rolling time. A 25mm layer thickness is very difficult to compact prior to cooling especially when paving in cold weather. To ensure adequate compaction the layer thickness should be closer to 37.5mm thick.

6.3 Effect of thickness on permeability at 7.0 ± 1.0 percent air voids

It is difficult to compact mixes to a reasonable density for thin lifts using the gyratory compactor. The problem is more pronounced when compacting SMA mixes. However, specimens compacted with vibratory compactor did achieve the target air voids at t/NMAS of 2.0, 3.0 and 4.0. The results in general show the permeability decreases as t/NMAS increases. Of all the mixes tested, only the 9.5 mm and 12.5 mm NMAS SMA mixes compacted at t/NMAS of 2.0 had permeability values more than 125 x 10^{-5} cm/sec. Results from Tables 36 and 37 are interesting in that specimens that had similar air void content, gradation and thickness had different permeability values. In most cases, specimens compacted with the vibratory compactor had much lower permeability than specimens compacted with gyratory compactor. This could likely be explained by a study conducted by Cooley and Kandhal (14) comparing compaction performed by vibratory and gyratory compactor. Specimens compacted by vibratory had more compaction at the top whereas gyratory-compacted samples showed less compaction in the top and bottom and more in the middle. This low compaction around the top, bottom, and outside edge for gyratory samples can significantly increase the permeability.

6.4 Evaluation of Factors Affecting Permeability

Observation of Figures 65 and 66 suggests that there is no significant difference between fine and coarse-graded mixes based on laboratory permeability tests. Cooley et al. (15) suggested a critical in-place air void content of 7.7 percent for both 9.5 and 12.5 mm NMAS coarse-graded mixes (based on field permeability value of 100 x 10^{-5} cm/sec). Using the critical value, the 9.5 mm coarse-graded mix has a lab permeability

value of 60 x 10^{-5} cm/sec and the 12.5 mm coarse graded mix has a lab permeability value of 24 x 10^{-5}cm/sec. The field permeability test is really an index and not a true measure of permeability so there is no surprise that there is a difference between field and lab results.

The selected factors identified by the multiple linear regression are interesting in that NMAS was not among the factors identified as affecting permeability. However, this can likely be explained in that of the 37 projects included in this study, 34 had either a 9.5 or 12.5 mm NMAS. Therefore, there was a little variation in NMAS, which would cause it not to be identified during the regression.

7.0 CONCLUSIONS

Based upon the results of this study, the following conclusions can be drawn.

The density that can be obtained under normal rolling conditions is clearly related to the t/NMAS. For improved compactibility it is recommended that the t/NMAS be at least 3 for fine graded mixes and at least 4 for coarse graded mixes. The data for SMA indicates that the ratio should also be at least 4. Ratios less than these suggested numbers could be used but it would generally require more compactive effort to obtain the desired density. In most cases a t/NMAS of 5 does not result in the need for more compactive effort to obtain maximum density. However, care must be exercised when the thickness gets too large to ensure that adequate density is obtained.

The results of the evaluation of the effect of mix temperature on the relationship between density and t/NMAS indicate that one of the reasons for low density at thinner sections (lower t/NMAS) is the more rapid cooling of the mixture. Hence, for thinner

layers it is even more important that rollers stay very close to the paver so that rolling can be accomplished prior to excessive cooling. For the conditions of this study the mixes placed at 25mm thickness cooled twice as fast as mixes placed at 37.5mm thickness. For thicker sections (larger t/NMAS) rate of cooling is typically not a problem.

The in-place void content is the most significant factor impacting permeability of Superpave pavements. This is followed by coarse aggregate ratio and VMA. As the values of coarse aggregate ratio increases, permeability increases. Permeability decreases as VMA increases.

The variability of permeability between various mixtures is very high. Some mixtures are permeable at the 8 to 10 percent void range and others do not seem to be permeable at these higher voids. However, to ensure that permeability is not a problem the in-place air voids should be between 6 and 7 percent or lower. This appears to be true for a wide range of mixtures regardless of NMAS and grading.

8.0 REFERENCES

1. Roberts, F.L., P.S. Kandhal, E.R. Brown, D.Y. Lee, and T.W, Kennedy. Hot Mix Asphalt Materials, Mixture Design, and Construction. NAPA Education Foundation, Lanham, MD. Second Ed., 1996.
2. Zube, E. "Compaction Studies of Asphalt Concrete Pavements as Related to the Water Permeability Test." Highway Research Board, Bulletin 358, 1962.
3. Brown, E.R., R. Collins, and J.A. Brownfield. "Investigation of Segregation of Asphalt Mixtures in the State of Georgia." Transportation Research Record 1217, 1989.

4. Choubane, B., G.C. Page, and J.A. Musselman. “Investigation of Water Permeability of Coarse Graded Superpave Pavements.” Journal of the Association of Asphalt Paving Technologists, Volume 67, 1998.

5. Ford, M.C., and C.E. McWilliams. “Asphalt Mix Permeability.” University of Arkansas, Fayettville, AR, 1988.

6. Hudson, S.B., and R.L. Davis. “Relationship of Aggregate Voidage to Gradation.” Association of Asphalt Paving Technologists, Volume 34, 1965.

7. Mallick, R.B., L.A. Cooley, Jr., and M. Teto. “Evaluation of Permeability of Superpave Mixes in Maine, Final Report. Technical Report ME-001, November 1999.

8. Musselman, J.A., B. Choubane, G.C. Page, and P.B. Upshaw. “Superpave Field Implementation: Florida’s Early Experience.” Transportation Research Record 1609, 1998.

9. Westerman, J.R. AHTD’s Experience with Superpave Pavement Permeability. Presented at Arkansas Superpave Symposium, January 21, 1998.

10. ‘Superpave Construction Guidelines.’ National Asphalt Pavement Association. Special Report 180. Lanham, Maryland. October 1997.

11. Garcia, J., K. Hansen. “HMA Pavement Mix Type Selection Guide.” National Asphalt Pavement Association. Information Series 128, 2001.

12. Cooley, Jr., L.A., B.D. Prowell, M.R. Hainin, M.S. Buchanan, and J. Harrington. Bulk Specific Gravity Round Robin Using the Corelok Vacuum Sealing Device. National Center for Asphalt Technology (NCAT) Report No. 02-11. November 2002.

13. The Asphalt Handbook. Asphalt Institute Manual Series No. 4 (MS-4) 1989.

14. Cooley, Jr., and P.S. Kandhal, "Evaluation of Density Gradients in Loaded Wheel Tester Samples," Journal of Testing and Evaluation, Volume 28, No. 6, November 2000.

15. L.A.Cooley, Jr.E.R. Brown, and S. Maghsoodloo. "Development of Critical Field Permeability and Pavement Density Values for Coarse-Graded Superpave Pavements." Prepared for Presentation and Publication at the 80th Annual Meeting of the Transportation Research Board. January 2001.